FACTORS CONTRIBUTING TO HUMORAL IMMUNITY AGAINST PNEUMONIC PLAGUE

A Dissertation presented to the Faculty of the Graduate School
at the University of Missouri

In Partial Fulfillment
Of the Requirements for the Degree

Doctor of Philosophy

by
NICHOLAS A. EISELE

Dr. Deborah M. Anderson, Dissertation Supervisor

MAY 2012

The undersigned, appointed by the Dean of the Graduate School, have examined the dissertation entitled

FACTORS CONTRIBUTING TO HUMORAL IMMUNITY
AGAINST PNEUMONIC PLAGUE

Presented by Nicholas A. Eisele

A candidate for the degree of Doctor of Philosophy

And hereby certify that in their opinion it is worthy of acceptance.

_____
Professor Deborah M. Anderson

_____
Professor George C. Stewart

_____
Professor Michael J. Calcutt

_____
Professor Michael L. Misfeldt

_____
Professor Francis J. Schmidt

The work presented within is dedicated to my friends and family. Without your constant love, support and devotion none of this would be possible. It is also dedicated to the loving memory of Daniel P. Saathoff; a person whose kindness and sincerity will always move me.

ACKNOWLEDGMENTS

Many people were instrumental for the completion of the work presented within. I first acknowledge my advisor, Dr. Deborah M. Anderson for her guidance, support, and dedication during my graduate career. I also thank the members of my doctoral committee, Dr. Michael J. Calcutt, Dr. George C. Stewart, Dr. Michael L. Misfeldt, and Dr. Francis J. Schmidt for always challenging me to think comprehensively and providing direction for my research. In addition, I also thank all of the members of the Anderson lab, especially David M. Bland, Miqdad Dhariwala, Lauren L. Keleher, Dr. Hanni Lee-Lewis, Dr. Yuqing Chen, Dr. Ami Patel, Dr. Andrew Kocsis, and Eric Coate for providing insightful discussions and technical assistance regarding many of the experiments performed within. I am also thankful for the undergraduate workers in the lab who have sustained the momentum of my work by maintaining the infrastructure of the lab.

The completion of this dissertation would not be possible without the support of researchers all over the University of Missouri campus. Dr. Curtis J. Pritzl and Dr. Daniel E. Hassett were instrumental in the formulation of several of the techniques presented within and assisted in data analysis. In addition, I acknowledge Dr. Charles R. Brown for graciously providing genetically modified mice, technical assistance regarding assay development, and invaluable feedback. I also thank Dr. Cynthia Besch-Williford at RADIL and the members of the Histology lab for helpful feedback, data analysis, and technical assistance with experiments requiring histopathological analysis.

I am also thankful to Dr. Olaf Schneewind of the University of Chicago and Howard T. Ricketts Laboratory at Argonne National Laboratory for hosting me for several weeks in order to carry out a transposon screen. In addition, I recognize Timothy Hermanas for creating the library and aiding me in logistics required to perform the screen. I also thank Karyl Kopaskie, Sao Mai Nguyen-Mau, and Dr. Bill Blaylock for providing additional support and camaraderie. Furthermore, I also acknowledge Emily Traw and Dr. Lauriane Quenee for assisting with administrative paperwork required to begin work in the HTRL.

The majority of my graduate work was funded by the NIH/NIGMS Cell and Molecular Biology training grant T32 GM008396. Thus, I would like to thank Dr. Mark Hannink for annually renewing my funding by this grant, and allowing me to obtain additional training which has undoubtedly contributed significantly to my development as a scientist. I also thank Debbie Allen for her help with logistical issues and organizing events associated with the training grant.

I also recognize administrative staff members in several departments. In the department of Veterinary Pathobiology I thank Darlene Ward, Anne Chegwidden, Ellen Abbott, and Jan Nicholson for all that they have done for me and the program. In addition, I thank Jana Clark in the Molecular Microbiology & Immunology departmental office for help with everything from registering for classes to filing paperwork with the graduate school. Without the help of such a great administrative team none of this work would be possible.

Last, but certainly not least, I thank all of the friends I have made at the University of Missouri. In particular, I am thankful to Dr. Bruno Marchand, Erkan

Osman, Dr. John Crawford Hardaway, Jordan Wilkins, David Bland, and Lauren Keleher for supporting me and providing friendship that has undoubtedly contributed to the successful completion of my Ph.D.

TABLE OF CONTENTS

LIST OF ILLUSTRATIONS

Figure Page

LIST OF TABLES

ABSTRACT

Yersinia pestis is the etiologic agent of plague and is responsible for more human deaths throughout history than any other bacterial pathogen. Today, naturally occurring cases are rare due in large part to the advent of basic sanitation. However, after the Anthrax attacks in 2001, there has been an increased need to better understand pathogens that could be weaponized. During infection, the *Y. pestis* Type III secretion system (T3SS) injects effector proteins into target host cells and is essential for virulence. Immunity to plague is conferred to the host via antibodies that target LcrV, an essential component of the T3SS. Although protective anti-LcrV antibodies block injection, the precise mechanism of protection has yet to be elucidated. As such, we sought here to better define the requirements for humoral immunity to plague. We found that protective antibodies not only block T3S, but also opsonize bacteria for phagocytic uptake. Thus, we next investigated the role of macrophages in disease clearance and found that while cells limit the replication of bacteria, they are unable to clear infection. Thus we hypothesized that another immune cell is important for disease clearance and found that recruitment and activation of neutrophils is essential for clearing infection in the presence of anti-LcrV antibodies. Taken together the data support a model whereby protective antibodies block T3S injection while simultaneously opsonizing bacteria for phagocytic uptake. However, although macrophages limit bacterial replication, cells are unable to kill organisms and rely on neutrophils to clear the infection.

CHAPTER 1

THE PLAGUE BACILLUS, *YERSINIA PESTIS*

Adapted from: *Nicholas A. Eisele and Deborah M. Anderson, "*Host Defense and the Airway Epithelium: Frontline Responses That Protect against Bacterial Invasion and Pneumonia*," Journal of Pathogens, vol. 2011, Article ID 249802, 16 pages, 2011. doi:10.4061/2011/249802*

And: *Eisele, N.A., Brown, C.R., and Anderson, D.M.,"* Phagocytes and humoral immunity to pneumonic plague*." Adv Exp Med Biol. 2012. In Press*

1.1 Introduction

Yersinia pestis is the causative agent of bubonic, pneumonic and septicemic plague and is responsible for more human deaths throughout history than any other bacterial pathogen [1]. Bacteria are found endemically throughout the world and are thought to have evolved from the enteric pathogen *Yersinia pseudotuberculosis* approximately 20,000 years ago [2]. Organisms are maintained enzootically in sylvatic or urban cycles through alternating transmission events between fleas and rodents [3]. After taking a blood meal from an infected mammal, bacteria colonize the mid-gut of the flea, forming a biofilm that blocks blood from entering the flea digestive tract. This causes the

insect to starve and attempt to take repeated blood meals from naïve hosts, ultimately leading to the regurgitation of bacteria into the bite site.

After the subcutaneous injection of bacteria, organisms migrate to the nearest lymph node via an unknown mechanism and begin to replicate. High level cell division and subsequent induction of local pro-inflammatory responses cause excessive swelling and pain in the lymph node, leading to the development of the characteristic bubo(s) associated with the disease. In a high number of cases, tissue necrosis eventually develops which gives bacteria access to the circulatory system and the ability to spread through the host systemically, resulting in septicemic plague. Here, organisms are able to invade and colonize organs throughout the host.

When bacteria reach the lung, affected mammals develop secondary pneumonic plague. In humans, this is a highly contagious form of disease as bacteria are easily spread from person-to-person via aerosolized droplets. It is thought that as little as 300 colony forming units (CFUs) are enough to cause disease [4]. Once inhaled, bacteria will colonize the airspaces of the lung resulting in primary pneumonic plague. Primary lung infection presents as a biphasic disease in that during the first 24-36 hours of infection little inflammation is observed [5, 6]. After the initial quiescent period (~48 hours post-infection), the lung environment then abruptly turns pro-inflammatory, accompanied by rapid bacterial growth and tissue necrosis [5]. Pulmonary infection ultimately results in a patchy bronchopneumonia containing necrotic lesions composed of fibrin,

neutrophils, and bacterial colonies [1]. In humans, symptoms include fever, headache, weakness, bloody sputum, and dyspnea. If left untreated, infection is nearly always fatal.

Due to its high virulence and the ease of pulmonary transmission, there have been countless naturally occurring plague epidemics within three pandemics recorded throughout history [7]. Although we are considered to still be experiencing the third pandemic, typically less than 3,000 cases are reported per annum worldwide, with only 5-15 of these in the United States [8]. However, after the Anthrax attacks of 2001 (Amerithrax), which resulted in the infection of 22 people and 5 deaths, increased attention has been given to biological agents that could result in a mass-casualty incident if intentionally deployed. Indeed, *Y. pestis* has been utilized as bioweapon in several conflicts throughout history. As a result of these circumstances, the Centers for Disease Control and Prevention (CDC) has classified the bacterium as a Category A Select Agent, leading to an increased push to better understand the pathogenesis of the organism, as well as toward the development of novel therapeutics which could be stored in the CDC National Strategic Stockpile in order to quickly and effectively respond to an incident.

1.2 Mechanisms of Virulence in Pneumonic Plague

The immunocompetent mammalian lung is well equipped to withstand insult by many threats, be it particle or biological. Thus, successful pathogens must evolve to avoid or eliminate these defenses in order to establish a

replicative niche. Given its extreme virulence, as well as the rapidity of disease, it is no surprise that *Y. pestis* has acquired many mechanisms to subvert these obstacles.

Y. pestis has acquired mechanisms to modify its lipopolysaccharide (LPS) structure in response to temperature which limits recognition of the bacterium by toll-like receptor 4 (TLR4). When grown at lower temperatures, that would be encountered while colonizing the flea vector (21-27°C), *Y. pestis* expresses a mixture of tri-acylated, tetra-acylated, penta-acylated, and hexa-acylated lipid A structures which may be beneficial for growth in this environment [9, 10]. However, when grown at the mammalian body temperature (37°C), tri-acylated and tetra-acylated lipid A structures predominate, with no detectable hexa-acylation. Consequently, LPS isolated from bacteria grown at 37°C does not significantly stimulate TLR4, and NF-κB is not activated in human inflammatory cells, thereby delaying production of TNF-α and IL-8 [11-13]. LPS isolated from bacteria grown at 37°C is not only nonstimulatory, but also inhibits TLR4 activation. Shown in mixing experiments, *Y. pestis* LPS from bacteria grown at 37°C could suppress TLR4 activation elicited from normally pro-inflammatory LPS [14]. Similar results were seen in dendritic cells where it has also been shown that tetra-acylated LPS inhibited cell signaling through TLR2 and TLR9, and inhibited up regulation of the co-stimulatory molecules MHC-II, CD40, and CD86 [15]. Together, the data demonstrate that LPS modulates TLR signaling through multiple mechanisms and is of central importance to *Y. pestis* virulence.

Yersinia pestis also uses a Type III secretion system (T3SS) to control inflammatory responses during infection through the injection of *Yersinia* outer proteins (Yops) into the host cell cytosol. Injection of Yops blocks phagocytic uptake by neutrophils, macrophages, and dendritic cells and ultimately causes host cell death [16-18]. This effect has historically been attributed to interactions with macrophages and neutrophils; however, the T3SS is active against epithelial cells and lymphocytes *in vitro*, suggesting it is positioned to play multiple roles *in vivo*. Mutants that lack the T3SS are avirulent in pneumonic plague models, where they fail to evade early innate immune responses in the lung [19, 20]. Depletion of TNF-α but not IL-1β caused an increase in sensitivity of mice to *Y. pestis* lacking YopH, but not wild type bacteria, suggesting that YopH may impact the ability of the host to induce NF-κB responses. Another Type III effector protein, YopJ, has long been known to affect NF-κB responses in macrophages. Recently, YopJ was shown to have similar activity when injected into bronchial epithelial cells where it reduced NF-κB regulated gene expression, suggesting that this virulence factor may help prevent unwanted inflammatory responses during the early stages of infection [21]. However, YopJ is relatively dispensable for virulence during pneumonic plague, suggesting that additional mechanisms for suppressing NF-κB regulated genes in alveolar macrophages and epithelial cells dominate during infection [22].

Effective T3S into phagocytic and epithelial cells has been shown to be dependent on the adhesive properties conferred by membrane proteins. Three

proteins have been identified in *Y. pestis* that contribute this activity: Ail, Pla, and Psa. Ail (attachment-invasion locus) mediates binding to fibronectin, a component of the extracellular matrix [23]. Pla (plasminogen activator) has proteolytic and adhesive properties that also mediate binding to the extracellular matrix and perhaps other receptors on alveolar macrophages and dendritic cells [24-26]. Psa (pH 6 antigen) fimbriae bind to phosphatidylcholine, a component of cell membranes and surfactant, and to β1-linked, galactosyl-linked residues in glycosphingolipids [27, 28]. Psa appears to be more important for binding alveolar epithelial cells than to macrophages indicating it may play a central role in penetration of the airway epithelium [29]. However Psa is relatively dispensable for virulence during pneumonic plague whereas Pla and Ail are essential [29]. Loss of any or all of these factors markedly reduces Yop-induced cytotoxicity towards target cells and attenuates virulence [30-33].

Y. pestis has a rough LPS structure and does not synthesize an O-antigen domain. Instead, bacteria utilize the multifunctional proteins mentioned above to resist killing by host antimicrobial molecules. Ail is highly expressed on the bacterial membrane at 26°C and 37°C and confers resistance to complement-mediated killing by serum derived from humans, rats, rabbits, sheep, goats, and guinea pigs but is dispensable for resistance to mouse serum [34]. Accordingly, strains lacking *ail* are highly attenuated in a rat model of pneumonic plague but still exhibit an increase in the mean time to death in mice [35]. Thus, this observation may indicate a role for Ail in adhesion and internalization *in vivo*. In

addition, anti-microbial peptides such as cathelicidin and β-defensin have antimicrobial activity against attenuated strains of *Y. pestis in vitro*, and expression of the surface located virulence factors Pla and CaF1 (Capsular protein F1) modulate susceptibility to these peptides [36]. Pla is a serine protease with broad spectrum activity that plays an essential role in the development of pneumonic plague. Pla-catalyzed cleavage of cationic anti-microbial peptides provides a mechanism whereby *Y. pestis* can cleave and inactivate CAMPs [36]. Paradoxically, expression of CaF1, which forms anti-phagocytic pili on the *Y. pestis* cell surface at 37°C, can reduce the protective effects elicited by Psa and Pla, likely through steric interference or alteration of substrate specificity. Pla may also directly mediate serum resistance due to its proteolytic activity on C3 [25].

Yersinia species are thought to be capable of invading epithelial cells through interactions between one or more adhesins and host cell β1 integrins [37]. At least three pathways of invasion have been suggested based on interactions between enteropathogenic *Yersiniae* and epithelial cells. The most efficient invasion mechanism, mediated by the protein Invasin, is not likely not to occur in *Y. pestis* because this gene is not expressed [38]. Nevertheless, invasion of the bronchial or type II alveolar epithelial cells is an attractive model by which *Y. pestis* would successfully penetrate the epithelial barrier without causing inflammation at early stages of infection. Alternative mechanisms for how bacteria invade the epithelium involve the action of one or more toxins

produced by extracellular bacteria. In support of this model, Pla is required for *Y. pestis* to invade the lung parenchyma, suggesting it may have a role in enhancing penetration of the alveolar epithelium [33].

Even under conditions that support high level, simultaneous expression of virulence factors that suppress phagocytosis and contribute to the extracellular lifecycle of the organism, a small percentage of bacteria are engulfed by phagocytes *in vitro* [39]. Intracellular bacteria are equipped to resist antimicrobial activity and proliferate even in IFN-γ activated macrophages [40, 41]. Once phagocytosed by macrophages, bacteria prevent the acidification of vacuoles and begin replicating independent of the T3SS [42, 43]. Replication in activated macrophages requires the protein RipA which directly reduces NO levels without modulating inducible nitric oxide synthase (iNOS) expression [40]. Intracellular survival is also dependent on *phoPQ* (a two-component signal transduction system that responds to low [Mg^{2+}]), *ugd*, *pmrK* (predicted phagosomal antimicrobial peptide resistance genes), and *mgtC* (a low-Mg^{2+} acquisition gene) which are important for the early intracellular survival of *Y. pestis* [44-46]. In addition, antibody opsonization of *Y. pestis* promotes phagocytic uptake, but the bacteria are not killed by macrophages [47]. Together, the data suggest that survival in alveolar macrophages, neutrophils, and perhaps also epithelial cells lining the airway, may be an important virulence mechanism for invasive strategies utilized during pneumonic plague [29].

In addition to inhibiting bacteria from being internalized, T3S by extracellular bacteria also inhibits ROS production in phagocytic cells which is required to eliminate intracellular bacteria [18]. Neutrophils are resistant to Yop-induced apoptosis and inhibition of ROS production appears to prevent cells from undergoing phagocytosis-induced cell death (PICD), a mechanism used by neutrophils to contain infection and resolve inflammation [48, 49]. Thus, the data support a model whereby T3S blocking antibodies prevent Yop injection into neutrophils, allowing ROS production and subsequent killing of intra- and extracellular bacteria.

1.3 Disease Intervention and Vaccine Development

Although standard antibiotics that target Gram-negative bacteria elicit high levels of protection if administered before the onset of severe symptoms, several multi-drug resistant strains have been isolated in nature from affected individuals that are refractory to such treatment [50, 51]. Thus, in the event of the intentional release of bacteria into the environment, it is possible that the culprits would make use of similar or further genetically modified strains. To circumvent this issue, vaccination against the organism is a viable alternative for achieving protection from infection via natural or intentional exposure, as well as inoculation from multiple routes of infection. Testing this hypothesis, Alexandre Yersin first purified antiserum produced against whole killed cells and successfully used it to treat a plague patient in 1896 [52]. This discovery ultimately led to the development of the Cutter USP formalin-inactivated whole cell killed vaccine, as

well as lesser known attenuated strain vaccinations which were not licensed for use in the United States. However, due to a lack of data regarding vaccine efficacy in animals and humans, as well as moderate to severe side effects commonly associated with human and non-human primate vaccination, the Cutter USP vaccine is not available to the general public [53].

As a result, much work has been done over the years to identify specific antigens that elicit high levels of protection in animal models of plague. In analyzing the antibody repertoire of mammals vaccinated with killed whole cells or attenuated strains, it becomes evident that antibodies against Caf1 predominate. Indeed, antibodies elicited from vaccination or passive transfer targeting Caf1 are protective in animal models of plague [54, 55]. However, subsequent analysis indicates that strains lacking *caf1* display similar levels of virulence as wild type strains in several animal models of infection [55]. Nevertheless, given the level of protection achieved in the presence of Caf1, this antigen remains part of current vaccine formulations.

A second antigen, LcrV (Low Calcium Response Variable antigen or V-Antigen), has also been identified as essential for virulence. LcrV forms a pentamer on the fully polymerized T3SS needle tip and is thought to act as a scaffold for proteins that mediate insertion of the needle complex into the target host cell membrane [56]. Many vaccine platforms attempting to exploit LcrV immunogenicity have been developed, including live attenuated recombinant-(plant and bacterial), DNA-, virus vector-, and subunit-based vaccines [57]. Of

these, several subunit vaccines have undergone extensive testing and show promise in eliciting protection from pneumonic plague in mouse, rat, guinea pig, and non-human primate animal models of infection [58-61].

Effective vaccination likely relies on the ability to stimulate cell-mediated defenses, as IFNγ, TNFα, and iNOS are required for immune protection from pulmonary challenge in the presence of anti-LcrV antibodies [62]. Characterization of serum taken from vaccinated mice and non-human primates indicates that inducing an anti-LcrV IgG antibody response capable of neutralizing T3SS injection *in vitro*, and protecting mice from challenge after passive transfer *in vivo*, correlates with immune protection from pneumonic plague [55, 58, 60, 63-66]. However, although vaccines are capable of raising titers in humans, it is unclear how high antibody titers need to be in order to elicit protection [64]. Furthermore, the ability to induce sustained high-level or high-quality anti-LcrV IgG titers in vaccinated non-human primates has proven to be difficult, as achieving titers capable of protecting cohorts of cynomolgus macaques and, to an even greater extent, African green monkeys from pulmonary challenge is inconsistent [4, 58]. Thus, the correlates of immunity needed to protect humans from pneumonic plague remain unclear.

Along with the inadequacies associated with the current plague vaccines, induction of an immune response upon vaccination takes weeks, meaning that already infected individuals cannot be protected upon vaccine administration. An alternative to active vaccination is the passive transfer of immunity with

humanized anti-LcrV antibodies. Using libraries of monoclonal antibodies (MAbs), several protective epitopes of unknown importance to LcrV function have been identified. MAb7.3 binds amino acids 135-275, with N255 being essential for binding, and passive transfer protects mice from pneumonic challenge [67, 68]. Within this region, monoclonal antibody BA5 has recently been shown to bind amino acids 196-225 and elicits a comparable level of protection to MAb7.3 [69]. In murine models of pneumonic plague, anti-LcrV antibodies must be administered within 24-48 hours of infection to achieve sufficient protection [70]. Antibodies targeting LcrV block effector translocation while simultaneously neutralizing bacteria for uptake by phagocytes, but it is unclear if both of these activities are required for the antibody-mediated clearance of bacteria during pneumonic infection [66].

1.4 Considerations and Research Aims

Much progress has been made over the years in understanding *Y. pestis* pathogenesis in the lung, as well as the concomitant development of therapeutics used to prevent or treat infection. However, as alluded to above, there are currently many problems that the field faces due to a lack of understanding in several areas. Of these, a major concern is that the precise mechanism of antibody-mediated clearance of disease in the lung has yet to be elucidated. Determining the pathways driving humoral immunity in the lung is absolutely essential, as augmenting constituents important for bacterial clearance in the presence of antibodies may extend the period of time that anti-LcrV antibodies

can be delivered to affected individuals and/or improve antibody efficacy. As such, listed here are the specific research aims of this dissertation that serve to address these concerns:

- Define the role of opsonophagocytosis in humoral immunity to plague
- Better understand intracellular *Y. pestis*-macrophage interactions and its role during infection
- Identify host-factors necessary for the clearance of pneumonic plague in the presence of neutralizing antibodies.

In the subsequent chapters, the aims outlined above are directly addressed using a number of *in vitro* and *in vivo* techniques and infection models. Investigating these important points will not only provide a better understanding of the mechanisms behind the infection process, but also reveal information that is essential for the development of novel therapeutics and treatment regimens.

1.5 References

1. Pollitzer, R., *Plague*. 1954, Geneva, Switzerland: World Health Organization.

2. Achtman, M., et al., *Yersinia pestis, the cause of plague, is a recently emerged clone of Yersinia pseudotuberculosis.* Proc Natl Acad Sci U S A, 1999. **96**(24): 14043-8.

3. Eisen, R.J. and K.L. Gage, *Transmission of flea-borne zoonotic agents.* Annu Rev Entomol, 2012. **57**: 61-82.

4. Pitt, M.L. *Nonhuman Primates as a Model for Pneumonic Plague*. in *Public Workshop on Animal Models and Correlates of Protection for Plague Vaccines*. 2004. Gaithersburg, MD.

5. Lathem, W., et al., *Progression of primary pneumonic plague: A mouse model of infection, pathology, and bacterial transcriptional activity.* Proc Natl Acad Sci, 2005. **102**(49): 17786-91.

6. Price, P.A., J. Jin, and W.E. Goldman, *Pulmonary infection by Yersinia pestis rapidly establishes a permissive environment for microbial proliferation.* Proc Natl Acad Sci U S A, 2012. **109**(8): 3083-8.

7. Perry, R.D. and J.D. Fetherston, *Yersinia pestis--etiologic agent of plague.* Clin Microbiol Rev, 1997. **10**(1): 35-66.

8. CDC, *Plague Fact Sheet.* 2005.

9. Rebeil, R., et al., *Variation in lipid A structure in the pathogenic yersiniae.* Mol Microbiol, 2004. **52**(5): 1363-73.

10. Rebeil, R., et al., *Characterization of late acytransferase genes of Yersnia pestis and their role in temperature dependent lipid A variation.* J Bacteriol, 2006. **188**(4): 1381-8.

11. Montminy, S.W., et al., *Virulence factors of Yersinia pestis are overcome by a strong lipopolysaccharide response.* Nat Immunol, 2006. **7**(10): 1066-73.

12. Kawahara, K., et al., *Modification of the structure and activity of lipid A in Yersinia pestis lipopolysaccharide by growth temperature.* Infect Immun, 2002. **70**(8): 4092-8.

13. Matsuura, M., et al., *Immunomodulatory effects of Yersinia pestis lipopolysaccharides on human macrophages.* Clin Vaccine Immunol, 2010. **17**(1): 49-55.

14. Montminy, S., et al., *Virulence factors of Yersinia pestis are overcome by a strong lipopolysaccharide response.* Nat Immunol, 2006. **7**(10): 1066-73.

15. Telepnev, M.V., et al., *Tetraacylated lipopolysaccharide of Yersinia pestis can inhibit multiple Toll-like receptor-mediated signaling pathways in human dendritic cells.* J Infect Dis, 2009. **200**(11): 1694-702.

16. Adkins, I., et al., *Yersinia outer proteins E, H, P, and T differentially target the cytoskeleton and inhibit phagocytic capacity of dendritic cells.* Int J Med Microbiol, 2007. **297**: 235-44.

17. Bergsbaken, T., S. Fink, and B. Cookson, *Pyroptosis: host cell death and inflammation.* Nat Rev Microbiol, 2009. **7**: 99-109.

18. Spinner, J.L., J.A. Cundiff, and S.D. Kobayashi, *Yersinia pestis type III secretion system-dependent inhibition of human polymorphonuclear leukocyte function.* Infect Immun, 2008. **76**(8): 3754-60.

19. Bosio, C., A. Goodyear, and S. Dow, *Early interaction of Yersinia pestis with APCs in the lung.* J Immunol, 2005. **175**: 6750-6.

20. Cantwell, A., S. Bubeck, and P. Dube, *YopH inhibits early pro-inflammatory cytokine responses during plague pneumonia.* BMC Immunol, 2010. **11**: 29-40.

21. Zhou, L., A. Tan, and M.B. Hershenson, *Yersinia YopJ inhibits pro-inflammatory molecule expression in human bronchial epithelial cells.* Respir Physiol Neurobiol, 2004. **140**(1): 89-97.

22. Lemaitre, N., et al., *Yersinia pestis YopJ suppresses tumor necrosis factor alpha induction and contributes to apoptosis of immune cells in the lymph node but is not required for virulence in a rat model of bubonic plague.* Infect Immun, 2006. **74**(9): 5126-31.

23. Tsang, T.M., S. Felek, and E.S. Krukonis, *Ail binding to fibronectin facilitates Yersinia pestis binding to host cells and Yop delivery.* Infect Immun, 2010. **78**(8): 3358-68.

24. Lahteenmaki, K., et al., *Expression of Plasminogen Activator Pla of Yersinia pestis enhances bacterial attachment to the mammalian extracellular matrix.* Infect Immun, 1998. **66**(12): 5755-62.

25. Soleinde, O., et al., *A surface protease and the invasive character of plague.* Science, 1992. **258**: 1004-7.

26. Zhang, Y., et al., *Type III secretion decreases bacterial and host survival following phagocytosis of Yersinia pseudotuberculosis by macrophages.* Infect Immun, 2008. **76**(9): 4299-310.

27. Galvan, E., H. Chen, and D. Schifferli, *The Psa fimbriae of Yersinia pestis interact with phosphatidylcholine on alveolar epithelial cells and pulmonary surfactant.* Infect Immun, 2007. **75**(3): 1272-9.

28. Payne, D., et al., *The pH 6 antigen of Yersinia pestis binds to beta1-linked galactosyl residues in glycosphingolipids.* Infect Immun, 1998. **66**(9): 4545-8.

29. Liu, F., et al., *Effects of Psa and F1 on the adhesive and invasive interactions of Yersinia pestis with human respiratory tract epithelial cells.* Infect Immun, 2006. **74**(10): 5636-44.

30. Weening, E.H., et al., *The dependence of the Yersinia pestis capsule on pathogenesis is influenced by the mouse background.* Infect Immun, 2011. **79**(2): 644-52.

31. Felek, S., T.M. Tsang, and E.S. Krukonis, *Three Yersinia pestis adhesins facilitate Yop delivery to eukaryotic cells and contribute to plague virulence.* Infect Immun, 2010. **78**(10): 4134-50.

32. Kolodziejek, A.M., et al., *Outer membrane protein X (Ail) contributes to Yersinia pestis virulence in pneumonic plague and its activity is dependent on the lipopolysaccharide core length.* Infect Immun, 2010. **78**(12): 5233-43.

33. Lathem, W., et al., *A plasminogen activating proteas specifically controls the development of primary pneumonic plague.* Science, 2007. **215**: 509-13.

34. Schesser Bartra, S., et al., *Resistance of Yersinia pestis to complement dependent killing is mediated by the Ail outer membrane proteins.* Infect Immun, 2008. **76**(2): 612-22.

35. Kolodziejek, A., et al., *Outer membran protein X (Ail) contributes to Yersinia pestis virulence in pneumonic plague and its activity is dependent on LPS core length.* Infect Immun, 2010. **In press**.

36. Galvan, E., M. Lasaro, and D. Schifferli, *Capsular antigen fraction 1 and Pla modulate the susceptibility of Yersinia pestis to pulmonary antimicrobial peptides such as cathelicidin.* Infect Immun, 2008. **76**(4): 1456-64.

37. Isberg, R. and J. Leong, *Multiple b1 chain integrins are receptors for invasin, a protein that promotes bacterial penetraion into mammalian cells.* Cell, 1990. **60**: 861-71.

38. Simonet, M., et al., *Invasin production by Yersinia pestis is abolished by insertion of an IS200-like element within the inv gene.* Infect Immun, 1996. **64**(1): 375-9.

39. Pujol, C. and J. Bliska, *The ability to replicate in macrophages is conserved between Yersinia pestis and Yersinia pseudotuberculosis.* Infect Immun, 2003. **71**(10): 5892-9.

40. Pujol, C., et al., *Replication of Yersinia pestis in interferon γ-activated macrophages requires ripA, a gene encoded in the pigmentation locus.* Proc Natl Acad Sci, 2005. **102**(36): 12909-14.

41. O'Laughlin, J., et al., *Yersinia pestis two-component gene regulatory systems promote survival in human neutrophils.* Infect Immun, 2010. **78**(2): 773-82.

42. Pujol, C., et al., *Yersinia pestis can reside in autophagosomes and avoid xenophagy in murine macrophages by preventing vacuole acidification.* Infect Immun, 2009. **77**(6): 2251-61.

43. Goguen, J., J. Yother, and S. Straley, *Genetic analysis of the low calcium response in Yersinia pestis mu d1 (Ap lac) insertion mutants.* J Bacteriol, 1984. **160**(3): 842-8.

44. Grabenstein, J., et al., *The response regulator PhoP of Yersinia pseudotubeculosis is important for replication in macrophages and for virulence.* Infect Immun, 2004. **72**(9): 4973-84.

45. Grabenstein, J., et al., *Characterization of phagosome trafficking and identification of PhoP-regulated genes important for survival of Yersinia pestis in macrophages.* Infect Immun, 2006. **74**(7): 3727-41.

46. O'Loughlin, J.L., et al., *Yersinia pestis two-component gene regulatory systems promote survival in human neutrophils.* Infect Immun, 2010. **78**(2): 773-82.

47. Noel, B., et al., *Yersinia pestis can bypass protective antibodies to LcrV and activation with gamma interferon to survive and induce apoptosis in murine macrophages.* Clin Vacc Immunol, 2009. **16**(10): 1457-66.

48. Spinner, J.L., et al., *Neutrophils are resistant to Yersinia YopJ/P-induced apoptosis and are protected from ROS-mediated cell death by the type III secretion system.* PLoS One, 2010. **5**(2): e9279.

49. DeLeo, F.R., *Modulation of phagocyte apoptosis by bacterial pathogens.* Apoptosis, 2004. **9**(4): 399-413.

50. Galimand, M., et al., *Multidrug resistance in Yersinia pestis mediated by a transferable plasmid.* N Engl J Med, 1997. **337**(10): 677-80.

51. Guiyoule, A., et al., *Transferable plasmid-mediated resistance to streptomycin in a clinical isolate of Yersinia pestis.* Emerg Infect Dis, 2001. **7**(1): 43-8.

52. Hawgood, B.J., *Alexandre Yersin (1863-1943): discoverer of the plague bacillus, explorer and agronomist.* J Med Biogr, 2008. **16**(3): 167-72.

53. Gage, K.L.e.a., *Prevention of Plague: Recommendations of the Advisory Committee on Immunization Practices (ACIP).* National Center for Infectious Diseases - Division of Vector-Borne Infectious Diseases, 1996.

54. Cornelius, C.A., et al., *Yersinia pestis IS1541 transposition provides for escape from plague immunity.* Infect Immun, 2009. **77**(5): 1807-16.

55. Quenee, L.E., et al., *Yersinia pestis caf1 variants and the limits of plague vaccine protection.* Infect Immun, 2008. **76**(5): 2025-36.

56. Cornelis, G.R., *The type III secretion injectisome.* Nat Rev Microbiol, 2006. **4**(11): 811-25.

57. Rosenzweig, J.A., et al., *Progress on plague vaccine development.* Appl Microbiol Biotechnol, 2011. **91**(2): 265-86.

58. Quenee, L.E., et al., *Prevention of pneumonic plague in mice, rats, guinea pigs and non-human primates with clinical grade rV10, rV10-2 or F1-V vaccines.* Vaccine, 2011.

59. Quenee, L.E., et al., *Plague in Guinea pigs and its prevention by subunit vaccines.* Am J Pathol, 2011. **178**(4): 1689-700.

60. Williamson, E.D., et al., *Immunogenicity of the rF1+rV vaccine for plague with identification of potential immune correlates.* Microb Pathog, 2007. **42**(1): 11-21.

61. Williamson, E.D., et al., *Kinetics of the immune response to the (F1+V) vaccine in models of bubonic and pneumonic plague.* Vaccine, 2007. **25**(6): 1142-8.

62. Parent, M.A., et al., *Gamma interferon, tumor necrosis factor alpha, and nitric oxide synthase 2, key elements of cellular immunity, perform critical protective functions during humoral defense against lethal pulmonary Yersinia pestis infection.* Infect Immun, 2006. **74**(6): 3381-6.

63. Bashaw, J., et al., *Development of in vitro correlate assays of immunity to infection with Yersinia pestis.* Clin Vaccine Immunol, 2007. **14**(5): 605-16.

64. Williamson, E.D., et al., *Human immune response to a plague vaccine comprising recombinant F1 and V antigens.* Infect Immun, 2005. **73**(6): 3598-608.

65. Williamson, E.D., et al., *Recombinant (F1+V) vaccine protects cynomolgus macaques against pneumonic plague.* Vaccine, 2011. **29**(29-30): 4771-7.

66. Weeks, S., et al., *Anti-V antigen antibody protects macrophages from Yersinia pestis -induced cell death and promotes phagocytosis.* Microb Pathog, 2002. **32**(5): 227-37.

67. Hill, J., et al., *N255 is a key residue for recognition by a monoclonal antibody which protects against Yersinia pestis infection.* Vaccine, 2009. **27**(50): 7073-9.

68. Hill, J., et al., *Regions of Yersinia pestis V antigen that contribute to protection against plague identified by passive and active immunization.* Infect Immun, 1997. **65**(11): 4476-82.

69. Quenee, L.E., et al., *Amino acid residues 196-225 of LcrV represent a plague protective epitope.* Vaccine, 2010. **28**(7): 1870-6.

70. Hill, J., et al., *Synergistic protection of mice against plague with monoclonal antibodies specific for the F1 and V antigens of Yersinia pestis.* Infect Immun, 2003. **71**(4): 2234-8.

CHAPTER 2

DUAL-FUNCTION ANTIBODIES TO *YERSINIA PESTIS* LCRV REQUIRED FOR PULMONARY CLEARANCE OF PLAGUE

As found in: *Nicholas A. Eisele and Deborah M. Anderson (2009). "*Dual-function antibodies to *Yersinia pestis* LcrV required for pulmonary clearance of plague.*" Clin Vaccine Immunol 16(12): 1720-27.*

2.1 Abstract

Yersinia pestis causes pneumonic plague, a necrotic pneumonia that rapidly progresses to death without early treatment. Antibodies to the protective antigen LcrV are thought to neutralize its essential function in the type III secretion system (T3SS) and by themselves are capable of inducing immunity to plague in mouse models. To develop multivalent LcrV antibodies as a therapeutic treatment option, we screened for monoclonal antibodies (MAbs) to LcrV that could prevent its function in the T3SS. Although we were able to identify single and combination MAbs that provided the high-level inhibition of the T3SS, these did not promote phagocytosis *in vitro* and were only weakly protective in a mouse pneumonic plague model. Only one MAb, BA5, was able to protect mice from pneumonic plague. *In vitro*, MAb BA5 blocked the T3SS with efficiency equal to or even less than that of other MAbs as single agents or as

combinations, but its activity led to increased phagocytic uptake. Polyclonal anti-LcrV was superior to BA5 in promoting phagocytosis and also was more efficient in protecting mice from pneumonic plague. Taken together, the data support a hypothesis whereby the pulmonary clearance of *Y. pestis* by antibodies requires both the neutralization of the T3SS and the simultaneous stimulation of innate signaling pathways used by phagocytic cells to destroy pathogens.

2.2 Introduction

Yersinia pestis, the etiologic agent of bubonic, pneumonic, and septicemic plague, has been responsible for more human death than any other bacterial pathogen [1]. Fortunately, naturally occurring cases of plague in humans are now uncommon, largely due to advances in basic sanitation and public awareness of infectious disease [2]. Nevertheless, the disease remains endemic in many areas of the world, and periodic human bubonic and, to a lesser extent, pneumonic plague cases appear each year. *Yersinia pestis* is believed to have evolved recently from *Yersinia pseudotuberculosis*, acquiring flea transmission and respiratory invasion properties through mobile genetic elements [3, 4]. The flea transmission cycle provides an opportunity for further evolution, because the bacteria reside in the nonsterile environment of the flea gut, where the formation of a biofilm provides an opportunity for horizontal gene exchange with other microbes [5]. Multidrug-resistant *Y. pestis* isolates have been recovered from human plague patients, suggesting that the bacteria do indeed continue to evolve mechanisms of survival in the mammalian host [6-8]. For these reasons, as well as for its potential use as a biological weapon, *Y. pestis* continues to be a significant public health concern and is a priority pathogen for the development of new vaccines and alternative therapeutics [2, 9].

There currently are no plague vaccines that are licensed for human use in the United States. The licensing of current candidates is likely to fall under the U.S. Food and Drug Administration's Animal Rule for the demonstration of

efficacy and potency due to a lack of naturally occurring human plague cases [10]. Thus, efficacy trials and the evaluation of vaccine potency in humans will be dependent on our ability to understand the molecular mechanism of protection. Current subunit vaccine candidates are formulated from two protective antigens, Fraction 1 (F1) and LcrV, which are undergoing extensive testing to satisfy the Animal Rule requirements [11-18]. Both antigens elicit a neutralizing antibody response that can be translated to passive antibody or even gene therapies [17-22]. These protective antibodies act directly on the bacteria and alter its interactions with innate immune cells such that the host clears the infection. T-cell responses also are believed to play an important role in host defense against *Yersinia pestis* [23, 24].

CaF1, or F1, is an abundant cell surface antigen of the type I pilin family that forms a capsule-like structure on *Y. pestis* at 37°C [25]. Although F1 appears to be antiphagocytic, it is not essential for virulence and thus would not contribute to immunity against *Y. pestis* mutant *caF1* [26, 27]. In contrast, LcrV is essential for all forms of plague due to its role in the type III secretion system (T3SS) [28-30]. LcrV is positioned on the surface of bacteria at 37°C, where it mediates the translocation of anti-host factors, collectively known as *Yersinia* outer proteins (Yops), whose antiphagocytic, cytolytic, and proapoptotic activities allow *Yersinia* to avoid being killed by the host's immune system [31, 32]. Polyclonal antibodies to recombinant LcrV (α-LcrV) can bind to this needle tip and lead to the inhibition of the T3SS and the phagocytosis of the bacteria [33-35]. However, it remains

controversial whether the direct inhibition of the T3SS by α-LcrV leads to phagocytosis or if the direct promotion of phagocytosis leads to the inhibition of the T3SS because it cannot function intracellularly [13, 36]. Three monoclonal antibodies (MAbs) have been independently cloned that can protect mice from bubonic and pneumonic plague . Although it is unclear whether each of these targets the same epitope, deletion studies of LcrV antigen suggest multiple protective epitopes exist [17, 37-39].

We were interested in developing antibody therapeutics and maximizing the potency of anti-LcrV therapy. In this work, we investigated the mechanism of protection from pneumonic plague to determine if the multivalent occupancy of antibody to LcrV improved protection. We found that antibodies that promoted phagocytosis directly were more potent at neutralizing pneumonic plague, although the inhibition of the T3SS alone led to partial protection. Only a single LcrV epitope led to antibodies that by themselves promoted uptake, while the multivalent occupation of antigen with MAbs did not increase either phagocytosis or protection. These data provide new insight into the mechanism of LcrV and support the use of assays that measure the phagocytic uptake of *Y. pestis* as correlates of immunity for the evaluation of plague vaccines.

2.3 Materials and Methods

Bacterial strains. All *Y. pestis* strains used were taken from frozen stocks and streaked for isolation onto heart infusion agar (HIA) plates. For pneumonic plague challenge, *Y. pestis* CO92 was plated on HIA supplemented with 0.005%

(v/v) Congo Red and 0.2% (w/v) galactose to verify the presence of the pigmentation locus [40]. Pigmented, isolated colonies then were inoculated in heart infusion broth (HIB) supplemented with 2.5 mM $CaCl_2$ and grown for 18 to 24 hours at 37°C, followed by dilution to the desired dose in sterile phosphate-buffered saline (PBS). All experiments with *Y. pestis* CO92 were performed in compliance with Select-Agent regulations and in accordance with the guidelines outlined by the University of Missouri Institutional Biosafety Committee. For *in vitro* assays with macrophages, *Y. pestis* KIM D27, a nonpigmented strain originally isolated by R. Brubaker [41] was grown routinely fresh from frozen stock on HIA, followed by aerobic growth at 27°C in HIB overnight prior to use in experiments. An isogenic derivative of KIM D27 lacking the 70-kb virulence plasmid that encodes the T3SS was generated in our laboratory by introducing the suicide vector pCVD442 into pCD1, followed by selection for the loss of both; the resulting mutant strain was confirmed by PCR analysis and Western blotting [42]. The *Escherichia coli* strain JM109 (a gift from George Stewart) or DH5α was used routinely for cloning expression plasmids; *E. coli* BL21 (Novagen, Madison, WI) was used for protein purification. Ampicillin (Amp) was used at 100 μg/ml for experiments involving recombinant plasmids.

Plasmids. pNE071 expresses DsRed from the isopropyl-β-D-thiogalactopyranoside (IPTG)-inducible promoter on a pUC18 plasmid backbone. The DsRed gene was amplified from the pDsRed-Monomer vector (Clontech, Mountain View, CA) with primers that included NdeI and BamHI sites for cloning.

The *lacI*^{q} gene and downstream *tac* promoter originally were amplified from pGEX-2TK (GE Healthcare, Buckinghamshire, UK) [43] with abutted EcoRI and NdeI restriction sites, followed by being cloned into pDsRed Monomer vector such that these sequences replaced the endogenous promoter.

Production of rabbit antibody. Recombinant LcrV (rLcrV) was overexpressed in *E. coli* BL21 and purified as previously described [38]. rLcrV then was used as an antigen for the wiffle ball immunization of New Zealand White rabbits [44]. All experiments employing polyclonal α-LcrV came from the same immunized animal. Rabbit serum containing α-LcrV antibodies was applied to a Protein A column and purified by following the manufacturer's protocol (Sigma, St. Louis, MO). Samples then were applied to a PD-10 desalting column (GE Healthcare, Buckinghamshire, United Kingdom) and eluted in PBS. Total immunoglobulin G (IgG) was quantified using bovine IgG as a standard in a bicinchoninic acid protein assay (Pierce, Rockford, IL).

Cloning of LcrV MAb E11. All monoclonal antibody (MAb) clones except E11 were generated against recombinant LcrV in immunized BALB/c mice and are described elsewhere [45]. For the cloning of MAb E11, amino acids 241 to 270 of LcrV were chemically synthesized as a peptide conjugated to keyhole limpet hemocyanin (Biosynthesis, Inc., Lewisville, TX). This peptide conjugate was used by the University of Chicago Fitch Monoclonal Antibody Facility to immunize BALB/c mice for cloning antibodies with specificity to rLcrV. Positive clones were selected by screening for binding to rLcrV by enzyme-linked immunosorbent

assay (ELISA), and the MAb (E11) with greatest relative affinity for rLcrV was isotyped and selected for analysis.

Purification of MAbs. MAbs were produced and purified according to standard methods by the University of Chicago Fitch Monoclonal Antibody Facility. Briefly, B-cell hybridomas expressing monoclonal antibodies were grown either in culture or in a bioreactor in serum-free medium. Antibody was harvested from the culture supernatants and purified using Protein G affinity chromatography. MAbs were eluted in 0.1 M glycine hydrochloride, pH 2.6, and dialyzed in PBS for 24 h with two buffer exchanges. The MAb concentration was determined by Bradford assay using bovine IgG for a standard curve. MAbs were stored at −80°C.

ELISA. rLcrV was used as the capture antigen for both ELISA and competitive ELISA experiments. Ninety-six-well plates were coated with 100 μg rLcrV and blocked with 1% (w/v) bovine serum albumin (BSA) in wash buffer (0.01% (v/v) Tween in PBS). Wells then were probed with LcrV MAb for 2 h, followed by detection with phosphatase-labeled goat anti-mouse IgA+IgG+IgM (H+L) (KPL, Gaithersburg, MD) diluted 1:2,500 in blocking buffer and *p*-nitrophenyl phosphate (PNPP) substrate (Pierce, Rockford, IL) according to the manufacturer's recommendations. Absorbance at 405 nm was measured on a FLUOstar Optima plate reader (BMG Labtech, Durham, NC).

Competitive ELISA. MAbs were biotinylated with EZ-Link NHS-LC-LC-biotin (Pierce, Rockford, IL) per the manufacturer's recommendations. Ninety-six-well plates were coated and blocked as described above and then probed for 2 h with

1.0 µg biotinylated MAb mixed with unlabeled MAbs in increasing concentrations. To detect bound biotinylated MAb, 200 µl of streptavidin conjugated to horse radish peroxidase (Pierce, Rockford, IL) and diluted 1:7,500 in blocking buffer was added to each well for 1 h, followed by the addition of 100 µl *o*-phenylenediamine dihydrochloride (OPD) substrate prepared per the manufacturer's protocol for 30 min (Pierce, Rockford, IL). The reaction was stopped by the addition of 100 µl 1N HCl, and absorbance was measured at 490 nm.

Caspase-3 assay. The caspase-3 protocol was modified from a previously described assay for measuring the antibody blocking of the T3SS by the inhibition of caspase-3 activation [33]. RAW 264.7 macrophages (approximately 1×10^6) were plated in a 12-well culture dish in Dulbecco's modified Eagle's medium (DMEM) plus 5% (v/v) fetal bovine serum (FBS) at a confluence of 80 to 90%. Overnight cultures of *Y. pestis* KIM D27 and an isogenic derivative lacking pCD1 were diluted to an optical density at 600 nm (OD_{600}) of 0.05 in HIB and incubated at 28°C for 2 h, followed by 1 h of incubation at 37°C to prime for type III secretion. One milliliter of bacteria was centrifuged, washed with PBS, and resuspended in DMEM plus 5% (v/v) FBS. MAbs (100 µg per ml PBS) or an equal volume of PBS were preincubated with 50 µl bacteria in DMEM plus 5% (v/v) FBS at 37°C in a total volume of 100 µl. The preincubated cultures then were added to macrophages (at a multiplicity of infection [MOI] of 10:1), and the plate was centrifuged at 450 rpm (40 × *g*) for 5 min. Infected cells were allowed

to incubate at 37°C under 5% CO_2 for 3.5 h. To detect activated caspase-3, cells were scraped off the plate, washed with PBS, and lysed following one freeze-thaw cycle and ice incubation in lysis buffer (EnzChek caspase-3 assay; Invitrogen, Carlsbad, CA). The detection of activated caspase-3 proceeded by following the manufacturer's protocol.

Phagocytosis assay. The protocol for the phagocytosis assay was adapted from a recently described fluorescence-based gentamicin protection assay for quantifying phagocytosis in macrophages [46]. Wild-type *Y. pestis* KIM D27 and isogenic pCD1$^-$ carrying pNE071 were grown overnight at 28°C in HIB supplemented with Amp (HIB + Amp). RAW 264.7 macrophages were biotinylated with EZ-Link NHS-LC-LC-Biotin (Pierce, Rockford, IL), and then 1 × 10^6 cells were plated on poly-L-lysine (Sigma, St. Louis, MO)-coated coverslips in DMEM-5% (v/v) FBS. Bacterial cultures were diluted to an OD_{600} of 0.05 and grown in HIB + Amp for 2 h at 28°C and for 1 h at 37°C. One milliliter of the bacterial culture was centrifuged, washed once with PBS, and resuspended in DMEM-5% (v/v) FBS. For an MOI of 20, 100 µl of bacteria then were added to DMEM-5% (v/v) FBS and 100 µg total antibody or PBS in a final volume of 600 µl and were incubated for 1 h at 37°C. Suspensions were applied to macrophages in a final volume of 2 ml, spun at 450 rpm (40 × *g*) for 5 min, and then incubated for 30 min at 37°C under 5% CO_2. At this time, gentamicin (100 µg/ml) and IPTG (100 mM) were added, and cells were incubated for an additional 2 h. Cells then were fixed with 4% (w/v) paraformaldehyde and stained with 4′,6′-diamidino-2-

phenylindole (DAPI) and streptavidin conjugated to Alexa Fluor 488 (Invitrogen, Carlsbad, CA). Z-stacked images were acquired on an Olympus IX70 inverted widefield fluorescent microscope from at least four random fields of 50 macrophages, and bacteria were counted in single-blind fashion. Representative images were acquired using Zeiss LSM 510 META NLO confocal laser-scanning microscopy.

Animals. Six- to 8-week-old female C57BL/6 mice (16 to 20 g; Charles River Laboratories, Wilmington, MA) were used for plague challenge experiments. During challenge, mice were maintained in Select-Agent-approved containment facilities at the University of Missouri in accordance to the guidelines outlined by the institutional animal care and use committee. All infected mice were monitored regularly by daily weighing and the assignment of health scores. Animals were identified as moribund if they exhibited severe neurologic signs and were then euthanized. Those that survived to the end of the 14-day observation period were euthanized by CO_2 asphyxiation, followed by cervical dislocation, methods that are approved by the American Veterinary Medical Association guidelines on euthanasia.

Pneumonic plague challenge. Bacteria were grown as described above at 37°C then diluted in sterile PBS to 6,000 CFU/0.02 ml (corresponding to 20 50% lethal doses (LD_{50} [47-49]) immediately prior to use in challenge experiments. Groups of five mice were given antibody (400 µg/0.4 ml) or PBS by intraperitoneal injection 60 min prior to challenge. All animals were lightly anesthetized by

isoflurane inhalation prior to intranasal infection with *Y. pestis* CO92. Animals were observed for recovery from anesthesia and returned to housing.

Statistical analysis. One-way analysis of variance (ANOVA) was used to evaluate the statistical significance of caspase-3 data. Dunnett's test was used after ANOVA to account for type I errors, and multiple comparisons and the reported *p*-values are the combined result of both tests. The unpaired Student's *t*-test was used to evaluate the statistical significance of data collected from gentamicin protection assays. The log-rank test was used to evaluate the statistical significance of survival and mean time to death (MTTD).

2.4 Results

2.4.1. Characterization of Antibodies that Neutralize Yersinia pestis

We recently generated a library of MAbs following the vaccination of BALB/c mice with rLcrV. Within this library, six linear peptide epitopes were represented, with several others binding what appears to be one or more conformational epitopes (O. Schneewind, personal communication). In addition, we cloned a seventh MAb (E11) against a peptide of LcrV amino acids 241 to 270 conjugated to Keyhole limpet hemocyanin. This epitope was not represented in our original library, yet deletion studies suggested that this is a neutralizing epitope [38]. We were interested in developing a multivalent LcrV MAb therapy as a postexposure treatment option and sought to identify MAbs that neutralized LcrV function. Representative MAbs from each of the seven epitopes, all of which were of the IgG1 isotype, were selected and measured for relative affinity to

purified LcrV in an ELISA. Initial tests to determine binding titers between MAb AH1 and BA5 and rLcrV were performed, and 7.5 µg antibody per ml of PBS reproducibly resulted in binding at the peak of the titer curve (data not shown). Therefore, this amount of MAb was chosen to characterize the relative binding of all of the MAbs with antigen rLcrV. Although there were various degrees of binding between MAb and antigen, all MAbs had detectable binding to LcrV at 7.5 µg/ml (Figure. 2.1).

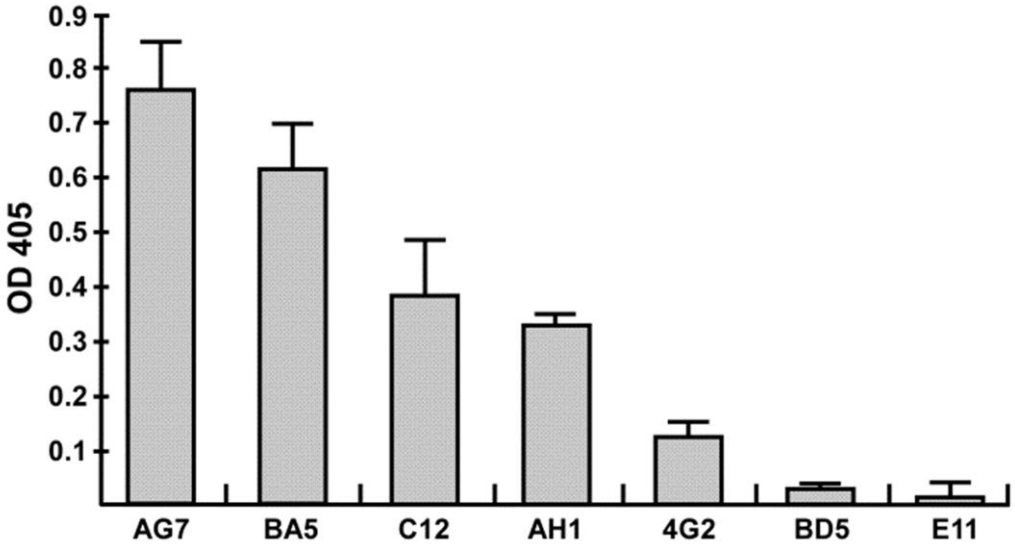

Figure 2.1. LcrV MAbs show similar binding to rLcrV. Ninety-six-well plates were coated with 100 µg rLcrV and probed with 7.5 µg MAb per ml PBS, followed by detection with phosphatase-labeled goat anti-mouse Ig antibody. Error bars represent the standard deviations from three separate assays.

Single MAbs initially were characterized for their ability to block the type III injection of Yops *in vitro*. For this analysis, we modified a caspase-3 assay that currently is used to evaluate the potency of LcrV vaccines [33, 50]. Wild-type *Y. pestis* KIM D27 injects effector Yops, one of which, YopJ, causes the activation of caspase-3 and the apoptosis of macrophages [51]. Isogenic *Y. pestis* lacking

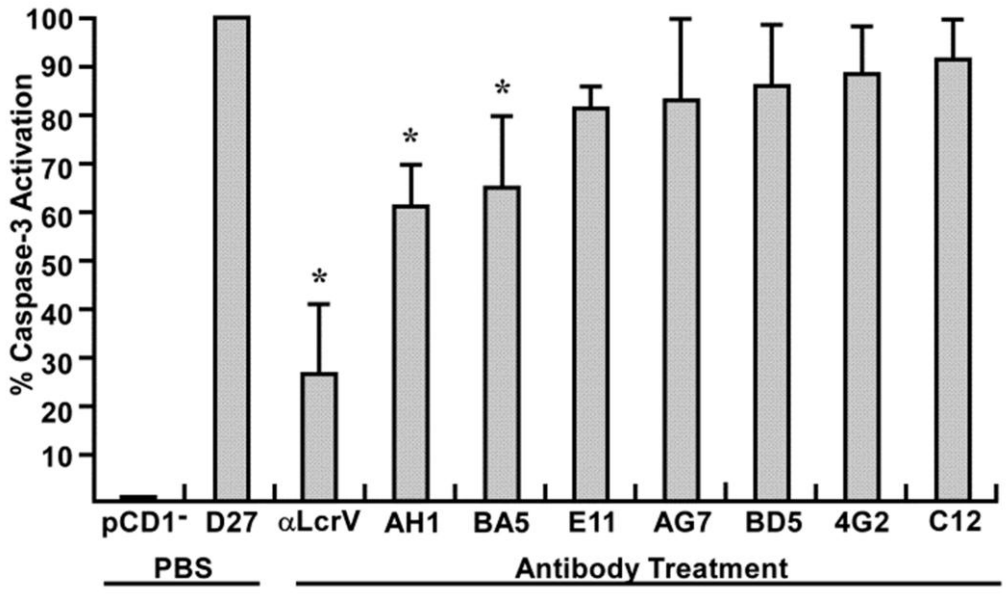

Figure 2.2. MAbs BA5 and AH1 block injection of YopJ into macrophages. One hundred micrograms of antibody or an equivalent volume of PBS was preincubated with *Y. pestis* KIM D27 at 37°C for 1 hour before infecting RAW 264.7 macrophage-like cells. pCD1⁻*Y. pestis* KIM D27 treated with PBS was used as a control for no injection. Pretreated bacteria then were added to macrophages at an MOI of 10. Caspase-3 activation was measured 3.5 hours after infection. Error bars represent the standard deviations from the means from at least six independent experiments. Statistical significance compared to results for untreated KIM D27 was evaluated by one-way ANOVA. *, p <0.05.

pCD1, which encodes the T3SS, are unable to activate caspase-3. For each experiment, both wild-type and pCD1⁻ *Y. pestis* KIM D27 strains were included and set to 100 and 0% caspase-3 activation, respectively. Initial tests were performed to monitor the concentration-dependent increase in antibody activity in this assay using 10 to 200 µg of purified polyclonal and monoclonal anti-LcrV. Results showed peak neutralization activity at 100 µg of antibody, and this amount was used to collect the data described below (data not shown). Preincubation with 100 µg of rabbit polyclonal α-LcrV blocked Yop injection, as only 27% caspase activation was observed (p <0.05 compared to results for the untreated wild-type infection of macrophages) (Figure. 2.2). However, two MAbs,

BA5 and AH1, were able to block injection, averaging 68 (p <0.05) and 61% (p <0.05), respectively, of the levels of the untreated control. Reducing the amount of BA5 or AH1 by half (50 µg) also reduced the inhibition of caspase activation, indicating that these MAbs blocked the T3SS in a concentration-dependent manner (data not shown). All other MAbs were unable to block the T3SS.

2.4.2. Identification of LcrV MAb Combinations that Exhibit Increased Activity against the T3SS

The multivalent occupancy of antigen by antibodies may lead to improved or even synergistic neutralizing activity. We tested this first by predicting which combinations of MAbs were likely to be capable of occupying LcrV simultaneously. For this, we used VMD 1.8.6 software [52] and the published structural information of LcrV [53]. This approach predicted that both BA5 and AH1 could bind antigen simultaneously. MAb E11 was predicted to bind an epitope that overlapped BA5, thus these two MAbs likely are unable to bind LcrV together. Both MAbs AG7 and 4G2 were predicted to bind antigen when both BA5 and AH1 were occupying LcrV. MAbs BD5 and C12 were predicted to be unable to occupy antigen with BA5 and AH1.

We tested combinations of MAbs, present in equal amounts that added up to 100 µg, in the caspase assay, and the results largely supported the structural predictions. Combining BA5 and AH1 led to better inhibition of caspase than using either MAb alone, with 51% blocking (p <0.05) compared to that of the untreated control (Figure 2.3). In contrast, E11 and BA5 did not improve the

blocking of the T3SS compared to that of untreated bacteria (78%, p >0.05), suggesting that these MAbs indeed are unable to bind antigen together. Double and triple combinations involving MAb BA5 and/or AH1 were tested, and the combination of BA5, AH1, and 4G2 was selected because it appeared to reproducibly provide the greatest increase in the neutralization of LcrV function (55% caspase activation; p <0.05).

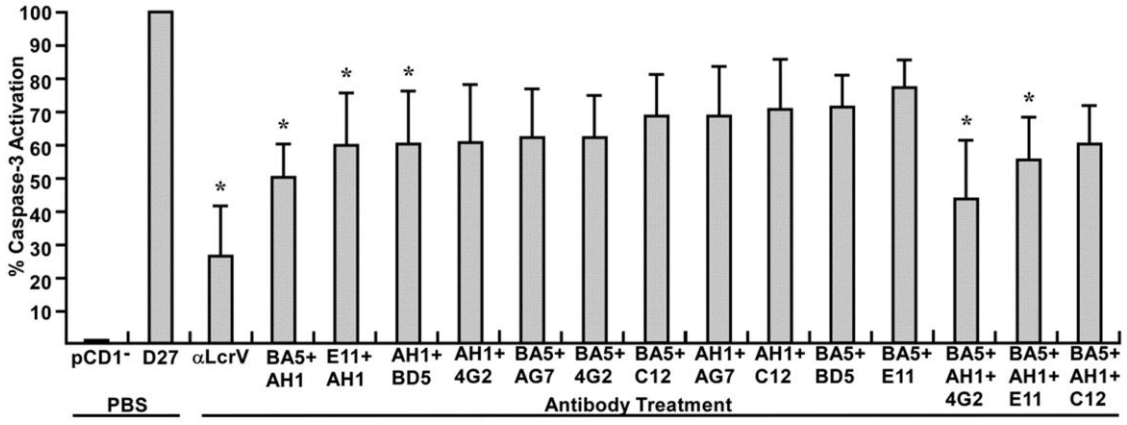

Figure 2.3. Multivalent antibody binding to LcrV results in the increased blocking of the T3SS. MAbs that were mixed in equal amounts, totaling 100 µg antibody, or an equivalent volume of PBS were preincubated with *Y. pestis* KIM D27 at 37°C for 1 hour before infecting RAW 264.7 macrophage-like cells at an MOI of 20. The infection of macrophages with pCD1^{-} *Y. pestis* KIM D27 treated with PBS was used as a control for no injection. Caspase-3 activation was measured 3.5 hours after infection. Error bars represent the standard deviations from the means from at least three independent experiments. Statistical significance compared to results for untreated KIM D27 was evaluated by one-way ANOVA. *, P < 0.05.

We confirmed that BA5, AH1, and 4G2 could bind LcrV together in a competitive ELISA. When BA5 was biotinylated, unlabeled BA5 could compete for the binding of rLcrV, but neither AH1 nor 4G2 was able to compete (Figure. 2.4A). Likewise, when AH1 was biotinylated, unlabeled AH1, but not BA5 or 4G2, was able to compete for the binding of rLcrV (Figure. 2.4B). Equal amounts of these MAbs were tested by ELISA at 0.1 µg total antibody per ml of

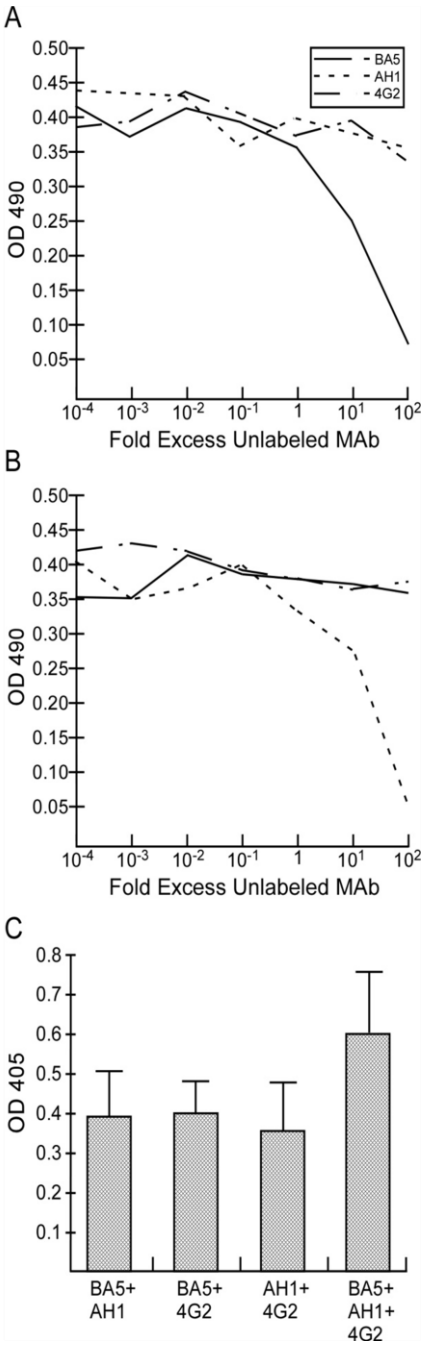

Figure 2.4. BA5, AH1, and 4G2 can bind rLcrV simultaneously. (A and B) Plates were coated with rLcrV and 1 µg biotinylated MAb BA5 (A) or AH1 (B), and increasing amounts of unlabeled MAb were allowed to bind. Bound biotinylated MAbs were detected with horseradish peroxidase-conjugated streptavidin. Competition for binding rLcrV was assessed by the displacement of biotinylation from the antigen. (C) Ninety-six-well plates were coated with 100 µg rLcrV and probed with 0.1 µg total MAb in equal concentrations, followed by detection with phosphatase-labeled goat anti-mouse Ig antibody. Error bars represent the standard deviations from the means from three separate assays.

PBS, and we found that each double combination, as well as the triple combination, appeared to bind antigen with similar affinity (Figure 2.4C). Taken together, these data indicate that MAb combinations that simultaneously bind LcrV result in the improved blocking of Yop injection compared to that of the single-MAb occupancy of antigen.

2.4.3. Multivalent MAb Occupancy of LcrV does not lead to Improved Protection from Pneumonic Plague

To compare the efficacy of individual MAbs to those of combinations of MAbs *in vivo*, a pulmonary model of infection was used. In this model, C57BL/6 mice were given 400 μg antibody by intraperitoneal injection 60 min prior to intranasal challenge with approximately 6,000 CFU *Y. pestis* CO92, which corresponds to 15-20 LD_{50} [49]. This antibody dose was chosen because it consistently led to full protection in this model with polyclonal α-LcrV, whereas 200 μg was only partially protective (data not shown). Control mice given PBS succumbed to disease rapidly, with 80% mortality and an MTTD of 5.1 days (Figure 2.5 and Table 1). In contrast, mice given purified rabbit polyclonal LcrV antibody were fully protected and survived challenge. All mice given 4G2 were susceptible to disease and died with an MTTD of 4.6 days (p >0.05 compared to results with an untreated control), suggesting that, similarly to published reports, LcrV MAbs that are unable to block the T3SS are not protective [33]. AH1 treatment protected 30% of mice upon challenge with no significant increase in the MTTD, but this was not a statistically significant increase in protection

compared to results for untreated mice (p >0.05 by log-rank test). Strikingly, however, BA5 was highly protective, providing 90% survival and a significant increase in time to death p <0.05 compared to results for the untreated control). Thus, even though AH1 and BA5 appeared equally capable of blocking the T3SS in the caspase assay, their protective properties differed substantially in the pulmonary infection model.

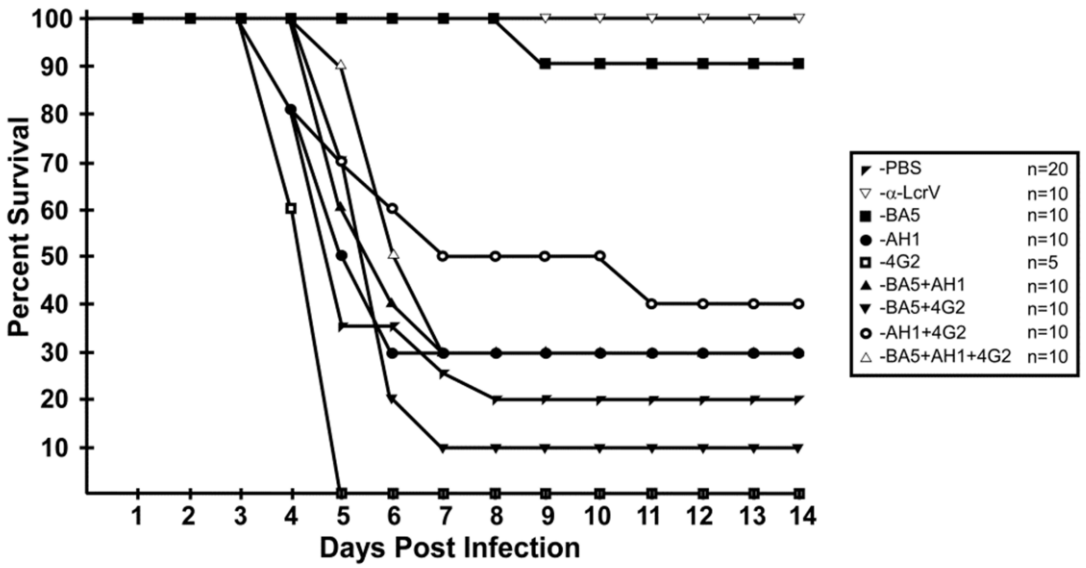

Figure 2.5. Multivalent occupancy of LcrV does not increase protection from pulmonary challenge by*Yersinia pestis*. C57BL/6 mice were given 400 µg total antibody by intraperitoneal injection 60 min prior to intranasal infection with 20 LD_{50} (6,000 CFU) *Y. pestis* CO92, and survival was monitored for a 14-day period. Data shown were generated in two independent challenges, with five mice per treatment group (n = 10 total) with the exception of 4G2, which was tested in only one experiment (n = 5 for 4G2). Statistical significance was evaluated by the log-rank test.

When 200 µg each of BA5 and AH1 was used as a therapeutic, instead of enhancing the neutralization of bacteria, as would be expected based on the caspase data, reduced protection was seen. Likewise, combining BA5 with 4G2 or with both AH1 and 4G2 resulted in reduced protection. Interestingly, an AH1

and 4G2 combination appeared to lead to partial protection (40%), although this protection was not statistically significant (p >0.05 compared to results for untreated controls). Thus, the single-dose administration of BA5 alone was the most potent therapy. This result is contrary to the data obtained from the caspase-3 assay, where AH1 was equal to BA5 in potency and combinations of these MAbs were superior. We therefore decided to investigate the potency of these antibodies in promoting phagocytosis directly to determine if this correlated with the protection data.

2.4.4. Antibody Protection of Pneumonic Plague Correlates with Opsonophagocytosis of Bacteria

Previous work on the mechanism of anti-LcrV on *Y. pestis* virulence has demonstrated that polyclonal antibodies may both neutralize the function of the T3SS and directly stimulate phagocytosis [33-35]. We therefore decided to quantify the ability of LcrV MAbs to stimulate the phagocytosis of bacteria by macrophages and to determine if this activity correlates with the protection we observed *in vivo*. *Y. pestis* carrying a plasmid expressing DsRed under an IPTG-inducible promoter was used in a microscopy-based gentamicin protection assay [46]. Briefly, bacteria were preincubated with PBS or anti-LcrV at 37°C prior to infecting RAW 264.7 macrophage-like cells. Phagocytosis proceeded for 30 min, and then gentamicin was added to kill any remaining extracellular bacteria. When only intracellular bacteria remained, IPTG was added to induce DsRed expression. The average number of intracellular bacteria, identified by red

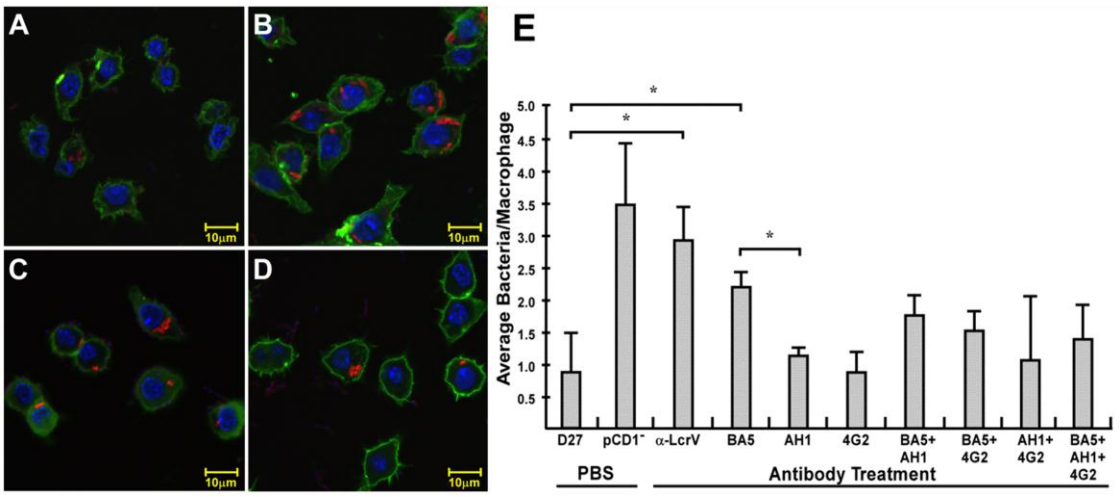

Figure 2.6. Antibodies that protect against pneumonic plague effectively opsonize bacteria. IPTG-inducible DsRed-expressing KIM D27 and KIM D27/pCD1⁻strains were incubated with 100 μg total antibody for 1 h and applied to RAW 264.7 macrophage-like cells at an MOI of 20. After 30 min of phagocytosis, gentamicin was added to kill extracellular bacteria, and IPTG was applied to samples for 2 h. Cells then were fixed and examined using confocal laser-scanning microscopy for representative images (A to D) or Z-stacking widefield fluorescent microscopy for quantification (E). Bacteria were counted in 50 macrophages from four random fields, and data were collected from at least three independent experiments. Statistical significance was evaluated using the unpaired Student's *t*-test. BA5 and polyclonal anti-LcrV treatment resulted in statistically significant increases in phagocytosis compared to that of PBS-treated controls (*, $p < 0.05$), while all other MAb treatments were not statistically different from PBS-treated controls.

fluorescence, was determined after visualization by microscopy (Figure. 2.6E). These data were collected from at least three independent experiments, each of which was counted blindly, with 50 macrophages counted in four sections of each slide. The phagocytosis index (PI) was calculated as the number of intracellular bacteria divided by the number of macrophages. Untreated wild-type KIM D27 bacteria often were found within macrophages, and a calculated PI of 1.0 was observed (Figure. 2.6A and E). In contrast, most of the macrophages infected with *Y. pestis* pCD1⁻ carried multiple bacteria, and a PI of 3.9 was observed (Figure. 2.6B). These data agree with previously published results and

show that bacteria that are unable to perform type III secretion are readily phagocytosed by macrophages [54].

TABLE 2.1. Summary of *in vitro* and *in vivo* activities of LcrV Antibodies

Treatment	% Survival[a]	MTTD	% Caspase-3 Activation[c]	Phagocytosis index[e]
PBS	20 (4/20)	5.1	100	0.95
Polyclonal	100 (10/10)[b]	n/a	26.6 (± 15.2)[d]	2.92[f]
BA5	90 (9/10)[b]	9.0	67.5 (±13.6)[d]	2.04[f]
AH1	30 (3/10)	5.0	61.4 (±9.0)[d]	1.12
4G2	0 (0/5)	4.6	87.2 (±10.6)	0.74
BA5+AH1	30 (3/10)	5.6	50.6 (±9.6)	1.39
BA5+4G2	10 (1/10)	5.8	63.4 (±12.0)	1.50
AH1+4G2	40 (4/10)	6.2	61.5 (±17.2)	1.21
BA5+AH1+4G2	30 (3/10)	6.1	55.8 (±12.7)	1.38

a. Protection from intranasal challenge with 20LD_{50} *Y. pestis* CO92; collected from two independent trials.
b. p <0.05 compared with PBS treated controls as determined by Log-Rank test.
c. % of untreated bacteria; average of 4 independent experiments with samples run in duplicate.
d. p <0.05 compared with PBS treated controls as determined by ANOVA.
e. Data collected from two independent experiments, counting 4 fields of 50 macrophages in each experiment.
f. p <0.05 compared with PBS treated controls as determined by unpaired Student's *t*-test

Wild-type bacteria coincubated with LcrV polyclonal antibodies resulted in increased uptake compared to that of untreated bacteria, with a PI of 2.9 (Figure. 2.6C). MAb BA5 also was able to promote uptake compared to that of the untreated control, with an average PI of 2.0 (P = 0.024) (Figure. 2.6D), while MAb AH1 was unable to promote phagocytosis more than the untreated control (PI of 1.1; P = 0.609), even though it is able to block the T3SS. Combinations of MAb BA5 with either AH1 or 4G2 reduced the PI from that of MAb BA5 alone, suggesting that reducing the amount of BA5 used in the assay reduced phagocytosis, and this could not be rescued by the multivalent binding of the other MAbs. Compared to the *in vivo* challenge results, MAb activity in the

phagocytosis assay closely matches observed activity during the pulmonary infection of mice with fully virulent *Y. pestis*. Taken together, these data suggest that neutralizing LcrV antibodies not only inhibit the T3SS but also directly promote phagocytosis, and both activities are required for protection from pneumonic plague.

2.5 Discussion

Vaccines formulated with F1 and LcrV appear to be highly effective in preventing plague. However, there is concern that their use by American civilians for biodefense may not be necessary or desired by the public, whose current concerns regarding vaccine safety may override their risk of exposure to *Y. pestis*. Because the antibody response strongly correlates with immunity to plague, we have been investigating defined antibody therapeutics as alternatives to vaccination. In this work, we studied defined, multivalent antibodies to LcrV with strong neutralizing activity *in vitro* as a preventive treatment for pneumonic plague in mice. Although LcrV MAb combinations could increase the neutralization of the T3SS, these MAbs by and large did not improve protection. Protective MAb BA5 exhibited biological activity similar to that of polyclonal anti-LcrV, and it was the only MAb treatment able to promote phagocytosis. Thus, it appears that antibodies must block the T3SS and stimulate phagocytic uptake to prevent rapid bacterial growth in the lung. Moreover, combinatorial MAb therapy targeting multiple defined cell surface antigens or elements of the T3SS that

enhance either phagocytic uptake or the inhibition of the T3SS may prove potent against pulmonary *Y. pestis* infections [55-57].

We described, for the first time, antibodies that could block the T3SS without promoting phagocytic uptake, allowing us to make direct comparisons of the contributions of these distinct functions. Although it remains difficult to determine whether BA5 activity in the T3SS assay is directly or indirectly caused by phagocytosis, it is likely that the binding of this antibody to the needle tip does inhibit the T3SS. Interestingly, protective LcrV MAb 7.3 was shown to effectively block the T3SS, which was believed to have an indirect impact on phagocytosis [13, 33, 58]. Recently, LcrV amino acid 255 was shown to be critical for MAb 7.3 binding, suggesting that MAb 7.3 and BA5 bind a similar epitope, while AH1 is distinct [59]. The comparison of antigen binding properties and different antibody isotypes might yield information about the true number of neutralizing epitopes as well as methods and formulations that can enhance their activity. It is conceivable that only a single LcrV epitope generates antibodies that both block the T3SS and stimulate phagocytosis and, therefore, are protective. The concentration of these antibodies in immune sera generally indicates protective immunity; however, the multivalent occupancy achieved by polyclonal antibody binding, which was highly active in both *in vitro* assays, may be protective without the development of high-titer antibody to the neutralizing epitope(s). Additional analyses comparing antigen binding between protective LcrV MAbs as well as

their *in vitro* activities ultimately might lead to the development of ELISA-based methods for correlates of protection.

Our results support the hypothesis that the antibody clearance of *Y. pestis* during respiratory infections is dependent on the activation of phagocytic cells such as macrophages and neutrophils, which perform the major defense against the acute infection of the mammalian lung [60-63]. Recently, it was shown that although gamma interferon and tumor necrosis factor alpha are important systemic host responses to plague, they are dispensable for antibody-induced immunity. This is a surprising result, because these cytokines broadly stimulate both innate and adaptive immune cells [64]. Future experiments will aim to understand key signaling pathways for the successful host defense of the mammalian lung against virulent *Yersinia pestis*.

2.6 Acknowledgements

This work was supported by the NIH/NIAID Region VII Midwest Regional Center of Excellence for Biodefense and Emerging Infectious Diseases (U54 AI157160) and the Region V Great Lakes Regional Center of Excellence for Biodefense and Emerging Infectious Diseases (U54 AI157153). N.A.E. is supported by a Cell and Molecular Biology Training grant (T32 GM008396).

We are grateful to Olaf Schneewind for the use of the anti-LcrV monoclonal antibody library, to Greg Purdy for the RAW 264.7 cell line, and to Sherrie Neff for excellent technical assistance with rabbit immunization and harvesting of immune sera. In addition, we thank Craig Franklin for help with

statistical analyses, Ami Patel for the quantification of microscopy, Hanni Lee-Lewis for the characterization of the peptide MAbs, and members of our laboratory for technical assistance with the biosafety level 3 experiments. The LcrV MAbs were cloned and produced by the GLRCE Animal Research and Immunology Core/Fitch Monoclonal Antibody Facility at the University of Chicago. Microscopy images were collected at the Molecular Cytology Core at the University of Missouri.

2.7 References

1. Fetherston, J. and R. Perry, *Yersinia pestis -- etiologic agent of plague.* Clin Microbiol Rev, 1997. **10**(1): 35-66.

2. Inglesby, T., et al., *Plague as a biological weapon: medical and public health management. Working group on civilian biodefense.* JAMA, 2000. **283**(17): 2281-90.

3. Achtman, M., et al., *Yersinia pestis, the cause of plague, is a recently emerged clone of Yersinia pseudotuberculosis.* Proc Natl Acad Sci, 1999. **96**: 14043-8.

4. Chain, P., et al., *Insights into the evolution of Yersinia pestis through whole-genome comparison with Yersinia pseudotuberculosis.* Proc Natl Acad Sci, 2004. **101**(38): 13826-31.

5. Hinnebusch, B., et al., *High-frequency conjugative transfer of antibiotic resistance genes to Yersinia pestis in the flea midgut.* Mol Microbiol, 2002. **2**: 349-54.

6. Galimand, M., et al., *Multidrug resistance in Yersinia pestis mediated by a transferable plasmid.* New Eng J Med, 1997. **337**(10): 677-80.

7. Guiyoule, A., et al., *Transferable plasmid-mediated resistance to streptomycin in a clinical isolate of Yersinia pestis.* Emerg Inf Dis, 2001. **7**(1): 43-8.

8. Welch, T., et al., *Multiple antimicrobial resistance in plague: An emerging public health risk.* PLoS One, 2007. **2**(3): 1-6.

9. Peters, N., et al., *The research agenda of the National Institute of Allergy and Infectious Diseases for antimicrobial resistance.* J Infect Dis, 2008. **197**(8): 1087-93.

10. Food and Drug Administration, H., *New drug and biological drug products; evidence needed to demonstrate effectiveness of new drugs when human*

efficacy studies are not ethical or feasible. Final rule. Fed Regist, 2002. **67**(105): 37988-98.

11. Williamson, E., et al., *A single dose sub-unit vaccine protects against pneumonic plague.* Vaccine, 2001. **19**: 566-71.

12. Williamson, E., et al., *Human immune response to a plague vaccine comprising recombinant F1 and V antigens.* Infect Immun, 2005. **73**(6): 3598-608.

13. Williamson, E., et al., *Immunogenicity of the rF1+rV vaccine for plague with identification of potential immune correlates.* Microb Path, 2007. **42**(1): 11-21.

14. Heath, D., et al., *Protection against experimental bubonic and pneumonic plague by a recombinant capsular F1-V antigen fusion protein vaccine.* Vaccine, 1998. **16**(11): 1131-7.

15. Andrews, G., et al., *Protective efficacy of recombinant Yersinia outer proteins against bubonic plague caused by encapsulated and nonencapsulated Yersinia pestis.* Infect Immun, 1999. **67**(3): 1533-7.

16. Welkos, S., S. Norris, and J. Adamovicz, *Modified caspase-3 assay indicates correlation of caspase-3 activity with immunity of nonhuman primates to Yersinia pestis infection.* Clin Vaccine Immunol, 2008. **15**(7): 1134-7.

17. Cornelius, C., et al., *Immunization with recombinant V10 protects cynomolgus macaques from lethal pneumonic plague.* Infect Immun, 2008. **76**(12): 5588-97.

18. Anderson, D., et al., *Pneumonic plague pathogenesis and immunity in Brown Norway rats.* Am J Path, 2009. **174**(3): 910-21.

19. Motin, V., et al., *Passive immunity to yersiniae mediated by anti-recombinant V antigen and protein A-V antigen fusion peptide.* Infect Immun, 1994. **62**(10): 4192-201.

20. Anderson, G., et al., *Protection of mice from fatal bubonic and pneumonic plague by passive immunization with monoclonal antibodies against the F1 protein of Yersinia pestis.* Am J Trop Med Hyg, 1997. **56**(4): 471-3.

21. Hill, J., et al., *Regions of Yesinia pestis V antigen that contribute to protection against plague identified by passive and active immunization.* Infect Immun, 1997. **65**(11): 4476-82.

22. Sofer-Podesta, C., et al., *Adenovirus-mediated delivery of an anti-V antigen monoclonal antibody protects mice against a lethal Yersinia pestis challenge.* Infect Immun, 2009. **77**(4): 1561-8.

23. Parent, M., et al., *Yersinia pestis V protein epitopes recognized by CD4 T cells.* Infect Immun, 2005. **73**(4): 2197-204.

24. Parent, M., et al., *Gamma Interferon, Tumor Necrosis Factor Alpha, and Nitric Oxid Synthase 2, key elements of cellular immunity, perform critical protective functions during humoral defense against lethal pulmonary Yersinia pestis infection.* Infect Immun, 2006. **74**(6): 3381-6.

25. Ben-Efraim, S., M. Aronson, and L. Bichowsky-Slomnicki, *New antigenic component of Pasteurella pestis formed under specific conditions.* J Bacteriol, 1961. **81**: 704-14.

26. Friedlander, A., et al., *Relationship between virulence and immunity as revealed in recent studies of the F1 capsule of Yersinia pestis.* Clin Infect Dis, 1995. **21**(supp 2): S178-81.

27. Du, Y., R. Rosqvist, and A. Forsberg, *Role of fraction 1 antigen of Yersinia pestis in inhibition of phagocytosis.* Infect Immun, 2002. **70**(3): 1453-60.

28. Skrzypek, E. and S. Straley, *Differential effects of deletions in lcrV on secretion of V antigen, regulation of the low-Ca^{2+} response, and virulence of Yersinia pestis.* J Bacteriol, 1995. **177**(9): 2530-42.

29. Quenee, L., et al., *Yersinia pestis caf1 variants and the limits of plague vaccine protection.* Infect Immun, 2008. **76**(5): 2025-36.

30. Cornelis, G., *The Type III injectisome.* Nat Rev Microbiol, 2006. **4**(11): 811-25.

31. Sarker, M., et al., *The Yersinia Yop virulon: LcrV is required for extrusion of the translocators YopB and YopD.* J Bacteriol, 1998. **180**(5): 1207-14.

32. Mueller, C., et al., *The V-antigen of Yersinia forms a distinct structure at the tip of the injectisome needle.* Science, 2005. **310**(5748): 674-6.

33. Weeks, S., et al., *Anti-V antigen antibody protects macrophages from Yersinia pestis-induced cell death and promotes phagocytosis.* Microb Path, 2002. **32**: 227-37.

34. Cowan, C., et al., *Anti-LcrV antibodies inhibits delivery of Yops by Yersinia pestis KIM5 by directly promoting phagocytosis.* Infect Immun, 2005. **73**(9): 6127-37.

35. Goure, J., et al., *Protective anti-V antibodies inhibit Pseudomonas and Yersinia translocon assembly within host membranes.* J Infect Dis, 2005. **192**: 218-25.

36. Zauberman, A., et al., *Neutralization of Yersinia pestis-mediated macrophage cytotoxicity by anti-LcrV antibodies and its correlation with protective immunity in a mouse model of bubonic plague.* Vaccine, 2008. **26**: 1616-25.

37. Vernazza, C., et al., *Small protective fragments of the Yersinia pestis V antigen.* Vaccine, 2009. **27**: 2775-80.

38. Overheim, K., et al., *LcrV plague vaccine with altered immunomodulatory properties.* Infect Immun, 2005. **73**(8): 5152-9.

39. Pullen, J., et al., *Analysis of the Yersinia pestis V protein for the presence of linear antibody epitopes.* Infect Immun, 1998. **66**(2): 521-7.

40. Surgalla, M.J. and E.D. Beesley, *Congo red-agar plating medium for detecting pigmentation in Pasteurella pestis.* Appl Microbiol, 1969. **18**(5): 834-7.

41. Brubaker, R.R., E.D. Beesley, and M.J. Surgalla, *Pasteurella pestis: Role of Pesticin I and Iron in Experimental Plague.* Science, 1965. **149**(3682): 422-4.

42. Donnenberg, M. and J. Kaper, *Construction of an eae deletion mutant of Enteropathogenic Escherichia coli by using a positive selection suicide vector.* Infect Immun, 1991. **59**(12): 4310-7.

43. Anderson, D. and O. Schneewind, *Yersinia enterocolitica type III secretion: an mRNA signal that couples translation and secretion of YopQ.* Mol Microbiol, 1999. **31**(4): 1139-48.

44. Clemons, D., et al., *Evaluation of a subcutaneously implanted chamber for antibody production in rabbits.* Lab Anim Sci, 1992. **42**(3): 307-11.

45. Quenee, L.E., et al., *Amino acid residues 196-225 of LcrV represent a plague protective epitope.* Vaccine, 2010. **28**(7): 1870-6.

46. Zhang, Y., et al., *Type III secretion decreases bacterial and host survival following phagocytosis of Yersinia pseudotuberculosis by macrophages.* Infect Immun, 2008. **76**(9): 4299-310.

47. Wang, S., et al., *A DNA vaccine producing LcrV antigen in oligomers is effective in protecting mice from lethal mucosal challenge of plague.* 22, 2004(3348-3357).

48. Lathem, W., et al., *Progression of primary pneumonic plague: A mouse model of infection, pathology, and bacterial transcriptional activity.* Proc Natl Acad Sci, 2005. **102**(49): 17786-91.

49. DeBord, K., et al., *Immunogenicity and protective immunity against bubonic plague and pneumonic plague by immunization of mice with the recombinant V10 antigen, a variant of LcrV.* Infect Immun, 2006. **74**(8): 4910-4.

50. Bashaw, J., et al., *Development of in vitro correlate assays of immunity to infection with Yersinia pestis.* Clin Vaccine Immunol, 2007. **14**(5): 605-16.

51. Monack, D., et al., *Yersinia signals macrophages to undergo apoptosis and YopJ is necessary for this cell death.* Proc Natl Acad Sci, 1997. **94**(19): 10385-90.

52. Humphrey, W., A. Dalke, and K. Schulten, *VMD: Visual molecular dynamics.* J Mol Graph, 1996. **14**(1): 27-38.

53. Derewenda, U., et al., *The structure of Yersinia pestis V-antigen, an essential virulence factor and mediator of immunity against plague.* Structure, 2004. **12**(2): 301-6.

54. Charnetzky, W. and W. Shuford, *Survival and growth of Yersinia pestis within macrophages and an effect of the loss of the 47-megadalton plasmid on growth in macrophages.* Infect Immun, 1985. **47**(1): 234-41.

55. Forman, S., et al., *yadBC of Yersinia pestis, a new virulence determinant for bubonic plague.* Infect Immun, 2008. **76**(2): 578-87.

56. Ivanov, M., et al., *Vaccination of mice with a Yop translocon complex elicits antibodies that are protective against infection with F1- Yersinia pestis.* Infect Immun, 2008. **76**(11): 5181-90.

57. Galvan, E., M. Lasaro, and D. Schifferli, *Capsular antigen fraction 1 and Pla modulate the susceptibility of Yersinia pestis to pulmonary antimicrobial peptides such as cathelicidin.* Infect Immun, 2008. **76**(4): 1456-64.

58. Hill, J., et al., *Synergistic protection of mice against plague with monoclonal antibodies specific for the F1 and V antigens of Yersinia pestis.* Infect Immun, 2003. **71**(4): 2234-8.

59. Hill, J., et al., *N255 is a key residue for recognition by a monoclonal antibody which protects against Yersinia pestis infection.* Vaccine, 2009. **27**(50): 7073-9.

60. Swain, S., et al., *Neither neutrophils nor reactive oxygen species contribute to tissue damage during Pneumocystis pneumonia in mice.* Infect Immun, 2004. **72**(10): 5722-32.

61. Sun, K., et al., *Interleukin-12 promotes gamma interferon-dependent neutrophil recruitment in the lung and improves protection against respiratory Streptococcus pneumoniae infection.* Infect Immun, 2007. **75**(3): 1196-202.

62. Bartlett, A., et al., *a-Toxin facilitates the generation of CXC chemokine gradients and stimulates neutrophil homing in Staphylococcus aureus pneumonia.* J Infect Dis, 2008. **198**: 1529-35.

63. Wilkinson, T., et al., *Trappin-2 promotes early clearance of Pseudomonas aeruginosa through CD14 dependent macrophage activation and neutrophil recruitment.* Am J Path, 2009. **174**(4): 1338-46.

64. Kummer, L., et al., *Antibodies and cytokines independently protect against pneumonic plague.* Vaccine, 2008. **26**: 6901-7.

CHAPTER 3

INTRACELLULAR *YERSINIA PESTIS* ESCAPES MACROPHAGES VIA THE INDUCTION OF TYPE III SECRETION SYSTEM-DEPENDENT AND INDEPENDENT CELL DEATH

3.1 Abstract

The Gram-negative bacterium *Yersinia pestis* causes bubonic, pneumonic, and septicemic plague in mammals and is thought to be responsible for more human deaths throughout history than any other bacterial pathogen. We and others have shown that fulminant disease is the result of high-level extracellular bacterial replication and that *in vitro* opsonophagocytosis of the organism by macrophages using Type III secretion (T3S) blocking antibodies correlates with protection in various animal models of infection. However, recent data suggest that even though opsonized bacteria are readily taken up by macrophages, intracellular organisms are not eliminated. Thus, we hypothesized that intracellular *Y. pestis* is not only able to survive within macrophages, but also escapes from the cell and participates in extracellular disease. In support of this notion, we show here that intracellular bacteria kill macrophages via mechanisms both dependent and independent of T3S. Treating bacteria with heat abrogates cell death after infection, indicating that inducing the T3SS-independent death of

host cells is an active process. To directly correlate cell death with intracellular colonization, we utilized an intracellular bacterial reporter strain and cell death marker to show that the majority of dead cells were indeed killed by intracellular infection. Interestingly, only bacteria capable of T3S accumulated in the supernatant outside of infected macrophages, indicating that once bacteria escape, T3S prevents re-entry into viable cells and maintains organisms in the extracellular milieu. Finally, to identify the bacterial factor or factors responsible for the T3SS-independent killing of macrophages by intracellular bacteria, we screened a Tn*5* mutagenesis library for strains that fail to elicit intracellular cell death. Taken together, the data suggest that intracellular *Y. pestis* escapes macrophages through inducing cell death independently of the major known virulence factors, leading to extracellular disease. However, in the absence of functional T3S, bacteria are sequestered intracellularly which likely facilitates disease resolution.

3.2 Introduction

Yersinia pestis is the causative agent of plague, a zoonotic disease usually transmitted by a flea vector [1]. Upon subcutaneous delivery of bacteria into the bite site of a naïve host, bacteria migrate to the nearest draining lymph node, possibly through a dendritic cell intermediate [2]. Here, bacteria rapidly divide and induce a strong program of inflammation within the lymphatic tissue. Bacteria may eventually invade the circulatory system of the infected host and replicate to markedly high numbers, resulting in septicemic plague. Eventually, organisms may also reach and colonize the lungs resulting in secondary pneumonic plague, a highly contagious form of the disease that is spread to new hosts via aerosolized droplets, leading to primary pneumonic plague.

During the late stages of all forms of disease, massive extracellular bacterial replication is thought to ultimately lead to the death of the host. To this end, *Y. pestis* expresses several virulence factors that maintain organisms in the extracellular milieu when grown at mammalian body temperatures. At 37ºC Caf1 pili assemble on the surface of bacteria and form a proteinaceous sheath that blocks the phagocytosis of organisms by macrophages [3]. However, despite being an effective mechanism that increases the pathogenicity of the organism *in vivo*, *caf1* mutants have been shown to retain virulence in several animal models of plague [4-7]. At this temperature, bacteria also express a Type III secretion system (T3SS) that directly injects effector proteins into the cytoplasm of target host cells [8]. Although effector injection has pleiotropic effects on the cell,

several function to inhibit cytoskeletal rearrangements, preventing phagocytosis of the organism [9]. Contrary to Caf1, numerous studies show that strains lacking T3SS capability are completely avirulent in animal models for all forms of plague (Reviewed in [1]).

Even with the presence of multiple systems that function to maintain bacteria extracellularly, a small percentage of infecting bacteria are taken up by phagocytes [10, 11]. Once inside the macrophage *Y. pestis* initially resides in a spacious endocytic compartment known as a *Yersinia* containing vacuole (YCV) which matures to acquire LAMP-1, Cathepsin-D and TROv, markers of late endosomes and lysosomes [12]. However, although lysosomal fusion is thought to occur, compartmental acidification is inhibited, leading to a near-neutral pH in the YCV [13]. In addition, YCVs can also enter the autophagous pathway, where compartments acquire markers of autophagosomes (LC3-II, LAMP-1) and a second phospholipid membrane [13, 14]. Again, YCV acidification is thought to be inhibited. In both cases, mature YCVs provide infecting bacteria with an environment permissive for survival and replication.

Several gene products have been identified as important for the intracellular survival and proliferation of *Y. pestis*. *phoPQ* encodes a two-component regulatory system that is thought to sense the low [Mg^{2+}] environment of endocytic compartments and is essential for intracellular survival [12, 15, 16]. Gene expression profiling of intracellular bacteria indicates that activation of the response regulator PhoP results in the expression of many genes. Of these,

mgtC, a gene predicted to promote low [Mg^{2+}] resistance, as well as *ugd* and *pmrK*, genes predicted to promote resistance to antimicrobial peptides, have been shown to be important for the early survival of intracellular *Y. pestis* [12].

Other gene products not predicted to be under the control of PhoPQ have also been identified as important for bacterial persistence within the YCV. RipA, a protein encoded within the 102-kb virulence-associated pigmentation locus (*pgm* locus), appears to directly reduce nitric oxide (NO) levels in interferon-γ (IFN-γ) activated macrophages and is thus required for replication in activated cells [17]. Stress-response genes also thought to be involved in quenching free radicals appear to be highly up regulated during intracellular infection [18]. Of these, the stress-induced genes y2313, y2315, y2316, and *orfX* (y2313-y2315-y2316-*orfX* operon) have been shown to be important for intracellular growth, but not survival. Interestingly, deletion of the y2313-y2316 portion of the operon, or *orfX* itself, results in an abnormal filamentous morphology and excessive accumulation of bacteria when inside of the macrophage. Complementing either y2313-y2315-2316 or *orfX in trans* restores the bacterium to a wild-type morphology. Further experimentation indicated that deletion of the entire y2313-y2316-*orfX* operon resulted in decreased T3S, leading to decreased cell death during extracellular infection. However, *in vivo* studies indicate that strains lacking this operon maintain virulence in a mouse model of septicemic plague [18].

Although the *Y. pestis* T3SS has been long known to be essential for virulence, the role of T3S in intracellular *Yersinia* virulence remains uncertain. The T3SS encoding virulence plasmid pCD1 is dispensable for bacterial survival inside of macrophages, and transcriptome data indicate that Yop (*Yersinia* outer protein) effectors and translocators are insignificantly regulated at 1.5, 4, and 8 hours post-infection (hpi) [18-20]. Nevertheless, ectopic overexpression of *yopJ* under the control of an inducible promoter in *Y. pseudotuberculosis* suggests that Yop injection likely occurs from within the YCV [21]. The LcrV translocator protein forms a pentamer on the tip of the T3SS needle and is essential for Yop injection. Protection from all forms of plague is conferred to the host by the presence of T3S neutralizing antibodies, and we have previously shown that protective anti-LcrV antibodies not only block T3S, but also opsonize the bacterium for efficient phagocytic uptake by macrophages [11, 22, 23]. However, recent data indicate that intracellular *Y. pestis* is not killed even in the presence of antibodies and that the host relies on neutrophil activity to fully clear disease, making the role of macrophages in innate- and humoral-based protection from disease unclear [16, 24].

Here, we sought to better understand the role of T3S and its effect on macrophages during intracellular infection. We hypothesized that intracellular *Y. pestis* is not only able to survive and replicate within macrophages, but subsequently escapes the cell by inducing cell death. In support of this notion, we found that intracellular *Y. pestis* is capable of killing macrophages by inducing

T3SS-dependent, as well as T3SS-independent cytotoxicity which was not contingent on high levels of bacterial replication or the *pgm* locus. Nevertheless, only bacteria capable of T3S were able to accumulate in infected cell culture supernatants and replicate efficiently. To investigate the role of T3SS-independent cell death we screened a transposon library for loss-of-function mutants and found several genetic elements required for intracellular bacteria to induce cytotoxicity. Taken together, the data support a model whereby *Y. pestis* escapes macrophages via the induction of cell death through T3SS-dependent as well as novel T3SS-independent mechanisms, leading to the release of phagocytosed bacteria into the extracellular milieu.

3.3 Materials and Methods

Bacterial Strains: Strains used in this study are indicated in Table 3.1. The Δ*lcrV* mutant was constructed using a previously described method by cloning a region 1000 bp upstream, and 1000 bp downstream of the *lcrV* open reading frame into the suicide vector pCVD442 using the following primers and restriction sites [25]:

V up- XbaI 5: 5’ AATCTAGATGCAGGGAGTTATTTGGCAT 3’

V up – EcoRI 3: 5’ AAGAATTCATTAAATAA TTTGCCCTCGCAT 3’

V Down – EcoRI 5: 5’ AAGAATTCTGCTAGATGACACGTCTGGT 3’

V Down – SphI 3: 5’ AAGCATGCGCCAGCCAA AAATCT TTGATG 3’

The Tn*5* recipient strain CO92pCD1^{-} was isolated by repeated passage of the wild-type CO92 parent strain on solid medium. PCR screening for *lcrH* and *yopB*, genes located on the pCD1 virulence plasmid, identified a single colony

that was cured for pCD1. Infecting mice with this isolate via subcutaneous and pulmonary routes of infection demonstrated a complete loss of virulence.

Bacterial Culture Conditions and Plasmids: Bacteria were streaked for isolation from frozen stocks on heart infusion agar and incubated for 48 hours at 26ºC in a static incubator. Single colonies were then grown overnight at 26ºC in heart infusion broth (HIB) shaking at 150 rpm. Strains auxotrophic for diaminopimelic acid synthesis were supplemented with 400 µg/ml 2,6-diaminopimelic acid (Sigma, St. Louis, MO) neutralized with an equivalent volume of ammonium hydroxide (1 mM). The plasmid pNE071 was constructed as previously described [11]. Briefly, pNE071 contains a pUC origin of replication and contains the DsRed open reading frame under the control of a *tac* promoter, and expresses the *lacI*^{q} repressor. Strains containing pNE071 were grown overnight in the presence of ampicillin (100 µg/ml).

Macrophage Infections: RAW 264.7 macrophage-like cells were routinely cultured in DMEM High Glucose with L-Glutamine (Life Technologies, Grand Island, NY) containing 10% (v/v) heat inactivated fetal bovine serum (Life Technologies, Grand Island, NY) and ciprofloxacin (10 µg/ml) at 37^{o}C containing 5% atmospheric CO_2. For infections, 1x10^{6} cells were plated in 12-well cell culture dishes in phenol red-free DMEM containing 5% (v/v) FBS and allowed to adhere overnight. Bacteria grown to stationary phase were prepared by diluting cultures 1:15 in fresh HIB and allowing organisms to re-enter log phase growth by incubating for 2 hours at 26ºC shaking at 150 rpm. Bacteria were washed

once with PBS then re-suspended in cell culture media. In experiments utilizing heat-treated bacteria, cultures were first heated at 56°C for 60 minutes in a water bath [26]. The OD_{600} was then measured using a spectrophotometer and used to calculate the indicated multiplicity of infection (MOI). After addition of bacteria to macrophages in duplicate wells, plates were centrifuged at 450 rpm (40 x *g*) to induce contact, then incubated at 37ºC for 30 minutes to allow for phagocytosis. At this time, gentamicin (50 µg/ml) was added to each well to kill off extracellular bacteria. For experiments measuring bacterial accumulation in the supernatant, the gentamicin-containing medium was removed after 1 hour and replaced with gentamicin-free cell culture medium.

LDH Measurement: 50 µl of cell culture supernatant was aspirated then clarified by centrifugation at 6000 rpm (3100 x *g*) for 5 minutes. Supernatants were transferred to a 96-well plate where 50 µl of Lactate Dehydrogenase (LDH) substrate reagent (Promega, Madison, WI) was then added. Wells containing unused cell culture media were included as blanks, and uninfected control cells were lysed with 0.04% (v/v) Triton-X 100 to obtain a value for the maximum amount of LDH possible within a well at a given time. Plates were incubated for 30 minutes at room temperature in the dark then fluorescence was measured on a plate reader (BMG FluoStar, BMG Labtech, Cary, NC) at an excitation/emission spectrum of 544/590. Values for duplicate wells were averaged then percent cytotoxicity for each sample was determined as:

$$\% \text{ Cytotoxicity} = (LDH_{Experimental} - LDH_{Blank})/(LDH_{Max} - LDH_{Blank}) \times 100.$$

Flow Cytometry: Macrophages grown in 6-well culture dishes were infected as described above with strains harboring pNE071. After allowing for phagocytosis and administration of gentamicin, 10 mM Isopropyl β-D-1-thiogalactopyranoside (IPTG) was added to cultures to induce DsRed expression in intracellular bacteria. At the indicated time points, cells were collected, stained, and fixed with the Live/Dead Fixable Green Dead Cell Stain Kit (Life Technologies, Grand Island, NY) per the manufactures recommendations. Cells were then analyzed by two-color analysis on a MoFlo XDP (Beckman Coulter, Brea, CA).

Inhibition of Caspase-1 and Caspase-3: Macrophage infections were carried out as described above. The irreversible inhibitor of Caspase-1, Z-YVAD-FMK, or Caspase-3, Z-DEVD-FMK, (Santa Cruz Biotechnology, Santa Cruz, CA) was then administered to infected cell cultures at the indicated concentrations at the time of gentamicin treatment. Compounds were dissolved in DMSO which was subsequently used as the vehicle control for experiments requiring inhibitors.

*Tn*5 *Screen:* Approximately 10,000 strains were isolated after transformation with the EZ-Tn*5* (R6Kγori/KAN-2) Tnp Transposome Kit (Epicentre, Madison, WI). Bacteria were grown in 96-well plates in duplicate directly from freezer stocks in HIB supplemented with kanamycin (25 µg/ml). $1x10^5$ macrophages were plated in 96-well plates containing control wells harboring uninfected macrophages, blank wells, and max-lysis wells. Macrophages were infected at an MOI of 50 with mutant bacteria or the parent strain, and then plates were centrifuged for 5 minutes at 450 rpm (40 x *g*). After 30 minutes of incubation at

37°C in 5% CO_2, media containing gentamicin (50 µg/ml) was added. Plates were incubated for 14-16 hours and then analyzed for LDH accumulation in cell culture supernatants directly in wells. Percent cytotoxicity for each strain was then measured as described above. A cutoff value for loss-of-function mutants was set at less than or equal to 50% of the cytotoxicity observed when normalized to the entire population of Tn*5* mutants tested, or for wild-type control values in the assay. Plotting the values for the mutants tested shows a normal distribution that averages 100.0% ± 33.0% of the cytotoxicity observed for the entire population of the library.

Statistical Analysis: Where comparing only two parameters, differences were determined to be significant when $p < 0.05$ by the Mann-Whitney *U*-test. Where making multiple comparisons, differences were determined to be significant when $p < 0.05$ by One Way Analysis of Various (ANOVA) followed by Dunnett's post-hoc test. Statistical analysis was performed using SigmaPlot 12.0 (Systat Software, San Jose, CA).

TABLE 3.1. Strains used in this Study

Strain Name	Relevant Characteristics[a]	Ref.[b]
KIM D27	pCD1$^+$, T3SS$^+$, *pgm*$^-$	[27]
KIM D27 pCD1	pCD1$^-$, T3SS$^-$, *pgm*$^-$	[11]
KIM D27Δ*lcrV*	pCD1$^+$, T3SS$^-$, *pgm*$^-$	This work
KIM D27Δ*dapAX*	pCD1$^+$, T3SS$^+$, *pgm*$^-$, Replication deficient	[28]
KIM D27Δ*dapAX*Δ*lcrV*	pCD1$^+$, T3SS$^-$, *pgm*$^-$, Replication deficient	This work
KIM6$^+$	pCD1-, T3SS$^-$, *pgm*$^+$	[29]
CO92pCD1$^-$	pCD1-, T3SS-, pgm+, Tn*5* recipient strain	This work

a. +, positive for the indicated attribute; -, negative for the indicated attribute
b. Reference of source

3.4 Results

3.4.1. Intracellular Y. pestis *Kills Macrophages in an Active Process via T3SS-Dependent and T3SS-Independent Cytotoxicity*

To first determine the requirements for intracellular bacteria to kill macrophages, we infected RAW 264.7 cells with KIM D27, KIM D27Δ*lcrV*, or KIM6^{+} grown overnight at 26ºC at an MOI of 10 or 50, then added gentamicin to kill extracellular bacteria. After 8 and 24 hpi we then quantified levels of the cell death indicator Lactate Dehydrogenase (LDH) in cell culture supernatants. For all strains tested at an MOI of 10, very little LDH accumulation was observed in supernatants at 8 hpi (data not shown). However, after 24 hours of infection, all three strains had elevated levels of LDH compared to uninfected controls (p <0.05), but no differences were observed when strains were compared to each other (p >0.05, Figure 3.1A). Conversely, at an MOI of 50, LDH release was significantly higher in macrophages infected with KIM D27 compared to uninfected cells, or cells infected with KIM D27Δ*lcrV* or KIM6^{+} at 8 hpi (p <0.05, Figure 3.1B). However, no differences were observed between T3SS^{+} and T3SS^{-} strains at 24 hpi (p >0.05).

To determine if high-level intracellular replication contributes to the cytotoxicity induced by bacteria, we next infected macrophages with bacteria auxotrophic for the synthesis of the cell wall constituent diaminopimelic acid (DAP). Strains deficient in the *dapA* gene are unable to undergo multiple rounds of cell division and eventually lyse due to osmotic stress [28]. Macrophages

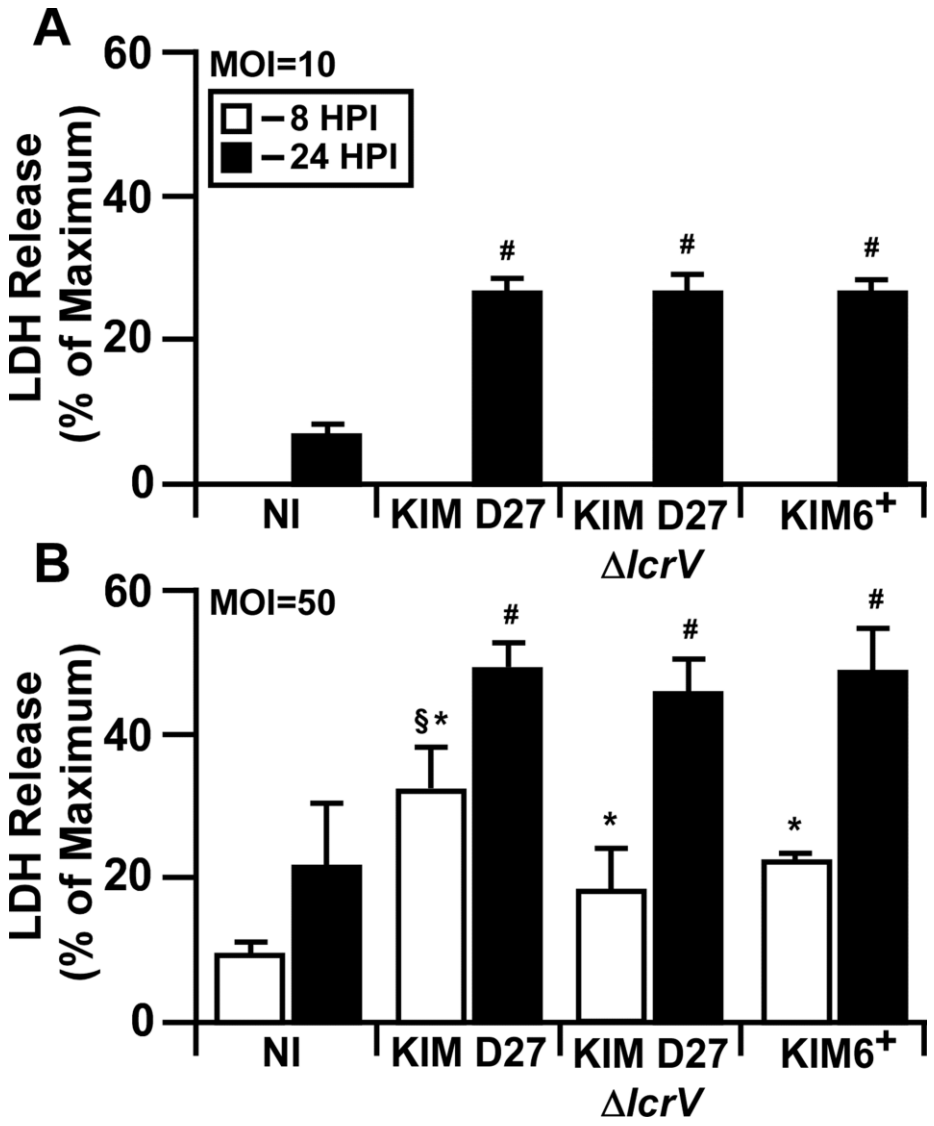

Figure 3.1. Intracellular *Y. pestis* induces T3SS-dependent and T3SS-independent cell death in macrophages. RAW 264.7 macrophages were left untreated or infected with the indicated strains at an MOI=10 (A) or 50 (B) then incubated for 8 (open bars) and 24 hours (black bars) in the presence of gentamicin. LDH accumulation was then measured in infected cell culture supernatants. Error bars indicate the SEM from three independent experiments. NI indicates no infection. * p <0.05 compared to uninfected controls at 8 hpi, # p <0.05 compared to uninfected controls at 24 hpi, § p <0.05 compared to all infection conditions at 8 hpi.

were infected at an MOI of 50 with KIM D27 or KIM D27Δ*dapAX* and cell culture supernatants were then analyzed for LDH accumulation at 8 and 24 hpi (Figure 3.2A). However, no significant differences in LDH release were observed

between replication proficient and replication deficient bacteria at either time point (p >0.05).

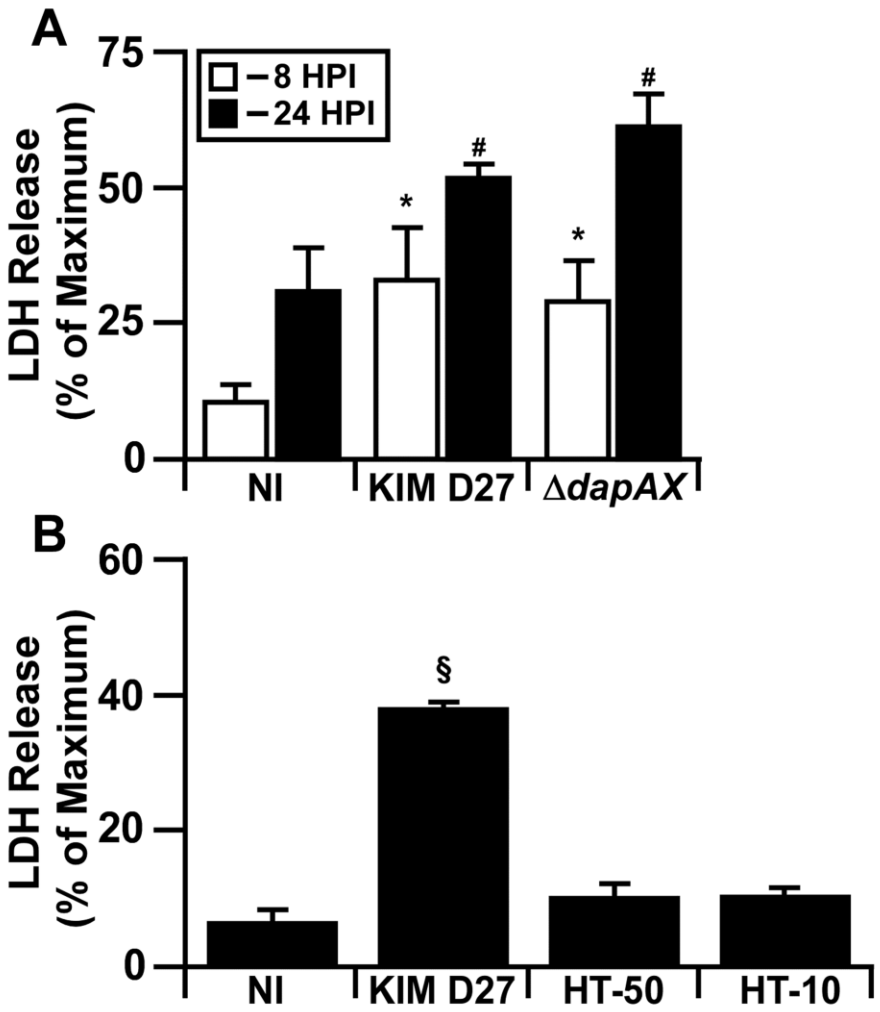

Figure 3.2. Induction of cell death by intracellular bacteria is independent of replication but requires an active process. (A) Macrophages were infected with the indicated strains at an MOI of 50 then incubated for 8 (open bars) and 24 hours (black bars) in the presence of gentamicin. LDH was then measured in infected cell culture supernatants (B) Macrophages were infected with viable bacteria at an MOI of 50 or bacteria that were heat-treated at an MOI of 50 or 10 (HT-50 and HT-10), then incubated for 24 hours in the presence of gentamicin. LDH accumulation was then measured. Error bars indicate the SEM from three independent experiments. NI indicates no infection, HT indicates heat-treated. * p <0.05 compared to uninfected controls at 8 hpi, # p <0.05 compared to uninfected controls at 24 hpi, § p <0.05 compared to all infection conditions.

To confirm that the induction of cell death by intracellular bacteria is the result of an active process, we next infected macrophages with viable or heat-treated KIM D27 and measured LDH accumulation in infected cell culture supernatants (Figure 3.2B). At 24 hpi with an MOI of 10, heat-treated bacteria elicited significantly less LDH release from infected cells compared to viable KIM D27 infected samples (p <0.05). Similar results were seen when macrophages were infected with heat-treated bacteria at an MOI of 50, or with bacteria that were killed by paraformaldehyde treatment (Figure 3.2B and data not shown). Taken together, the data suggest that although intracellular *Y. pestis* is able to kill the host cell via T3S, additional mechanisms that require an active process independent of the *pgm* locus or a high level of replication contribute to cytotoxicity elicited by intracellular bacteria.

3.4.2. Induction of LDH Release by Intracellular Infection is both Time- and Dose-Dependent

To better understand the kinetics of cell death caused by intracellular infection, we next performed a time course assay. Macrophages were either left untreated or infected with KIM D27 or KIM D27Δ*lcrV* (Figure 3.3A). At 6 hpi, little LDH had accumulated in cell culture supernatants for all samples. However, by 12 hpi LDH levels began to increase in infected cell culture supernatants for both strains compared to uninfected cells, and continued to rise through 18 hpi where signals began to saturate between 18 and 24 hpi (p <0.05). Similar to the results above, an elevated level of LDH was observed in the supernatants of cells

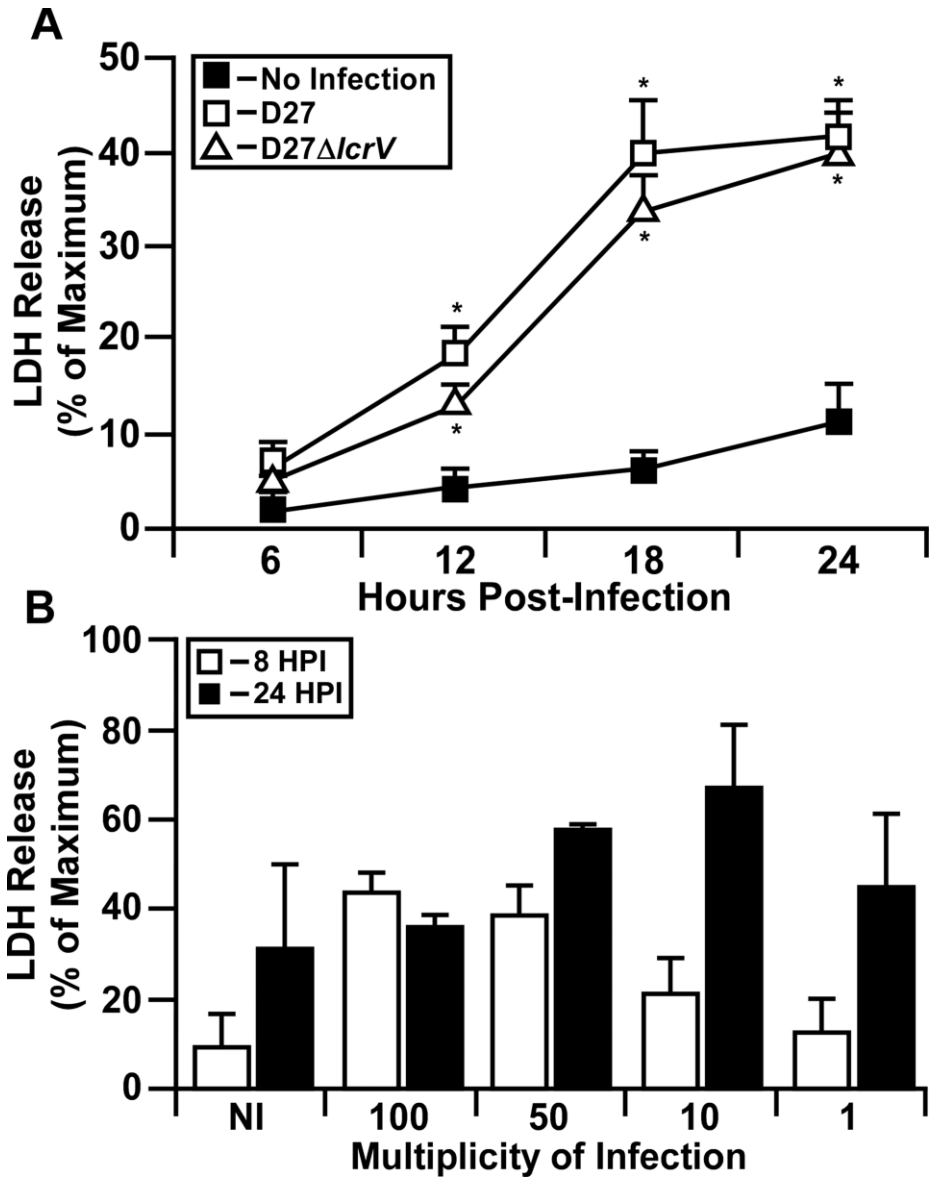

Figure 3.3. Intracellular *Y. pestis* induces cell death in a time- and dose-dependent manner. (A) Macrophages were left uninfected (black squares) or infected with KIM D27 (open squares) or KIM D27Δ*lcrV* (open triangles) and incubated in the presence of gentamicin. At the time points indicated LDH accumulation in infected cell culture supernatants was analyzed. Error bars represent the SEM from three independent experiments, * p <0.05 at the indicated time points compared to uninfected cells. (B) Macrophages were infected with KIM D27 at the indicated MOIs and incubated for 8 (open bars) or 24 (closed bars) hours where LDH accumulation was then measured. Error bars represent the SEM from two independent experiments.

infected with KIM D27 compared to KIM D27Δ*lcrV*, however differences were not determined to be statistically significant at the time points examined (p >0.05).

We next sought to determine if the intracellular bacterial burden correlates with the amount of LDH released from infected cells. Macrophages were infected at an MOI of 100, 50, 10, or 1 with KIM D27 then analyzed for LDH accumulation in the infected cell culture supernatants at 8 and 24 hpi (Figure 3.3B). As expected, cells infected at an MOI of 50 measured 39% LDH release which increased to 43% at an MOI of 100 at 8 hpi. Lowering the MOI to 10 and 1 decreased the level of LDH measured to 21% and 12%, respectively. However, at 24 hpi, LDH levels for cells infected at an MOI of 10 or 1 were increased compared to measurements taken at 8 hpi, and reached that for cells infected at an MOI of 50. Of note, the LDH level observed in the infected cell culture supernatants of macrophages that were administered an MOI of 100 or 50 was lower than macrophages infected with an MOI of 10 or 1 at 24 hpi. This is likely due to assay limitations as active LDH only remains in cell culture supernatants for approximately 9 hours, suggesting that the majority of cells in the assay had lysed at earlier time points. Taken together, these data suggest that cell death induced by intracellular bacteria is dependent on both time and intracellular concentrations of infecting organisms.

3.4.3. Cell Death Directly Correlates with Intracellular Infection

While the aforementioned results indicate that cell death is induced within a population of macrophages infected with *Y. pestis*, they do not show that intracellular infection directly correlates with killing on a per-cell basis. To address this issue, we utilized bacterial intracellular reporter strains and a

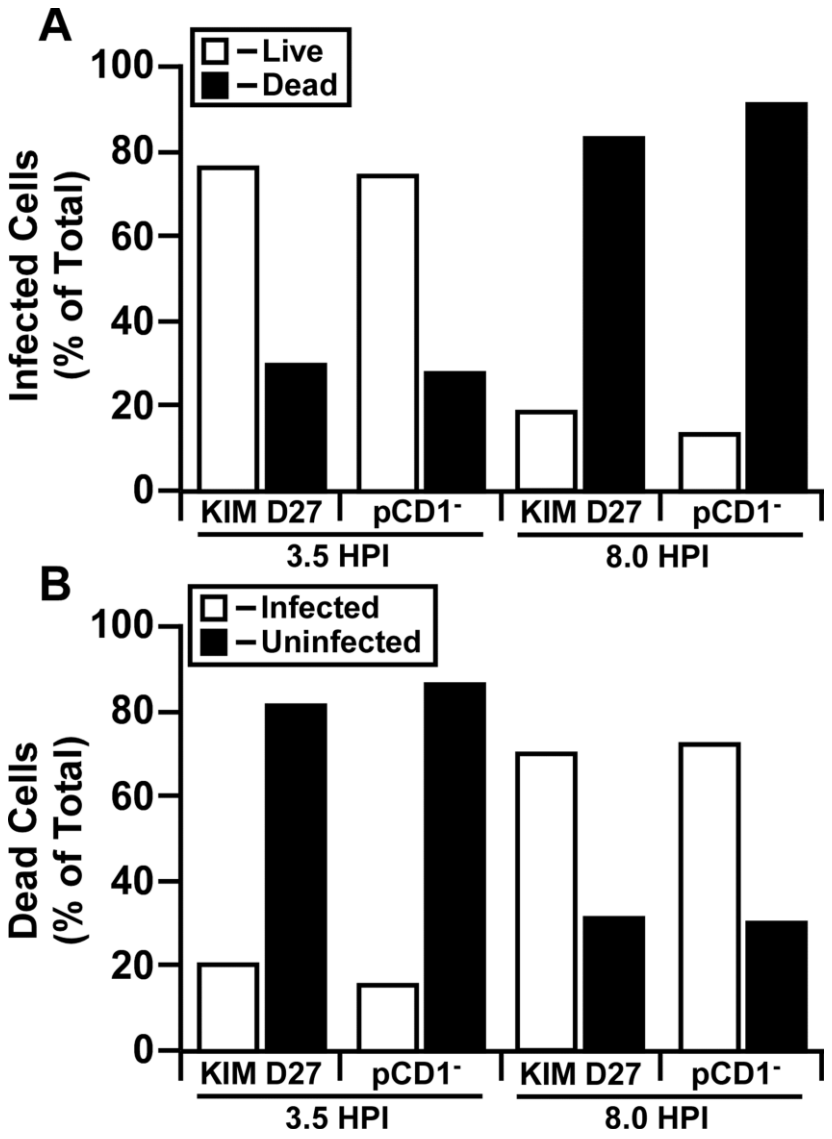

Figure 3.4. Intracellular *Y. pestis* infection directly correlates with cell death. Macrophages were infected with the indicated bacterial strains harboring pNE071 which expresses DsRed in the presence of IPTG. After allowing for phagocytosis, gentamicin and IPTG were added to infected cells which were subsequently collected at the indicated time points. Cells were then stained with a fixable Live/Dead cell death indicator and analyzed by flow cytometry. Data are representative of two technical replicates.

live/dead stain to measure the colocalization of infection and cell death by flow cytometry (Figure 3.4). At 3.5 hpi, infected cells were mostly viable and did not take up the live/dead stain when infected with a T3SS$^+$ or a T3SS$^-$ strain (Figure 3.4A). However, by 8 hpi, cells infected with either strain became largely

permeable to the live/dead stain, confirming that infected cells are indeed being killed over time by intracellular infection, regardless of T3S proficiency in the infecting strain. Consistent with the data above, macrophages infected with KIM D27 yielded a slightly higher percentage of cell death in infected cells than KIM D27pCD1^{-} at 8 hpi (17.8% vs. 15.1%).

In addition, when gating on cells that take up the live/dead stain, the majority of dead cells at 3.5 hpi are largely uninfected (Figure 3.4B). However, dead and infected cells are more prevalent at 8 hpi indicating that the majority of dead cells transition from uninfected to infected over the course of the experiment. These results indicate that intracellular *Y. pestis* infection directly correlates with the induction of cell death and provides additional evidence that both T3SS^{+} and T3SS^{-} bacteria are capable of killing macrophages from within.

3.4.4. Type III Secretion Allows Y. pestis *to Escape Macrophages*

The data presented above indicates that both T3SS^{+} and T3SS^{-} strains are capable of killing cells from within the YCV or the cytoplasm. Thus, we hypothesized that both strains would be able to escape the macrophage by inducing cell death. To test this notion, we infected macrophages with strains deficient in DAP synthesis and pulsed infected cells for 1 hour with gentamicin (Figure 3.5A). This protocol eliminates error that would arise from extracellular replication, allowing us to measure *de novo* bacterial escape from the cell at the indicated time points [28]. As expected, after replacing gentamicin containing medium with antibiotic free medium at 1 hpi, few bacteria were detected in the

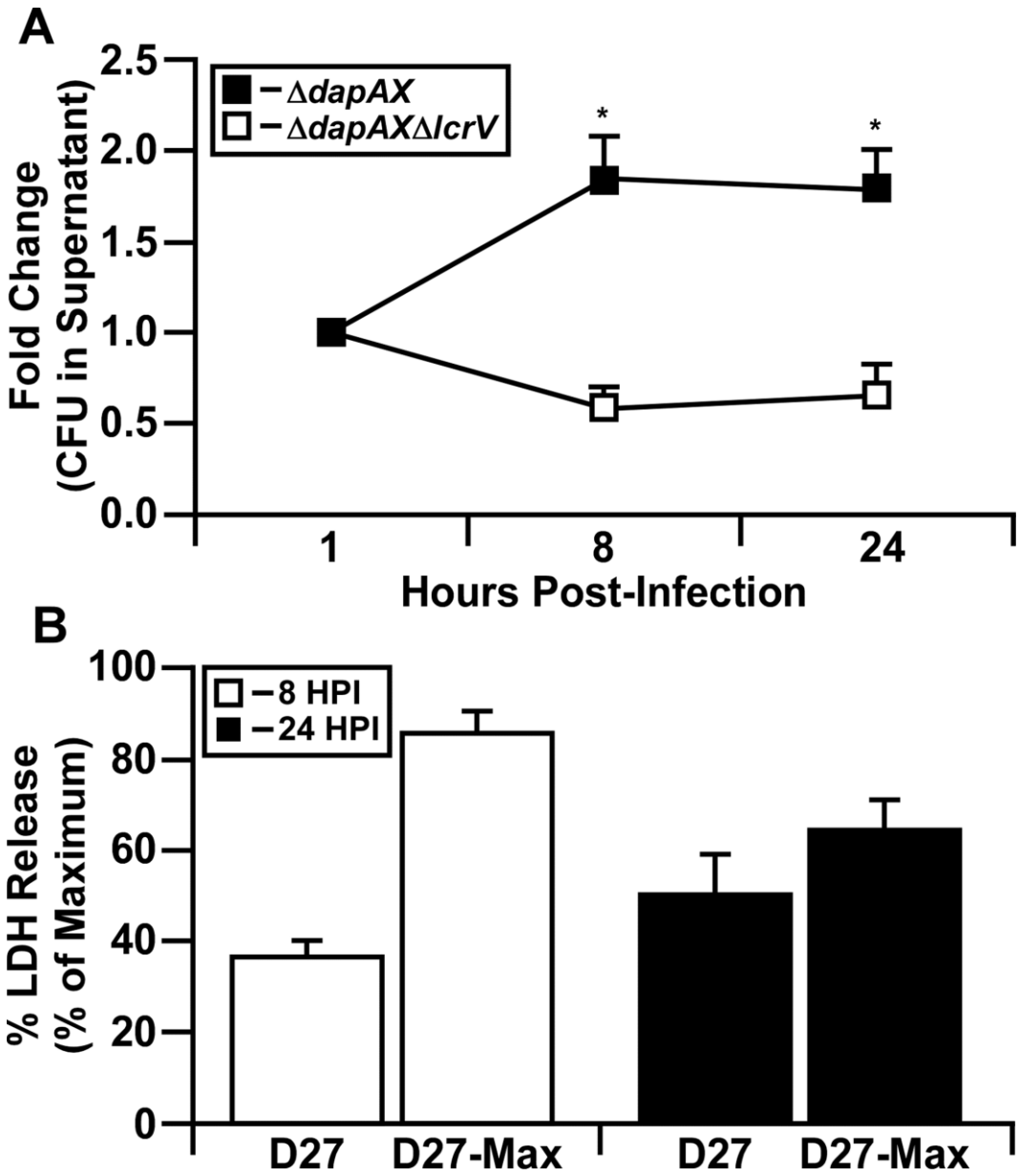

Figure 3.5. Type III secretion allows *Y. pestis* to escape macrophages. (A) Macrophages were infected with KIM D27Δ*dapAX* (black squares) or KIM D27Δ*dapAX*Δ*lcrV* (open squares) and pulsed for one hour with gentamicin. Bacteria in the infected cell culture supernatants were then plated solid media at the indicated time points and measured as the fold change from bacteria quantified at 1 hour post-infection. Error bars represent the SEM from three independent experiments, **p* <0.05 at the indicated time points. (B) Macrophages were infected with KIM D27 and incubated in medium containing gentamicin for 8 (open bars) or 24 (closed bars) hours then analyzed for LDH accumulation in cell culture supernatants. Infected cells were then lysed with Triton-X 100. Error bars represent the SEM from two independent experiments.

infected cell culture supernatants. However, by 8 and 24 hpi, a 1.8- and 1.6-fold increase was observed in the number of T3SS$^+$ bacteria in the infected cell culture supernatants, respectively. Unexpectedly, a 0.58- and 0.62-fold reduction in the number of T3SS$^-$ bacteria in the supernatant was measured at 8 and 24 hpi. Thus, although both T3SS$^+$ and T3SS$^-$ strains are able to kill macrophages from within, only T3SS$^+$ bacteria accumulate extracellularly.

Due to the discrepancy between the accumulation of LDH and the net loss of T3SS$^-$ bacteria in the supernatant, we hypothesized that viable macrophages within an infected cell population could phagocytose escaped bacteria. To this end, we infected macrophages with KIM D27 then measured LDH accumulation in the supernatant before and after lysis with Triton-X 100 at 8 hpi (Figure 3.5B). As expected, infected cells measured a ~40% increase in LDH accumulation compared to uninfected controls. However, after lysing this population an additional 48% increase in LDH was observed, indicating that at 8 hpi a large portion of macrophages within an infected cell population are still viable, even in the presence of T3S. However, at 24 hpi there was no difference between KIM D27-induced LDH accumulation and LDH released due to Triton-X 100 lysis. These data suggest that once T3SS$^-$ bacteria kill and escape the cell, viable macrophages phagocytose bacteria and sequester organisms intracellularly, resulting in the net reduction of extracellular bacteria. Conversely, T3SS$^+$ bacteria are able to remain outside of viable cells likely due to temperature-induced expression of, and injection with antiphagocytic effector proteins.

3.4.5. Intracellular Sequestration Limits Bacterial Replication

To better understand the implications of limiting the extracellular presence of *Y. pestis* we next measured the ability of T3SS$^+$ and T3SS$^-$ bacteria to replicate in a population of macrophages. Cells were infected with KIM D27 or KIM D27Δ*lcrV* at an MOI of 10 then pulsed with gentamicin for 1 hour. Infected macrophages were incubated for 1 or 20 hours and cells were then lysed, and the total bacteria present in the infection (extracellular and intracellular) were then plated on solid medium and quantified. Strikingly, macrophages infected with KIM D27 measured a 124.4-fold (± 28.4) increase in the number of total bacteria compared to a 50 fold (± 9.0) increase observed for KIM D27Δ*lcrV*, indicating that T3SS$^+$ bacteria increased in numbers to a greater extent than T3SS$^-$ bacteria in the presence of macrophages. Thus, T3SS-dependent extracellular replication after escape from the cell greatly contributes to *Y. pestis* replication in the presence of a population of macrophages.

3.4.6. Caspase-1- and Caspase-3-Independent Cell Death during Intracellular Infection

To better understand the mechanism of cell death induced by intracellular infection with *Y. pestis* we next determined the impact of cell death inhibitors on LDH release during KIM D27 infection. To investigate the role of pyroptosis we first administered the irreversible inhibitor of Caspase-1 Z-YVAD-FMK in increasing concentrations to macrophages and measured LDH release after 8 hours of infection (Figure 3.6A). However, no differences in LDH release were

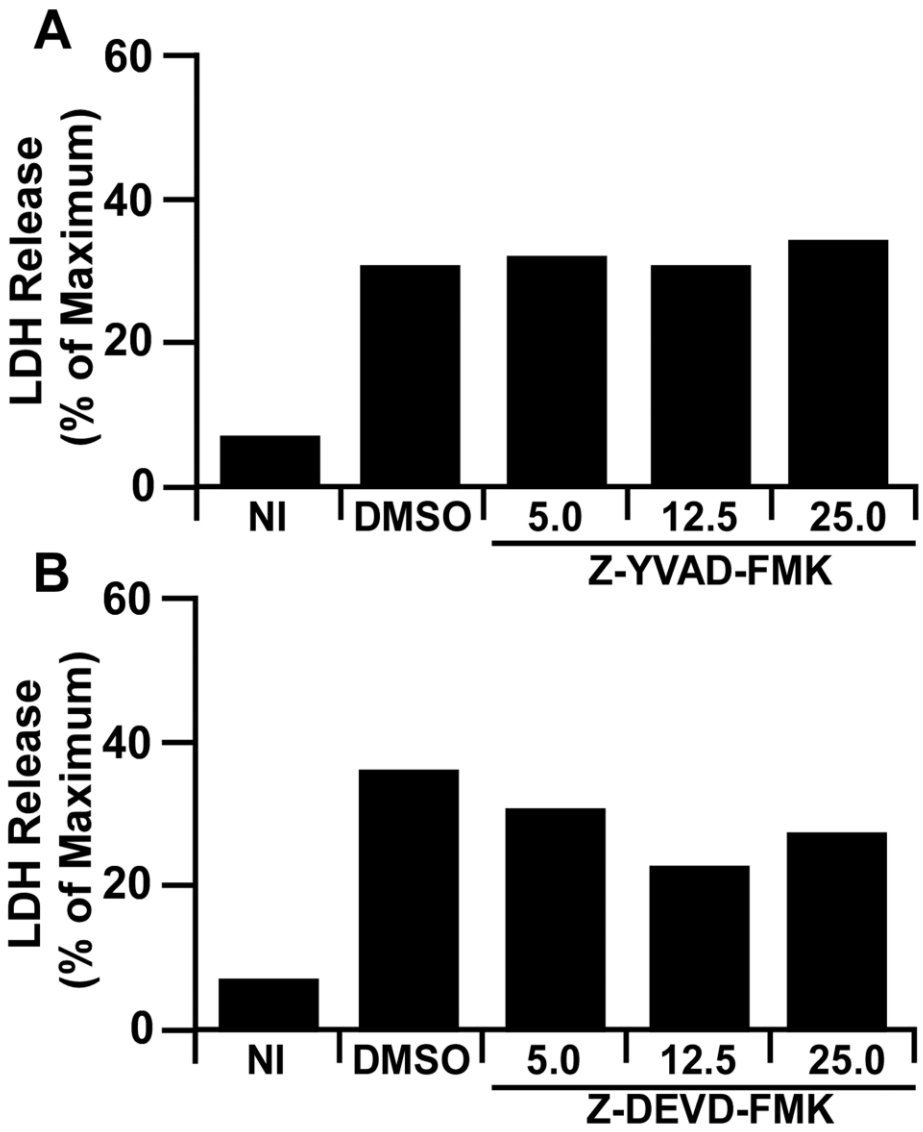

Figure 3.6. Apoptosis contributes to T3SS-dependent cell death by intracellular *Y. pestis*. Macrophages were infected with KIM D27 at an MOI of 50 then treated with the indicated concentrations (µg/ml of cell culture medium) of Z-YVAD-FMK (A), Z-DEVD-FMK (B), or the vehicle control DMSO at the time of gentamicin treatment. At 8 hpi LDH accumulation in infected cell culture supernatants was then analyzed. Data are representative of two independent experiments.

observed for any of the concentrations tested. We next investigated the impact of YopJ injection by determining role of apoptosis during infection.

Administering increasing concentrations of the irreversible inhibitor of Caspase-3

Z-DEVD-FMK resulted in a dose-dependent reduction of LDH release at 8 hpi. However, the inhibitory effect of the compound was abrogated between 12.5 and 25.0 µg/ml, indicating that Caspase-3 activation only partially contributes to the LDH release observed during infection. No effect on LDH release was observed at 24 hpi for either inhibitor (data not shown). Consistent with the results above, these data suggest that although the T3SS contributes to cell death during intracellular infection, a mechanism independent of pyroptosis and apoptosis is likely responsible for the LDH release observed during infection with T3SS$^-$ strains.

3.4.7. Identification of Bacterial Factors Required For the T3SS-Independent Induction of Cell Death

The data presented above indicates that *Y. pestis* can kill macrophages independently of T3S, the *pgm* locus, and high-level replication. To identify and investigate the role of bacterial factors that are required for the induction of T3S-independent cell death during intracellular infection we screened ~10,000 strains in a *Y. pestis* CO92pCD1$^-$ Tn*5* mutagenesis library for insertions that result in the loss of the bacterium's ability to promote cell death from within the cell (Figure 3.7).

Seventeen mutants reproducibly measured below the cutoff value for the screen (Table 3.2, boxed – See Materials and Methods). Interestingly, all but one of the loss-of-function insertions (YPO0425/*hmsT*), displayed a growth defect *in vitro* compared to the parent strain (which typically measured an

overnight OD_{600} of 1.2-1.4). Sequence analysis indicated that several of the mutants contain the same genomic insertion. An insertion in YPO1011 appeared in 3 mutants and is thought to encode an uncharacterized outer membrane TonB-dependent receptor. In these mutants, as well as one additional mutant, YPO3494 also contained sequence homology to the same inserted genomic region. This region likely encodes for *truB*, a tRNA pseudouridine synthase-B which catalyzes the pseudouridination of tRNA, a step important for tRNA structure and, consequently, efficient protein synthesis. Of note, these mutants were isolated from the same series of mutants and are overrepresented in the library because they are likely clones from a single transformation with the EZ-Tn*5* transposition vector.

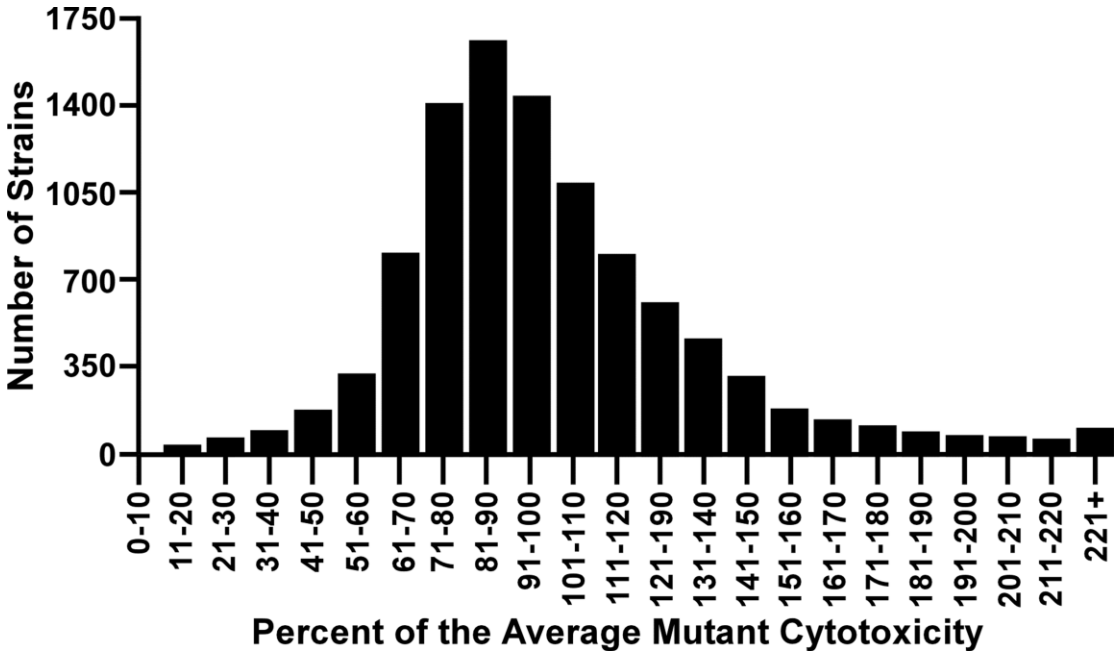

Figure 3.7. Distribution of the cytotoxicity observed for Tn*5* mutants. Approximately 10,000 strains transformed with the EZ-Tn*5* vector were analyzed for the ability to induce cell death after macrophage infection. Percent cytotoxicity was determined for each strain which was then normalized to the percent cytotoxicity observed for all strains tested.

TABLE 3.2. Tn*5* Mutants that reproducibly lost the ability to promote LDH release during intracellular infection

Insertion Site (YPO)[a]	Gene Homology[b]	Percent Cytotoxicity	Percent of Tn*5*[c]	Percent of WT[d]	OD_{600}[e]
4118	*glmS*	4.5%	12.3%	25.1%	0.195
ND[f]	ND	7.6%	20.5%	41.9%	0.279
ND	ND	11.3%	30.6%	24.8%	0.328
0425	*hmsT*	11.4%	30.8%	62.9%	1.375
033/0500	ND	12.9%	34.9%	28.3%	0.537
1558/1011/3288, 3494	*xonA*/*genF*/ *truB*	13.6%	36.8%	29.8%	0.722
2567/1011/3494	*pta*/*truB*	13.7%	37.0%	30.0%	0.721
2975/4119	*glmU*	14.2%	38.4%	31.1%	0.159
1019	*ptrA*	14.9%	40.3%	32.6%	0.475
3138	*ymoA*	15.0%	40.6%	46.2%	0.561
3307/pMT1.50c	*recA*	17.8%	48.1%	39.0%	0.112
ND	ND	19.3%	52.2%	42.3%	0.298
3494	*truB*	20.4%	55.2%	44.7%	0.297
0987	ND	21.2%	57.3%	46.4%	0.458
2870	*guaA*	21.6%	58.4%	47.3%	0.379
3720	*shlB*/*hpmB*	21.6%	58.4%	47.3%	0.544
1011/3494	*truB*	22.8%	61.7%	49.9%	0.412

a. Location of Tn*5* insertion based on sequence homology
b. Gene homology as annotated in the CO92 genome
c. Percent cytotoxicity taken as a percentage of the cytotoxicity determined for all mutants assayed.
d. Percent cytotoxicity taken as a percentage of the wild-type control
e. OD_{600} was measured at approximately 30 hours after inoculation
f. ND - No Data

3.5 Discussion

Although it has been appreciated for some time that *Y. pestis* is able to survive and replicate inside of macrophages, the exact role and the molecular mechanisms of intracellular colonization during infection have yet to be elucidated. Therefore, we sought to gain a better understanding of the interactions between intracellular bacteria and macrophages. Toward this end,

we hypothesized that bacteria egress the cell by initiating a program of cell death from within the YCV or the cytoplasm, leading to escape of the organism and exacerbated extracellular disease.

We first aimed to determine the requirements for intracellular *Y. pestis* to kill macrophages, as measured by LDH accumulation in infected cell culture supernatants. Consistent with previously published data, we found that T3S contributes to the death of macrophages during intracellular infection, as determined by an increase in LDH levels elicited from macrophages infected with KIM D27 compared to KIM D27Δ*lcrV* (Figure 3.1). Strikingly, we also observed a T3SS-independent mechanism of cell death which also contributed to the cytotoxicity observed during intracellular infection. This process was not reliant on virulence factors encoded within the *pgm* locus or excessive bacterial replication, as Congo Red binding and DAP synthesis were dispensable for this observation. Moreover, this process was independent of apoptosis and pyroptosis (Figure 3.6). Nevertheless, induction of cell death did rely on an active process, as elevated levels of LDH release were ablated in cultures infected with heat-treated bacteria (Figure 3.2). The observation that the *Y. pestis* T3SS is not required for the induction of cell death is in stark contrast to a study which showed that intracellular *Y. pseudotuberculosis* requires YopJ translocation to induce cell death from YCVs within bone marrow-derived macrophages [30]. Thus it is possible that the outcome of intracellular *Y. pestis* infection is distinct from that of *Y. pseudotuberculosis*.

To better understand the kinetics of cell death induction during intracellular infection we next performed a time course assay where LDH was measured at 6, 12, 18, and 24 hpi (Figure 3.3A). Similar to the data above, we found that as the infection progressed, T3SS$^+$ bacteria elicited increased levels of cell death compared to T3SS$^-$ bacteria. However, T3SS$^-$ bacteria were able to elicit significantly higher levels of cell death than uninfected controls, further supporting the conclusion that intracellular *Y. pests* can kill macrophages independent of T3S. We next sought to determine if the intracellular bacterial burden determines the amount of cell death observed, and found a positive correlation between MOI and LDH release at 8 hpi with all MOIs, and at 24 hpi with lower MOIs (Figure 3.3B). These data clearly demonstrate that infection-induced cell death in macrophages is both a time- and dose-dependent, and suggest the presence of a specific receptor-ligand interaction that activates a cell death pathway.

To rule out the possibility that a soluble intermediate is leading to the death of infected cells within a population, we next showed that intracellular infection directly correlates with the induction of cell death by measuring the colocalization of intracellular bacterial reporter strains with a cell death indicator. At early time points (3.5 hpi), gating on both T3SS$^+$ and T3SS$^-$ infected cells indicates that cells are largely viable (Figure 3.4A). However, as the infection progressed, infected cells more readily took up the cell death stain. In addition, when gating on dead cells, uninfected cells predominated at 3.5 hpi, while

infected cells predominated at 8 hpi (Figure 3.4B). In other words, infected cells transition from a live to dead status, and dead cells transition from an uninfected to an infected status throughout the course of the experiment, supporting the conclusion that intracellular *Y. pestis* infection directly leads to the death of the host cell.

Given that intracellular infection with viable bacteria resulted in a significant amount of cell death independent of T3S, we hypothesized that both $T3SS^+$ and $T3SS^-$ strains would escape the cell and accumulate in infected cell culture supernatants. We first tested this by comparing KIM D27 and KIM D27Δ*lcrV* directly and determined that greater numbers of $T3SS^+$ bacteria accumulated in infected cell culture supernatants compared to $T3SS^-$ bacteria over the time course of the experiment (data not shown). However, we also noticed that as bacteria escaped macrophages, organisms began to replicate. Thus, small differences in the number of CFUs between infection conditions present after pulsing with gentamicin could amplify exponentially through the course of the experiment.

To circumvent this issue, we again made use of strains auxotrophic for DAP synthesis so that small differences would not amplify over time as replicating bacteria lyse, and *de novo* bacterial release from infected macrophages could be determined at the time points tested. Similar to the data obtained for replication-proficient bacteria, we found that there were greater numbers of $T3SS^+$ bacteria in cell culture supernatants compared to $T3SS^-$

bacteria, which unexpectedly measured a net reduction in extracellular bacteria over time (Figure 3.5A). Unlike replication-proficient KIM D27Δ*lcrV* bacteria which accumulated in a delayed manner compared to KIM D27, the KIM D27Δ*dapAX*Δ*lcrV* strain unexpectedly measured a net decrease in the number of extracellular CFUs. This observation is likely an artifact of the strain being inhibited in replication while simultaneously being sequestered intracellularly.

To reconcile the discrepancy between the observation that both $T3SS^+$ and $T3SS^-$ strains are able to kill macrophages from within, yet only $T3SS^+$ bacteria accumulate outside of cells, the data suggest that unique interactions between escaped extracellular bacteria and viable macrophages result in such opposing fates. We therefore hypothesized that while $T3SS^-$ bacteria kill and escape the cell, viable macrophages within an infected cell culture subsequently phagocytose escaped bacteria and sequester organisms intracellularly. Conversely, during infection with $T3SS^+$ organisms, bacteria thermally up regulate expression of the T3SS injectasome, as the infection is carried out at 37°C, and re-entry of bacteria into viable cells is then inhibited due to extracellular Yop injection. In support of this notion, we show at 8 hpi the amount of LDH present within an infected cell culture is significantly increased by lysing the remaining infected cells with Triton-X 100, suggesting that viable macrophages indeed make up part of the infected cell population (Figure 3.5B). Furthermore, when measuring the entire bacterial population present within an infection at 20 hpi (extra- and intracellular), less $T3SS^-$ bacteria are present,

suggesting that intracellular sequestration limits bacterial replication (Section 3.4.5). Results shown in Figure 3.4 also confirm these data as cells examined by flow cytometry show there is a small percentage of both Live/Infected and Live/Uninfected cells present within an infected cell population.

We next sought to identify and investigate the role of the bacterial factor(s) responsible for the T3SS-independent induction of cell death during intracellular infection. To this end, we performed a screen of ~10,000 Tn*5* mutants constructed in a strain lacking pCD1 for genetic elements that lead to the diminution of LDH release during infection (Figure 3.7, Table 3.2). Unexpectedly, metabolic defects limiting replication in nutrient-rich broth may have an impact on the ability of bacteria to induce cell death during intracellular infection, as strains measuring lower overnight optical densities elicited lower LDH release. However, these data conflict with the results above which demonstrated no defect in a DAP auxotroph to induce cell death (Figure 3.2A). Additional experimentation will be required to better understand this discrepancy. Nevertheless, the results of the screen suggest several possible mechanisms that could be used by *Y. pestis* to escape the macrophage.

Several regulators of virulence were identified as being important for intracellular bacteria to induce cytotoxicity. Sequence analysis indicates a disruption of YPO0425 (*hmsT*) results in a 69% reduction of LDH release (Table 3.2) and, as discussed above, did not demonstrate an overnight growth defect (Table 3.2). HmsT is a diguanylate cyclase that converts 2 GTP into cyclic

diguanylate (c-di-GMP) which is degraded/regulated by the phosphodiesterase, HmsP [31, 32]. In addition, sequence data obtained for another loss-of-function mutant indicates an insertion in YPO2870 which encodes the GMP synthase GuaA (*guaA*), an enzyme important for the synthesis of the GTP precursor GMP [33]. C-di-GMP is an important signaling molecule in the regulation of bacterial virulence and acts as a second messenger thought to promote sessile growth in the environment [34, 35]. As such, production of high levels of c-di-GMP by bacteria has been attributed to the inhibition of motility and promotion of biofilm synthesis [31, 36]. In *Y. pestis*, HmsT generates c-di-GMP at temperatures between 26°C and 30°C (temperatures thought to be encountered by the flea) leading to the biosynthesis of extracellular poly-β-1,6-GlcNAc by the *hmsHFRS* operon located in the *pgm* locus [37]. Thus, *hmsT* is essential for bacterial biofilm formation in the flea. However, strains that overproduce c-di-GMP due to a mutation in *hmsP* retain virulence in bubonic and pneumonic models of plague [38]. Further experimentation will be required to determine if a deficiency in *hmsT*-dependent production of c-di-GMP and/or *guaA*-dependent production of GMP is the reason for the decrease in cell death. It should be noted that although c-di-GMP is an indirect activator of the inflammasome, it is unlikely that this activity leads to T3SS-independent cell death, as inhibiting Caspase-1 had no effect on LDH release (Figure 3.6).

Another insertion identified in the screen thought to regulate virulence was in the open reading frame of the thermoregulator *ymoA*. YmoA is a histone-

like protein and a temperature-dependent transcriptional modulator that is thought to function by altering DNA topology via interactions with the H-NS nucleoprotein [39, 40]. YmoA has previously been shown to have negative regulatory activity on the expression of the plasmid encoded *Yersinia* T3SS and chromosomally encoded Invasin (*inv*) in enteropathogenic *Yersiniae* at low temperatures, while displaying positive activity on the chromosomally encoded enterotoxin *yst* (Yst) in *Y. enterocolitica* [41-43]. Although YmoA could influence T3SS-dependent cell death, the screen was performed in a strain lacking pCD1, thus the data suggest that *ymoA* may have a modulatory role on factors required for the T3SS-independent induction of cell death by intracellular bacteria. Future studies aim to determine if c-di-GMP or YmoA may regulate factors needed for escape from the YCV and the macrophage, as well as the role of temperature in infection-induced cytotoxicity.

In addition to *hmsT* and *ymoA*, another gene insertion that resulted in a reduction of LDH release during infection has also been associated with virulence. An insertion in YPO3720 lead to a reduction of LDH release by about 53% compared to the parent strain, and sequence homology indicates that this region is similar to the *Edwardsiella tarda* and *Serratia marcescens* hemolysin *shlB/hpmB* (Table 3.2). In *S. marcescens,* the outer membrane protein ShlB has been well characterized and is required for ShlA secretion, which subsequently mediates cytotoxicity toward, and invasion of cultured epithelial cells, as well as virulence in the lung [44-48]. In *E. tarda*, a gene with homology to *shlB/hpmB*

acts as an invasin and promotes entry into cultured epithelial cells, as well as early growth of the organism within the cell [49]. Interestingly, a gene with homology to *shlA* is immediately downstream of *shlB* in a putative bicistronic operon in the *Y. pestis* CO92 genome, suggesting that an insertion in *shlB* could prevent the expression of both genes. In *L. monocytogenes, e*scape from the vacuole is mediated by the hemolysin Listeriolysin O (LLO), which has been shown to be essential for egress from the phagosome to the cytoplasm [50]. Strains lacking LLO are hypocytotoxic and avirulent in animal models of infection [51]. This is an attractive model to explain the T3SS-independent cytotoxicity observed for *Y. pestis* and will be examined further.

Lastly, the insertion that lead to the greatest defect in the induction of cell death during intracellular infection was in YPO4118, which encodes the ribozyme/riboswitch *glmS*, a glucosamine-fructose-6-phosphate aminotransferase [52]. A second mutant strain with an insertion in the same genomic region displayed cytotoxicity below the cutoff value in the initial screen (37.6% of Tn*5*), but failed to elicit the same low level of cytotoxicity when analyzed a second time (66.3% of Tn*5*). Nevertheless, the values obtained in both analyses were well below 100% of that observed for the entire population of Tn*5* mutants and will be analyzed further. A second insertion in YPO4119 shows sequence homology to *glmU*, a gene located immediately upstream of *glmS* on the *Y. pestis* CO92 chromosome. *glmU* is thought to encode a protein that catalyzes the acetylation of glucosamine-1-phosphate and uridylation of N-

acetylglucosamine-1-phosphate to produce uridine dihosphate- N-acetylglucosamine (UDP-GlcNAc).

Sugar moieties play an important role in bacterial structure and function, such as cell wall and LPS biosynthesis, as well as in virulence [53]. In *Campylobacter jejuni,* protein glycosylation plays an integral role in attachment and invasion of human intestinal epithelial cells, and the colonization of intestinal tissues in mice [54, 55]. In addition, UDP-GlcNAc has been shown to be transferred to Rho, Rac, and Cdc42 by *Clostridium novyi* alpha-toxin to inhibit GTPase activity, leading to breakdown of the cytoskeleton [56, 57]. Although the role of protein glycosylation in *Y. pestis* virulence is unknown, a similar mechanism could be utilized by bacteria given the dose dependent requirement for the induction of cell death, and the loss of this activity in these mutants.

It is important to note that we also found a significant number of strains that resulted in the over-stimulation of LDH release, leading to a hypercytotoxic phenotype. Using the inverse parameters for loss-of-function strains (i.e. 150% of the average cytotoxicity observed for the entire population of Tn*5* mutants) 788 strains (7.9%) were determined to be gain-of-function mutants (Figure 3.7). Unexpectedly, sequence analysis indicates that several of the most cytotoxic strains have defects in genes known to promote the intracellular survival of *Y. pestis*. The *wecBC* operon is important for the synthesis of the eneterobacterial common antigen (ECA) and was previously shown to promote intracellular survival via an unknown mechanism [58]. In our screen, these strains measured

229.7% and 291.0% cytotoxicity when normalized to the value observed for the entire Tn*5* library tested, respectively. In addition, *wecB* insertions were found in two independent isolates.

Previous work in *F. tularensis* has shown that a hypercytotoxic phenotype associated with a mutant strains is indicative of the inability of the bacterium to survive intracellularly [59]. This was shown by Peng et al. where strains known to be hypercytotoxic were transformed with a reporter containing the luciferase gene under the control of a CMV promoter. Therefore, if intracellular bacteria are killed via lysis, the reporter is free to be expressed by the host cell. Indeed, hypercytotoxic mutants elicited higher levels of luciferase expression from the host cell than wild-type strains. In the subsequent analysis it was determined that defective intracellular survival leads to the lysis of the bacterium and release of PAMPs/DAMPs which activate the inflammasome, resulting in pyroptosis of the host cell. Thus, further examination of the hypercytotoxic strains identified in the screen could lead to the identification of novel factors necessary for the intracellular survival and proliferation of *Y. pestis*.

Taken together, the data support a working model whereby *Y. pestis* is capable of killing macrophages via established, as well as novel pathways leading to egress from the cell and extracellular disease. As shown in Figure 3.8, after being taken up by macrophages bacteria reside in a YCV. Upon thermally-induced expression of the T3SS, bacteria inject cytotoxic effect proteins into the host cell cytosol, leading to Caspase-3 directed apoptosis. In addition, via an

unknown mechanism, bacteria also induce cell death independent of T3S. Nevertheless, only bacteria capable of T3S accumulate outside of cells due to the extracellular injection of effectors that inhibit phagocytosis, and lead to exacerbated cell death, possibly freeing additional intracellular bacteria. Conversely, T3SS$^-$ bacteria are re-phagocytosed and sequestered intracellularly.

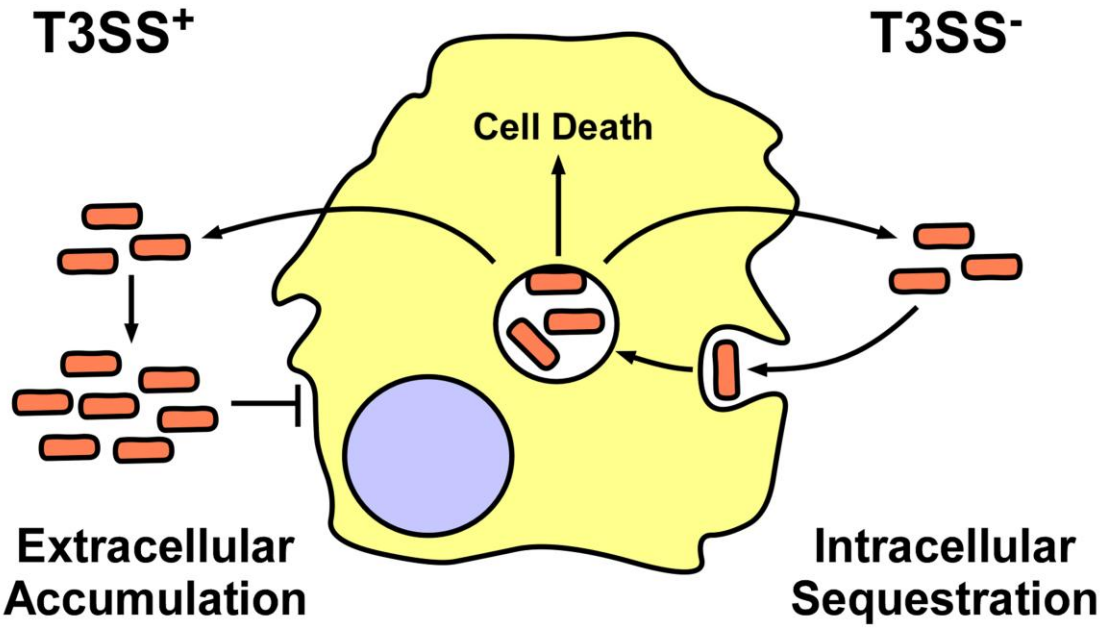

Figure 3.8. Model for the escape of *Yersinia pestis* from macrophages. After phagocytosis, bacteria reside in a YCV. From within this compartment, bacteria induce cell death via T3SS-mediated Yop injection, as well as though T3SS-independent pathways and both activities lead to the escape of bacteria from the cell. However, only in the presence of T3S are bacteria able to remain extracellular and promote further cell death via Yop injection.

It has not escaped our attention that this model provides a possible mechanism for the role of macrophages in the antibody-mediated clearance of plague. We have previously shown that protective anti-LcrV antibodies not only block T3S into macrophages, but also opsonize bacteria for phagocytic uptake [11]. However, Noel et al. showed that *Y. pestis* is able to survive in cells even when pre-opsonized with protective antibodies [16]. Given that bacteria lacking

LcrV are inhibited in their replication in the presence of macrophages, the same mechanism could control the replication of neutralized *Y. pestis* during infection, leading to an inhibition of bacterial growth at sites of infection and improved disease outcome. Directly testing this hypothesis would provide to a better understanding of the role of macrophages in the immune clearance of *Y. pestis* in the lung.

It is likely that the bacterial factor or factors necessary for intracellular *Y. pestis* to promote cell death independent of T3S is/are represented in strains identified in the loss-of-function transposon screen. Future studies aim to fully characterize these mutants and determine if losing the ability to promote cell death in the absence of T3S is detrimental to virulence *in vivo*. Furthermore, since T3SS-independent LDH release did not rely on Caspase-1 or Caspase-3, we aim to determine the cell death pathway responsible for this process and its role during intracellular infection. It is unknown whether *Y. pestis* utilizes an intracellular lifecycle to promote disease. Thus, better understanding this potentially important aspect of plague would not only provide an improved understanding of *Y. pestis* pathogenesis, but could lead to the development of novel therapeutics and intervention strategies useful for combatting disease.

3.6 Acknowledgements

NAE is supported by the NIH/NIGMS cellular and molecular biology training grant T32 GM008396. We thank Olaf Schneewind, Timothy Hermanas, Emily Traw, Lauriane Quenee, the University of Chicago, and the rest of the

members of the Howard T. Ricketts Laboratory at Argonne National Laboratory for providing the Tn*5* library. We also thank Susan Gater at the University of Missouri Laboratory for Infectious Disease Research for technical assistance with experiments requiring flow cytometry. Finally, we thank David Bland for providing critical comments regarding the manuscript.

3.7 References

1. Perry, R.D. and J.D. Fetherston, *Yersinia pestis--etiologic agent of plague.* Clin Microbiol Rev, 1997. **10**(1): 35-66.

2. Zhang, S.S., et al., *Plasminogen activator Pla of Yersinia pestis utilizes murine DEC-205 (CD205) as a receptor to promote dissemination.* J Biol Chem, 2008. **283**(46): 31511-21.

3. Du, Y., R. Rosqvist, and A. Forsberg, *Role of fraction 1 antigen of Yersinia pestis in inhibition of phagocytosis.* Infect Immun, 2002. **70**(3): 1453-60.

4. Weening, E.H., et al., *The dependence of the Yersinia pestis capsule on pathogenesis is influenced by the mouse background.* Infect Immun, 2011. **79**(2): 644-52.

5. Quenee, L.E., et al., *Yersinia pestis caf1 variants and the limits of plague vaccine protection.* Infect Immun, 2008. **76**(5): 2025-36.

6. Cornelius, C.A., et al., *Yersinia pestis IS1541 transposition provides for escape from plague immunity.* Infect Immun, 2009. **77**(5): 1807-16.

7. Davis, K.J., et al., *Pathology of experimental pneumonic plague produced by fraction 1-positive and fraction 1-negative Yersinia pestis in African green monkeys (Cercopithecus aethiops).* Arch Pathol Lab Med, 1996. **120**(2): 156-63.

8. Cornelis, G.R., *The type III secretion injectisome.* Nat Rev Microbiol, 2006. **4**(11): 811-25.

9. Matsumoto, H. and G.M. Young, *Translocated effectors of Yersinia.* Curr Opin Microbiol, 2009. **12**(1): 94-100.

10. Charnetzky, W.T. and W.W. Shuford, *Survival and growth of Yersinia pestis within macrophages and an effect of the loss of the 47-megadalton plasmid on growth in macrophages.* Infect Immun, 1985. **47**(1): 234-41.

11. Eisele, N.A. and D.M. Anderson, *Dual-function antibodies to Yersinia pestis LcrV required for pulmonary clearance of plague.* Clin Vaccine Immunol, 2009. **16**(12): 1720-7.

12. Grabenstein, J.P., et al., *Characterization of phagosome trafficking and identification of PhoP-regulated genes important for survival of Yersinia pestis in macrophages.* Infect Immun, 2006. **74**(7): 3727-41.

13. Pujol, C., et al., *Yersinia pestis can reside in autophagosomes and avoid xenophagy in murine macrophages by preventing vacuole acidification.* Infect Immun, 2009. **77**(6): 2251-61.

14. Klein, K.A. and J.B. Bliska, *How Yersinia pestis becomes a foreign obstruction in the digestive system of the macrophage.* Autophagy, 2009. **5**(6): 882-3.

15. Grabenstein, J.P., et al., *The response regulator PhoP of Yersinia pseudotuberculosis is important for replication in macrophages and for virulence.* Infect Immun, 2004. **72**(9): 4973-84.

16. Noel, B.L., et al., *Yersinia pestis can bypass protective antibodies to LcrV and activation with gamma interferon to survive and induce apoptosis in murine macrophages.* Clin Vaccine Immunol, 2009. **16**(10): 1457-66.

17. Pujol, C., et al., *Replication of Yersinia pestis in interferon gamma-activated macrophages requires ripA, a gene encoded in the pigmentation locus.* Proc Natl Acad Sci U S A, 2005. **102**(36): 12909-14.

18. Fukuto, H.S., et al., *Global gene expression profiling of Yersinia pestis replicating inside macrophages reveals the roles of a putative stress-induced operon in regulating type III secretion and intracellular cell division.* Infect Immun, 2010. **78**(9): 3700-15.

19. Straley, S.C. and P.A. Harmon, *Growth in mouse peritoneal macrophages of Yersinia pestis lacking established virulence determinants.* Infect Immun, 1984. **45**(3): 649-54.

20. Pujol, C. and J.B. Bliska, *The ability to replicate in macrophages is conserved between Yersinia pestis and Yersinia pseudotuberculosis.* Infect Immun, 2003. **71**(10): 5892-9.

21. Zhang, Y., G. Romanov, and J.B. Bliska, *Type III secretion system-dependent translocation of ectopically expressed Yop effectors into macrophages by intracellular Yersinia pseudotuberculosis.* Infect Immun, 2011. **79**(11): 4322-31.

22. Smiley, S.T., *Immune defense against pneumonic plague.* Immunol Rev, 2008. **225**: 256-71.

23. Quenee, L.E. and O. Schneewind, *Plague vaccines and the molecular basis of immunity against Yersinia pestis.* Hum Vaccin, 2009. **5**(12): 817-23.

24. Eisele, N.A., et al., *Chemokine receptor CXCR2 mediates bacterial clearance rather than neutrophil recruitment in a murine model of pneumonic plague.* Am J Pathol, 2011. **178**(3): 1190-200.

25. Donnenberg, M.S. and J.B. Kaper, *Construction of an eae deletion mutant of enteropathogenic Escherichia coli by using a positive-selection suicide vector.* Infect Immun, 1991. **59**(12): 4310-7.

26. Parent, M.A., et al., *Cell-mediated protection against pulmonary Yersinia pestis infection.* Infect Immun, 2005. **73**(11): 7304-10.

27. Brubaker, R.R., E.D. Beesley, and M.J. Surgalla, *Pasteurella pestis: Role of Pesticin I and Iron in Experimental Plague.* Science, 1965. **149**(3682): 422-4.

28. Bland, D.M., et al., *Novel Genetic Tools for Diaminopimelic Acid Selection in Virulence Studies of Yersinia pestis.* PLoS One, 2011. **6**(3): e17352.

29. Une, T. and R.R. Brubaker, *In vivo comparison of avirulent Vwa- and Pgm- or Pstr phenotypes of yersiniae.* Infect Immun, 1984. **43**(3): 895-900.

30. Zhang, Y., et al., *Type III secretion decreases bacterial and host survival following phagocytosis of Yersinia pseudotuberculosis by macrophages.* Infect Immun, 2008. **76**(9): 4299-310.

31. Kirillina, O., et al., *HmsP, a putative phosphodiesterase, and HmsT, a putative diguanylate cyclase, control Hms-dependent biofilm formation in Yersinia pestis.* Mol Microbiol, 2004. **54**(1): 75-88.

32. Simm, R., et al., *Phenotypic convergence mediated by GGDEF-domain-containing proteins.* J Bacteriol, 2005. **187**(19): 6816-23.

33. Lambden, P.R. and W.T. Drabble, *The gua operon of Escherichia coli K-12: evidence for polarity from guaB to guaA.* J Bacteriol, 1973. **115**(3): 992-1002.

34. Camilli, A. and B.L. Bassler, *Bacterial small-molecule signaling pathways.* Science, 2006. **311**(5764): 1113-6.

35. Mills, E., et al., *The bacterial second messenger c-di-GMP: mechanisms of signalling.* Cell Microbiol, 2011. **13**(8): 1122-9.

36. Sun, Y.C., et al., *Differential control of Yersinia pestis biofilm formation in vitro and in the flea vector by two c-di-GMP diguanylate cyclases.* PLoS One, 2011. **6**(4): e19267.

37. Bobrov, A.G., et al., *Insights into Yersinia pestis biofilm development: topology and co-interaction of Hms inner membrane proteins involved in exopolysaccharide production.* Environ Microbiol, 2008. **10**(6): 1419-32.

38. Bobrov, A.G., et al., *Systematic analysis of cyclic di-GMP signalling enzymes and their role in biofilm formation and virulence in Yersinia pestis.* Mol Microbiol, 2011. **79**(2): 533-51.

39. Banos, R.C., et al., *A global modulatory role for the Yersinia enterocolitica H-NS protein.* Microbiology, 2008. **154**(Pt 5): 1281-9.

40. Jackson, M.W., E. Silva-Herzog, and G.V. Plano, *The ATP-dependent ClpXP and Lon proteases regulate expression of the Yersinia pestis type III secretion system via regulated proteolysis of YmoA, a small histone-like protein.* Mol Microbiol, 2004. **54**(5): 1364-78.

41. Cathelyn, J.S., et al., *The RovA regulons of Yersinia enterocolitica and Yersinia pestis are distinct: evidence that many RovA-regulated genes were acquired more recently than the core genome.* Mol Microbiol, 2007. **66**(1): 189-205.

42. Ellison, D.W. and V.L. Miller, *H-NS represses inv transcription in Yersinia enterocolitica through competition with RovA and interaction with YmoA.* J Bacteriol, 2006. **188**(14): 5101-12.

43. Cornelis, G.R., et al., *ymoA, a Yersinia enterocolitica chromosomal gene modulating the expression of virulence functions.* Mol Microbiol, 1991. **5**(5): 1023-34.

44. Hertle, R., et al., *Specific phosphatidylethanolamine dependence of Serratia marcescens cytotoxin activity.* Mol Microbiol, 1997. **26**(5): 853-65.

45. Hertle, R., et al., *Cytotoxic action of Serratia marcescens hemolysin on human epithelial cells.* Infect Immun, 1999. **67**(2): 817-25.

46. Hertle, R. and H. Schwarz, *Serratia marcescens internalization and replication in human bladder epithelial cells.* BMC Infect Dis, 2004. **4**: 16.

47. Schiebel, E., H. Schwarz, and V. Braun, *Subcellular location and unique secretion of the hemolysin of Serratia marcescens.* J Biol Chem, 1989. **264**(27): 16311-20.

48. Schiebel, E. and V. Braun, *Integration of the Serratia marcescens haemolysin into human erythrocyte membranes.* Mol Microbiol, 1989. **3**(3): 445-53.

49. Strauss, E.J., N. Ghori, and S. Falkow, *An Edwardsiella tarda strain containing a mutation in a gene with homology to shlB and hpmB is*

defective for entry into epithelial cells in culture. Infect Immun, 1997. **65**(9): 3924-32.

50. Schnupf, P. and D.A. Portnoy, *Listeriolysin O: a phagosome-specific lysin.* Microbes Infect, 2007. **9**(10): 1176-87.

51. Glomski, I.J., A.L. Decatur, and D.A. Portnoy, *Listeria monocytogenes mutants that fail to compartmentalize listerolysin O activity are cytotoxic, avirulent, and unable to evade host extracellular defenses.* Infect Immun, 2003. **71**(12): 6754-65.

52. Tinsley, R.A., J.R. Furchak, and N.G. Walter, *Trans-acting glmS catalytic riboswitch: locked and loaded.* RNA, 2007. **13**(4): 468-77.

53. Raetz, C.R., et al., *Lipid A modification systems in gram-negative bacteria.* Annu Rev Biochem, 2007. **76**: 295-329.

54. Szymanski, C.M., D.H. Burr, and P. Guerry, *Campylobacter protein glycosylation affects host cell interactions.* Infect Immun, 2002. **70**(4): 2242-4.

55. Karlyshev, A.V., et al., *The Campylobacter jejuni general glycosylation system is important for attachment to human epithelial cells and in the colonization of chicks.* Microbiology, 2004. **150**(Pt 6): 1957-64.

56. Selzer, J., et al., *Clostridium novyi alpha-toxin-catalyzed incorporation of GlcNAc into Rho subfamily proteins.* J Biol Chem, 1996. **271**(41): 25173-7.

57. Busch, C., et al., *Characterization of the catalytic domain of Clostridium novyi alpha-toxin.* Infect Immun, 2000. **68**(11): 6378-83.

58. Klein, K.A., et al., *A Transposon Site Hybridization Screen Identifies galU and wecBC as Important for Survival of Yersinia pestis in Murine Macrophages.* J Bacteriol, 2012. **194**(3): 653-62.

59. Peng, K., et al., *Elevated AIM2-mediated pyroptosis triggered by hypercytotoxic Francisella mutant strains is attributed to increased intracellular bacteriolysis.* Cell Microbiol, 2011. **13**(10): 1586-600.

CHAPTER 4

CHEMOKINE RECEPTOR CXCR2 MEDIATES BACTERIAL CLEARANCE RATHER THAN NEUTROPHIL RECRUITMENT IN A MURINE MODEL OF PNEUMONIC PLAGUE

As found in: *Eisele, N. A., H. Lee-Lewis, et al. (2011). "*Chemokine receptor CXCR2 mediates bacterial clearance rather than neutrophil recruitment in a murine model of pneumonic plague*." Am J Pathol 178(3): 1190-1200.*

4.1 Abstract

Pulmonary infection by *Yersinia pestis* causes pneumonic plague, a necrotic bronchopneumonia that is rapidly lethal and highly contagious. Acute pneumonic plague accompanies the up regulation of pro-inflammatory cytokines and chemokines suggesting that the host innate immune response may contribute to the development of disease. To address this possibility, we sought to understand the consequences of neutrophil recruitment during pneumonic plague and we studied the susceptibility of C3H-HeN mice lacking the CXC chemokine KC or its receptor CXC receptor 2 (CXCR2) to pulmonary *Y. pestis* infection. We found that without *Kc* or *Cxcr2*, disease progression was accelerated both in bacterial growth and development of primary bronchopneumonia. When examined in an antibody clearance model, *Cxcr2*$^{-/-}$

mice were not protected by neutralizing *Y. pestis* antibodies, yet bacterial growth in the lungs was delayed in a manner associated with a neutrophil-mediated inflammatory response. After this initial delay, however, robust neutrophil recruitment in *Cxcr2*$^{-/-}$ mice correlated with bacterial growth and the development of fulminant pneumonic and septicemic plague. In contrast, attenuated *Y. pestis* lacking the conserved pigmentation locus could be cleared from the lungs in the absence of CXCR2 indicating virulence factors within this locus may inhibit CXCR2 independent pathways of bacterial killing. Together, the data suggest CXCR2 uniquely induces host defense mechanisms that are effective against virulent *Y. pestis* raising new insight into the activation of neutrophils during infection.

4.2 Introduction

The mammalian respiratory tract has limited host defense mechanisms against pathogenic microbes. Upon infection, alveolar macrophages, fibroblasts, and endothelial and epithelial cells produce chemokines to attract immune effector cells such as neutrophils, macrophages and NK cells to the lungs [1]. Two families of chemokines, CC and CXC, predominantly signal these cells in response to recognition of invading microbes using pattern recognition receptors or as a response to lung injury induced by the pathogen. In addition to signaling the induction of adhesive factors, such as integrins, necessary for neutrophil chemotaxis, CXC chemokines also signal activation of these cells to enable an increase in intracellular Ca^{+2} which is necessary for exocytosis and other effector responses that stimulate killing of microbes [2]. Antibodies that opsonize the pathogen accelerate the activation of these signaling pathways, as well as additional pathways involving the complement or Fcγ receptors and improve the efficiency of phagocytic killing by neutrophils [3]. These multiple signaling pathways of neutrophil recruitment and activation induced by antibodies ensure a robust response to infection.

CXC chemokines are potent neutrophil attractants and are involved in host defense against extracellular pathogens. In mice, chemokines KC and MIP-2 are part of the CXC family and are considered likely functional homologues of human interleukin-8 (IL-8) [4, 5]. Secretion of KC and macrophage inflammatory protein-2 (MIP-2) induces extravascular migration of neutrophils to sites of infection,

cellular apoptosis and tissue damage by signaling predominantly through CXC receptor 2 (CXCR2) [6]. *Cxcr2* is highly homologous between mouse and human and is expressed by a variety of immune cells, including neutrophils, monocytes, eosinophils, mast cells, basophils, and lymphocytes [7]. CXC chemokine secretion can be triggered through recognition of bacterial peptidoglycan or lipopolysaccharide (LPS) causing migration of neutrophils to an infection site and the activation of clearance mechanisms [8-11]. Likewise, CXC chemokines are also produced in response to apoptosis or host cell damage resulting in infiltration of neutrophils to injured tissue to clean up dead cells [12]. Mice unable to signal through CXCR2 are more susceptible to many bacterial and even some viral infections, both respiratory and nonrespiratory, but less susceptible to inflammatory injury [10, 13-19]. For many respiratory infections, absence of *Cxcr2* results in increased colonization and decreased neutrophil recruitment to the infected site. For example, in response to *Streptococcus pneumoniae* infection, wild-type mice recruit more neutrophils than *Cxcr2*$^{-/-}$ mice during 48 to 72 hours, and these numbers decline in time as the mice clear the infection [15]. Similarly, in response to Rhinovirus infection, *Cxcr2*$^{-/-}$ mice recruit fewer neutrophils over at least a 96-hour time period as compared to wild-type mice and this decrease is associated with an increase in disease in the mutant mice [13]. Many other examples of bacterial infections that are cleared by CXCR2 dependent recruitment of neutrophils during the early innate immune response

have been described, and in each case, *Cxcr2* mutants have decreased neutrophil chemotaxis associated with increased bacterial load.

CXCR2 is also associated with neutrophil-induced host injury, such as what occurs in the lungs during bacterial sepsis [20, 21]. CXCR2-dependent infiltration and activation of neutrophils to the lungs causes acute injury and pneumonia independent of bacterial colonization of the respiratory tract, suggesting unregulated migration and activation of neutrophils severely damages host tissues [22, 23]. Small molecule antagonists of CXCR2 can inhibit lipopolysaccharide-induced lung pathology by blocking neutrophil migration to the infection site, suggesting that preventing the activation of CXCR2 can prevent septicemic disease [24].

Primary pneumonic plague is a deadly bronchopneumonia that develops following inhalation of *Y. pestis*. The disease is similar in rodents and man, and is characterized by parenchymal congestion by polymorphonuclear cells, large bacterial colonies, alveolar destruction, and edema [25-27]. *Y. pestis* virulence factors manipulate innate immune responses to avoid detection and promote disease [28]. Pattern recognition receptors such as toll-like receptors 2, 4, or 5 do not appear to be activated during infection due in large part to the presence of a noncanonical lipopolysaccharide, and a lack of flagellin, which helps prevents an initial inflammatory response in the host [29]. Further immune modulation and cytotoxicity is conferred by a type III secretion system (T3SS) by which extracellular bacteria target macrophages and other immune cells to inject them

with proteins that inhibit phagocytosis, alter inflammatory signaling pathways, modulate NF-κB signaling, and result in the death of the target cell [28, 30]. Late-stage disease involves a large induction of IFN-γ, chemokines, and other systemic pro-inflammatory cytokines [26, 31, 32]. Neutrophil infiltration is prominent in pathological lesions of moribund mice and rats and is associated with bacteria and tissue necrosis [26, 27, 31-33]. These observations suggest that *Y. pestis* replication strongly promotes neutrophil infiltration during late stage disease, but this response is ineffective and may even be detrimental to the host.

Immunity to the plague can be conferred by antibodies to low calcium response V-antigen LcrV, a component of the T3SS system required for immune evasion and disease [34-37]. Neutralizing LcrV antibodies block the T3SS and promote phagocytosis, and both activities are required for immunity, suggesting that opsonization of bacteria plays an important role in clearance [38-40]. The type III secretion system is a strategy of extracellular bacteria; however *Y. pestis* is capable of surviving inside activated macrophages in a manner dependent on the pigmentation (*pgm*) locus, a 102-kb pathogenicity island required for development of pneumonic and bubonic plague [33, 41-46]. Furthermore, antibody-mediated phagocytosis of *Y. pestis* does not lead to its destruction inside activated macrophages *in vitro*, leaving the mechanism of immunity uncertain [47].

In this work, we addressed the role of chemokines and neutrophils in plague, both during disease and in clearance after treatment with protective LcrV

antibodies that broadly stimulate innate immune activation. We studied mice defective in signaling through CXC chemokines and characterized host responses to pulmonary *Y. pestis* challenge. We found that CXCR2 provided protective responses in both models but had minimal impact on neutrophil recruitment to infected sites. Early containment of the infection was seen in anti-LcrV treated *Cxcr2*$^{-/-}$ mice in a manner that was associated with neutrophil recruitment and little to no damaged lung tissue. Despite these seemingly protective responses, however, *Cxcr2*$^{-/-}$ mice later developed systemic disease and acute bronchopneumonia that were indistinguishable from untreated mice, suggesting that other, seemingly redundant, pathways of neutrophil recruitment and activation may be ineffective against *Y. pestis*. Systemic ablation of neutrophils also resulted in loss of antibody protection that mimicked the loss of protection seen in *Cxcr2*$^{-/-}$ mice consistent with CXCR2 as the primary mechanism for inducing bacterial clearance. Deletion of the *pgm* locus rendered *Y. pestis* sensitive to CXCR2-independent clearance, indicating this region encodes virulence factors that likely inhibit activation of neutrophils. Together the data support a model whereby CXCR2 signaling of neutrophils is necessary to destroy virulent *Y. pestis*, whereas other chemotactic pathways stimulate recruitment of neutrophils that are inactivated by products of the *pgm* locus allowing rapid bacterial replication and fulminant disease.

4.3 Materials and Methods

Bacterial Strains. All *Y. pestis* culture strains used were taken from frozen stocks and streaked for isolation onto heart infusion agar (HIA) plates. The plates used for *Y. pestis* CO92 were supplemented with 0.005% (w/v) Congo Red and 0.2% (w/v) galactose to screen for bacteria that retain the pigmentation locus [48]. For the pneumonic plague challenge, a single, red-pigmented colony was used to inoculate heart infusion broth (HIB) supplemented with 2.5 mM $CaCl_2$ and grown 18 to 24 hours at 37°C, at 120 rpm. All handling of samples containing live *Y. pestis* CO92 was performed in a select agent authorized BSL3 facility under protocols approved by the University of Missouri Institutional Biosafety Committee. Nonpigmented *Y. pestis* CO92 and KIM D27 were routinely grown fresh from frozen stock on HIA, followed by aerobic growth at 27ºC in HIB overnight before use in experiments [33, 42].

Animals. All animal procedures were in strict accordance with the National Institutes of Heath Guide for the Care and Use of Laboratory Animals and were approved by the University of Missouri Animal Care and Use Committee. C3H-HeNCrl (C3H) mice were used for studies on host responses to plague and were the parent strain of the $Kc^{-/-}$ and $Cxcr2^{-/-}$ mice. Wild-type C3H mice were purchased from Charles River Laboratories (Wilmington, MA). Knockout mice were bred and housed in barrier containment facilities at the University of Missouri. Males and females, ranging from 15 to 50 g were used for challenge experiments. During challenge, mice were maintained in select agent approved

animal containment facilities at the University of Missouri. All infected mice were monitored regularly by daily weighing and assignment of health scores. Animals that survived to the end of the 14 day observation period or were identified as moribund (defined by pronounced ataxia sometimes accompanied by severe dyspnea) were euthanized by CO_2 asphyxiation followed by bilateral pneumothorax. These methods are approved by the American Veterinary Medical Association Guidelines on Euthanasia.

Pneumonic Plague Challenge. *Y. pestis* CO92, grown as previously described at 37°C, were diluted in sterile PBS to 400, 4000 or 6000 colony forming units (CFU)/0.02 ml just before use for challenge experiments. Actual dose and retention of the pigmentation locus were determined by plating in triplicate on HIA with Congo Red. Where indicated, for some intranasal infections involving nonpigmented *Y. pestis* strains, mice were given 500 μg $FeCl_2$ in H_2O by intraperitoneal injection just before challenge. All animals intranasally infected with *Y. pestis* were first lightly anesthetized by isoflurane inhalation. Animals were observed for recovery from anesthesia and returned to housing.

Purification of Antibody. Rabbit polyclonal LcrV was produced as previously described; serum antibody titer to recombinant LcrV was 10^5 for all experiments [39]. For purification, rabbit serum containing α-LcrV antibodies was applied to a protein G column and purified according to the manufacturer's protocol (Sigma, St. Louis, MO). Samples were then applied to a PD-10 buffer exchange column (GE Healthcare, Buckinghamshire, UK) and eluted in PBS. Total IgG was

quantified using bovine IgG as a standard in a BCA protein assay (Pierce, Rockford, IL).

Antibody Treatment. For pneumonic plague challenges, 400 µg/0.4 ml purified antibody was given by intraperitoneal injection 60 minutes before infection. Untreated control mice were given 400 µl sterile PBS by intraperitoneal injection 60 minutes before challenge. In some experiments, mice were given rat anti-mouse Gr-1 (RB6.8C5) monoclonal antibodies (BD Pharmingen, San Jose, CA) intraperitoneally in 100 µg (100 µg/100 µl) or 200 µg (200 µg/200 µl) doses at the times indicated. Control mice in these experiments were given equivalent volumes of PBS.

Quantification of Bacterial Load in Blood and Tissues. Immediately after euthanasia, blood was collected directly from the heart by cardiac puncture. Lungs, spleens and livers were collected aseptically and homogenized in 1 ml sterile PBS. Serial dilutions of the blood and homogenized tissues were then plated onto HIA plates for quantification of bacterial load (CFU/mL or CFU/organ, respectively).

Histopathological Evaluation of Tissues. Lungs were perfused with 10% (v/v) formalin before removal; all other tissues were collected and placed in 10% (v/v) formalin. All tissues were fixed for a minimum of 48 hours. Fixed tissues were embedded in paraffin and sections were cut and stained with H&E. For histological scoring of neutrophil infiltration (judged by staining positive for Gr-1 by immunohistochemistry), bacterial colonies, congestion, edema and alveolar

destruction, lung lobes were evaluated in a single blind fashion by a veterinarian with expertise in the pathological analysis of disease in rodents.

Immunohistochemistry. Tissues that had been fixed in 10% (v/v) formalin as previously described were sectioned onto slides for immunohistochemical analysis. Slides were stained with rat anti-mouse F4/80 (Serotec, Oxford, UK) or monoclonal anti-Gr-1 (RB6.8C5 [49]) and detection was achieved by secondary staining with biotinylated rabbit anti-rat IgG and HRP-streptavidin (Dako, Carpenteria, CA). Staining and detection were carried out according to the manufacturer's guidelines.

Statistical Analysis. Survival and mean time to death were evaluated for statistical significance between groups using the Mann-Whitney rank sum test. Pathological scores were evaluated by one way ANOVA followed by Dunn's method for multiple comparisons. Percent weight loss compared to pre-challenge weight as well as neutrophil recruitment in lesions with and without bacteria were evaluated by Student's *t*-test. Significance was concluded if $p < 0.05$.

4.4 Results

4.4.1. CXC Chemokines Contribute to the Clearance of Y. pestis *CO92 from the Lung.*

CXC chemokines, such as KC, are produced by resident macrophages and other phagocytic cells of the mammalian lung in response to bacterial invasion. High level production of KC is stimulated during pneumonic plague in

mice, suggesting it may be active in promoting neutrophil recruitment to infected areas [31]. To understand the consequences of KC production, we challenged C3H-HeN mice carrying a homozygous deletion of *KC* (*Kc*$^{-/-}$) by intranasal instillation of *Y. pestis* CO92 and followed the development of disease for a 14 day period. At a challenge dose of 4,000 CFU, 100% of *Kc*$^{-/-}$ mice succumbed to infection compared to only 20% of wild-type mice (Figure 4.1A; $p < 0.05$). These results strongly suggest that KC serves a protective role in host defense against pulmonary *Y. pestis* challenge.

We also tested whether KC was important to antibody-mediated immunity to *Y. pestis* in a passive transfer of immunity model. In this model, opsonized *Y. pestis* would be predicted to broadly stimulate the innate immune system, including production of pro-inflammatory cytokines and chemokines as well as complement and Fcγ receptor (FcR) allowing us to ascertain whether CXCR2 is uniquely required for host defense or if other neutrophil recruitment or activation pathways can be substituted. Anti-LcrV treated *Kc*$^{-/-}$ mice appeared only partially protected and 40% died with a mean time to death of 5.75 days compared to 100% survival in wild-type (Figure 4.1B, $p > 0.05$). These results are consistent with the involvement of KC in antibody-mediated immunity, but suggest that other protective signaling mechanisms also occur. Moribund *Kc*$^{-/-}$ mice that were not treated with anti-LcrV typically exhibited both severe dypsnea and ataxia. Lungs from these mice were examined for histopathology by staining with hematoxylin and eosin (H&E) and by immunohistochemistry to identify injury, neutrophil

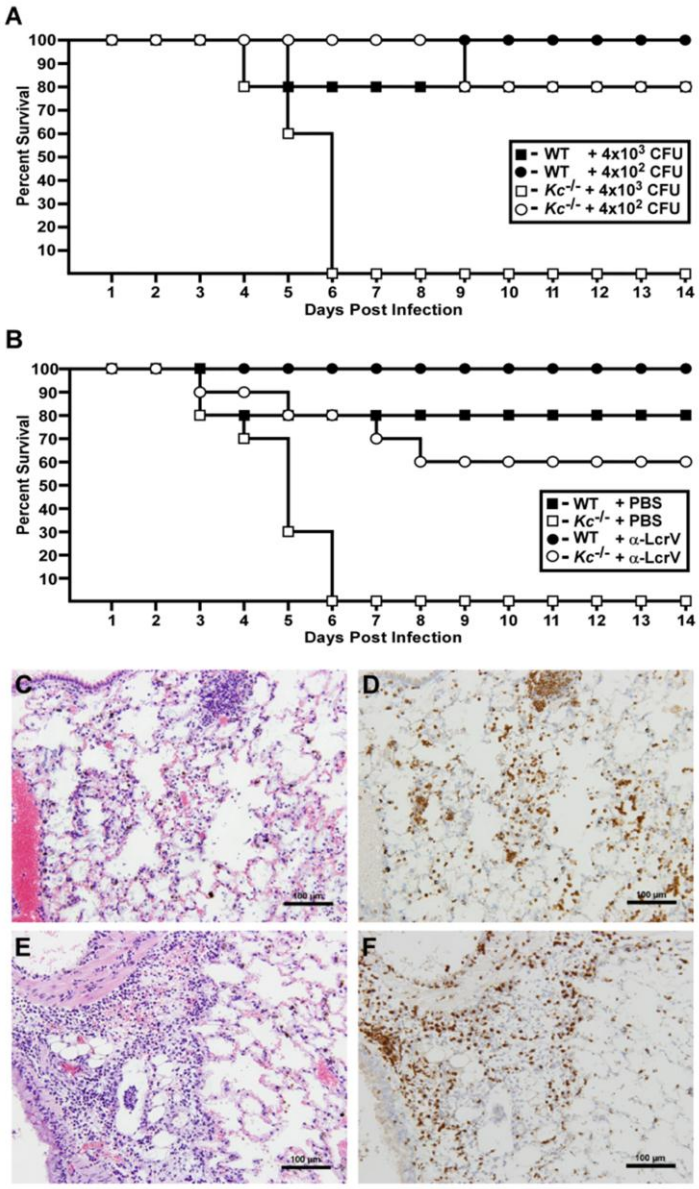

Figure 4.1. KC contributes to protection against pneumonic plague. (A) Wild-type (WT, n=5) or *Kc*$^{-/-}$ C3H mice (n=5) were challenged by intranasal (IN) infection with the indicated doses of *Y. pestis* CO92 and survival was monitored for 14 days. (B) Mice were given 400µg anti-LcrV polyclonal antibody (n=3 for Wild-type; n=5 for *Kc*$^{-/-}$); or PBS (n=5 for wild-type; n=5 for *Kc*$^{-/-}$) by intraperitoneal (IP) injection 60 minutes prior to IN challenge with *Y. pestis* CO92 and survival was monitored over a 14 day period; Data shown were collected in one of two independent experiments with equivalent challenge doses and similar results (n=10 *Kc*$^{-/-}$ mice were analyzed for treated and untreated groups). Lungs from moribund mice were inflated with 10% (v/v) formalin, fixed for 48 hours before staining with hemotoxylin and eosin (C&E) or anti-Gr-1 (D&F). Both wild-type (C-D) and *Kc*$^{-/-}$ (E-F) mice developed acute bronchopneumonia with infiltration of neutrophils. Representative images are shown at 20X magnification.

infiltration, and bacterial burden to characterize the development of pneumonic plague. Immunohistochemistry with anti-Gr-1, an antibody that stains neutrophils and some monocytes, was also performed to confirm the identity of these cells. Wild-type and *Kc*$^{-/-}$ mice both developed acute bronchopneumonia, characterized by large bacterial colonies, cellular debris and infiltration of neutrophils that was indistinguishable from one another (Figure 4.1C-F). In each strain, spleens and livers of moribund mice showed evidence of advancing systemic disease, characterized by tissue necrosis and hemorrhage in the spleen and multiple foci of inflammation in the liver (data not shown). Together, these results suggest that KC production, whether during untreated or antibody-treated infection, plays a protective role against pneumonic plague.

4.4.2. CXCR2 is Essential for Protection Against Pneumonic Plague.

In mice, KC and other CXC chemokines signal through CXCR2 to recruit neutrophils during bacterial infections [50]. Therefore, we analyzed *Cxcr2*$^{-/-}$ mice to understand the role of neutrophil infiltration at a more global level. Groups of five to eight wild-type C3H or *Cxcr2*$^{-/-}$ mice were treated with PBS just before intranasal challenge with 6,000 CFU *Y. pestis* CO92. Wild-type and *Cxcr2*$^{-/-}$ mice were similarly susceptible to acute disease which developed within 4 days of infection (Figure 4.2, $p > 0.05$). In contrast, while wild-type mice were protected by neutralizing antibodies and did not develop signs of disease, all but one *Cxcr2*$^{-/-}$ mouse succumbed to the infection ($p < 0.05$, compared to wild-type treated mice with anti-LcrV). Notably, these mice were initially protected by the antibodies

which provided an extension in the mean time to death (6.3 days for treated mice compared to 4.4 days for untreated mice, p <0.005). These results suggest that CXCR2 independent responses lead to early containment but not clearance of *Y. pestis*.

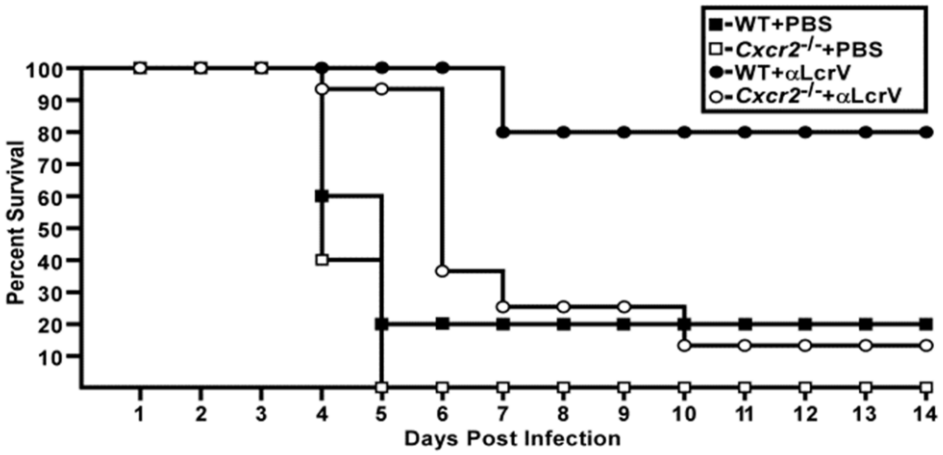

Figure 4.2. *Cxcr2* is essential for protection against pneumonic plague. Wild-type (n=5) or *Cxcr2*$^{-/-}$ (n=5) C3H mice were given PBS or 400 µg anti-LcrV polyclonal antibody (n=13 for *Cxcr2*$^{-/-}$) by IP injection 60 minutes prior to IN infection with 6,000 CFU *Y. pestis* CO92 and survival was monitored over a 14 day period. Data for *Cxcr2*$^{-/-}$ treated with anti-LcrV were collected in 2 independent experiments.

4.4.3. Neutrophil Infiltration Correlates with Bacterial Replication and Lung Injury.

We next compared disease progression between wild-type and *Cxcr2*$^{-/-}$ mice from both antibody-treated and PBS-treated groups. In this experiment, wild-type or *Cxcr2*$^{-/-}$ mice were treated with either PBS or anti-LcrV via intraperitoneal injection 60 minutes before challenge by intranasal instillation of *Y. pestis* CO92. At 60 hours post-infection, we examined either bacterial load or pathology of the lungs, liver and spleen of these mice. All PBS-treated *Cxcr2* mutant mice had a high titer of bacteria in the lungs which only occasionally had

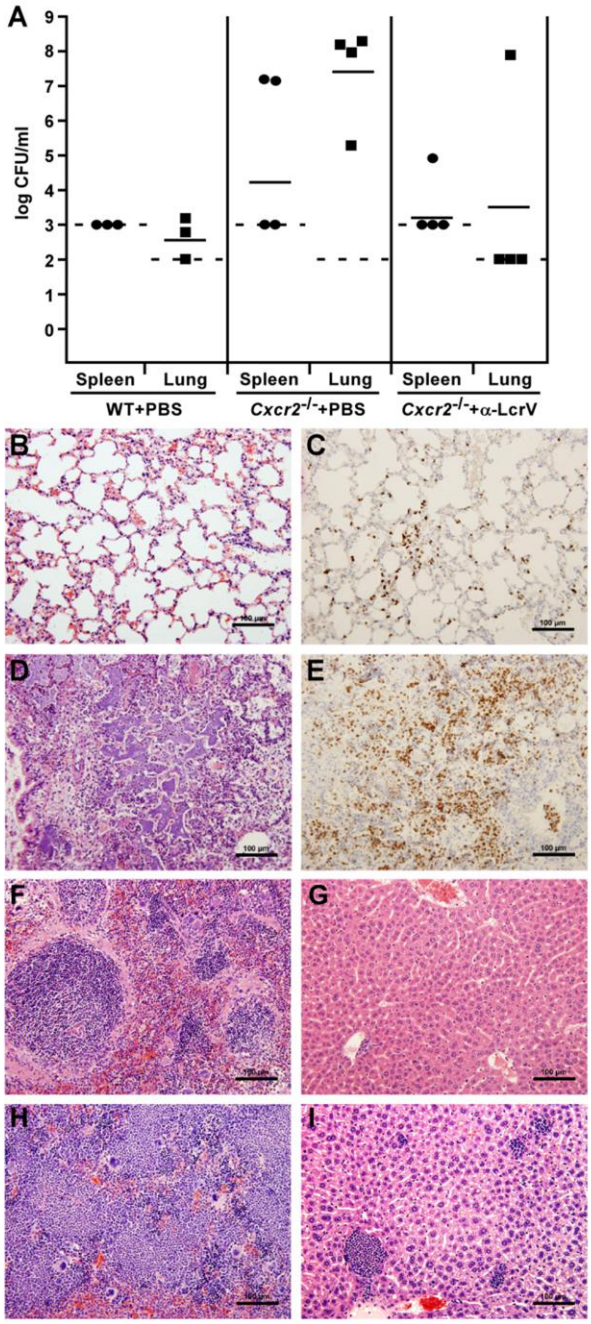

Figure 4.3. Primary pneumonic plague develops more rapidly in *Cxcr2*$^{-/-}$ mice. Wild-type (n=3) or *Cxcr2*$^{-/-}$ (n=4) C3H mice were given PBS IP 60 minutes prior to IN infection with 6,000 CFU *Y. pestis* CO92. Mice were euthanized 60 hours post-infection and tissues were harvested and diluted in PBS to analyze for bacterial burden (A) or fixed in 10% (v/v) formalin to analyze by histopathology (B-I). WT lungs (B-C), spleen (F) and liver (G); *Cxcr2*$^{-/-}$ lungs (D-E), spleen (H) and liver (I). Anti-mouse Gr-1 was used in immunohistochemistry for identification of neutrophils (C, E). Dashed lines indicate the limit of detection and solid lines indicate the geometric mean of the samples (A). Images are shown at 20X magnification.

disseminated to distal tissues, suggestive of primary pneumonic plague (Figure 4.3A). Analyses of histological sections confirmed these observations, whereas wild-type PBS-treated mice had only mild to moderate infiltration of neutrophils and no visible bacteria (Figure 4.3B-C), all *Cxcr2*$^{-/-}$ mice treated with PBS had severe bronchopneumonia, with neutrophils surrounding foci of bacteria (Figure 4.3D-E). The liver and spleen from these mice had developed minor to moderate disease indicating systemic spread of the infection (Figure 4.3F-I).

In contrast, we recovered bacteria from only one of four anti-LcrV treated *Cxcr2*$^{-/-}$ mice at 60 hours post-infection, indicating that fewer than 100 CFU were generally present in the lungs at this time point. Nevertheless, histological analyses of the lungs from anti-LcrV treated *Cxcr2*$^{-/-}$ mice at 60 hours post-infection revealed moderate infiltration of neutrophils in all three animals examined, two of which harbored occasional bacteria (Figure 4.4E-F, see Supplemental Table S4.1). Similarly, inflammatory responses were also seen in the liver and spleen (Figure 4.4G-H, see Supplemental Table S4.2). In contrast, lungs, liver and spleen from wild-type anti-LcrV treated mice had few to no disease lesions nor neutrophils at 60 hours post-infection (Figure 4.4A-D; see Supplemental Table S4.3). Together these results suggest that *Cxcr2* mutant mice initially contain the infection after treatment with protective antibodies.

We next evaluated bacterial load and disease severity in antibody-treated *Cxcr2*$^{-/-}$ mice challenged with *Y. pestis* CO92 after 90 hours post-infection, when mice in this group showed signs of acute disease. All mice examined harbored a

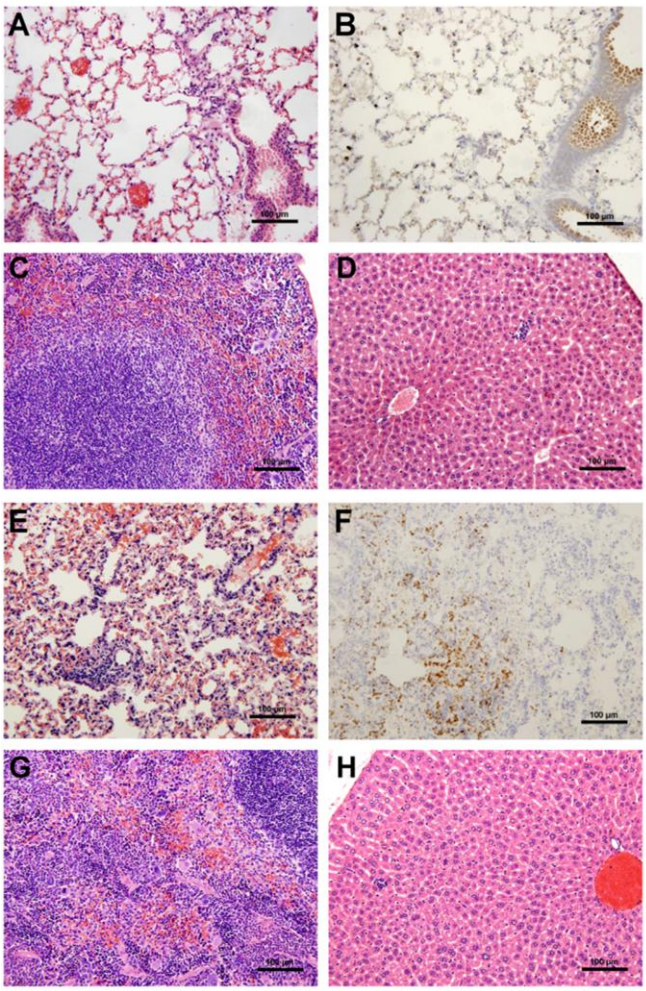

Figure 4.4. Anti-LcrV antibody treatment slows the progression of disease in *Cxcr2*$^{-/-}$ mice. WT and *Cxcr2*$^{-/-}$ mice, treated with 400 µg anti-LcrV polyclonal antibody IP 60 min prior to IN challenge with 6,000 CFU *Y. pestis* CO92 as above, were euthanized 60 hours post-infection, tissues harvested and fixed in 10% (v/v) formalin for histochemical and immunohistochemical analysis. WT lungs (A-B), spleen (C) and liver (D); C*xcr2*$^{-/-}$ lungs (E-F), spleen (G) and liver (H). Immunohistochemistry with anti-Gr-1 was used to identify neutrophils (B and F). Images are shown at 20X magnification.

high titer of bacteria in the lungs (Figure 4.5A). Five of six mice examined also harbored detectable amounts of bacteria in the blood, indicating systemic disease. A second group of four anti-LcrV treated *Cxcr2*$^{-/-}$ mice, also euthanized 90 hours post-infection, was examined by histopathology of formalin-fixed

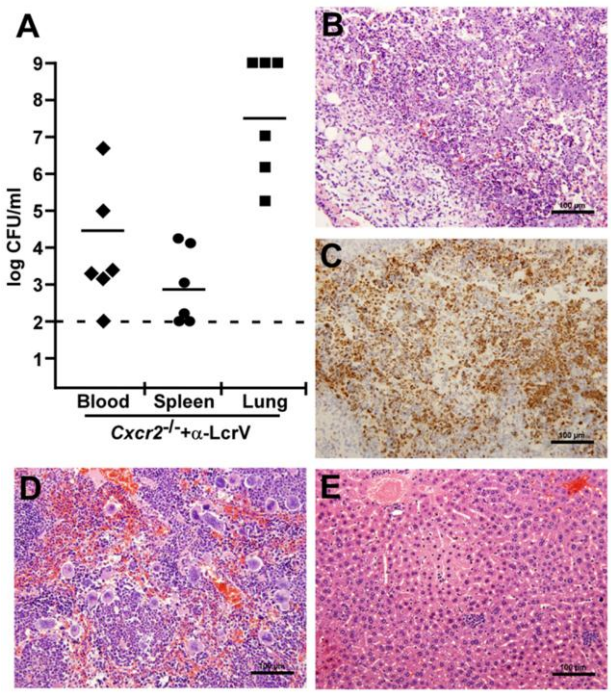

Figure 4.5. Anti-LcrV antibody treatment initially contains the infection but does not prevent development of pneumonic or septicemic plague. *Cxcr2*$^{-/-}$ mice (n=6) were given 400 µg anti-LcrV polyclonal antibodies and challenged IN with 6,000 CFU *Y. pestis* CO92. Blood, spleen, and lung were analyzed for bacterial burden at 90 hours post-infection, when death is first seen for this group (A). (B-E) A second group *Cxcr2*$^{-/-}$ mice (n=4) was challenged with the same dose following anti-LcrV treatment, euthanized 90 hours post-infection and lungs (B-C), spleen (D) and liver (E) were removed, formalin fixed, stained, and analyzed for histopathology. Tissue sections were also stained with anti-Gr-1 to identify neutrophils that had been recruited to the lung (C). Images are shown at 20X magnification.

tissues. Lungs of antibody-treated mice showed moderate to severe bronchopneumonia with infiltration of neutrophils surrounding large bacterial colonies (Figure 4.5B-C, see Supplemental Table S4.1). This suggests that these mice still developed bronchopneumonia despite the delay in time to disease. However, consistent with systemic bacterial dissemination, spleens of these mice were also necrotic and the livers exhibited hepatitis with multiple foci of inflammation and thus it appears septicemic plague had also developed

(Figure 4.5D-E, see Supplemental Table S4.2).

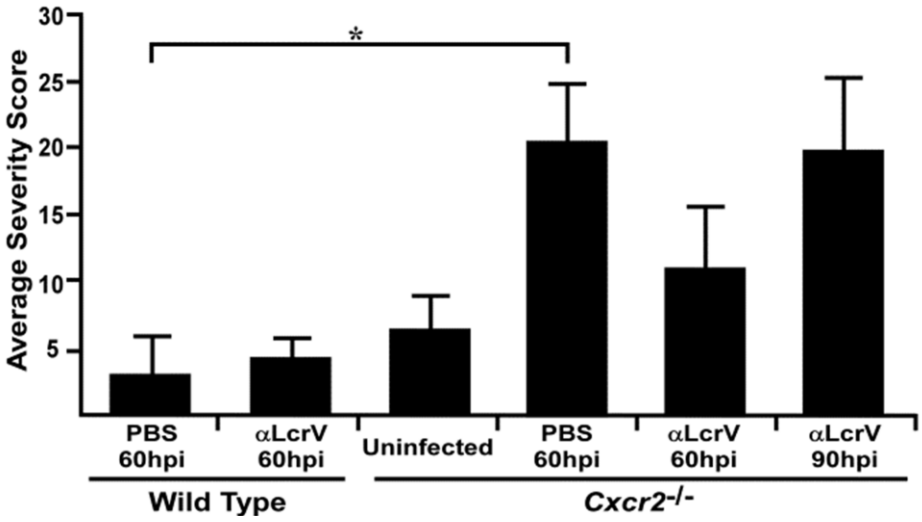

Figure 4.6. Quantitative histochemistry shows efficient neutrophil recruitment to the lungs of *Cxcr2*$^{-/-}$ mice despite the failure to prevent bacterial growth and disease. Disease severity scores, based on parenchyml congestion, neutrophil recruitment, edema, and alveolar destruction, were determined by analyzing three lung lobes for each mouse and the average score per group was plotted. Group sizes ranged from 2-5 (n=5, uninfected *Cxcr2*$^{-/-}$; n=4 WT + PBS, 60hours; n=2 WT + anti-LcrV, 60 hours; n=3 *Cxcr2*$^{-/-}$ + PBS, 60 hours; n=3 *Cxcr2*$^{-/-}$ + anti-LcrV, 60 hours; n=4 *Cxcr2*$^{-/-}$ + anti-LcrV, 90 hours).*p <0.05 as determined by one way ANOVA; hpi indicates hours post infection.

To quantify the degree of disease in the lungs, severity scores indicative of pneumonic plague at 60 and 90 hours post-infection were determined. Edema, alveolar destruction, neutrophil infiltration and parenchymal congestion were used as indicators of pneumonia. Assignment of scores corresponding to none through severe (scale of 0 to 3) for each criterion was performed for three lung lobes by examination of slides stained with H&E and anti-Gr-1, and a total score was determined for each mouse (Figure 4.6). Average scores within each group indicated that PBS-treated *Cxcr2*$^{-/-}$ mice developed severe pneumonia by

TABLE 4.1. Average severity score at 60 hours post infection per lung sample

Bacteria	Pathological Lesion[a]	Wild-Type + PBS	*Cxcr2*$^{-/-}$ + PBS	*Cxcr2*$^{-/-}$ + anti-LcrV
-	Neutrophil Infiltration[b]	1 (± 1.00)	1.67 (±0.44)	0.33 (±0.44)
	Alveolar Destruction	0	0	0
	Pulmonary Edema	0	0	0
	Parenchyml Congestion	0.13 (±0.19)	1.5 (±1.00)	0.67 (±0.44)
+	Neutrophil Infiltration[b]	NA	2.50 (±0.67)	2.00 (±0.00)*
	Alveolar Destruction	NA	2.58 (±0.39)**	2.25 (±0.17)**
	Pulmonary Edema	NA	1.17 (±0.56)	1.50 (±0.33)*
	Parenchyml Congestion	NA	2.50 (±0.67)	2.50 (±0.33)*

a. Lesions observed and scored from hematoxylin and eosin stain of formalin fixed tissues
b. Neutrophil enumeration from immunohistochemistry anti-Gr-1 stain of formalin fixed tissues
NA=Not Applicable; bacteria were not seen in any lobe.
() ± the standard deviation from the mean
*p <0.05, **p <0.001 compared to no bacteria of the same group; evaluated by Student's *t*-test

60 hours post-infection whereas wild-type mice did not (p <0.05, evaluated by one way ANOVA). At this time point, anti-LcrV treated *Cxcr2*$^{-/-}$ mice showed moderate neutrophil infiltration and few pathological lesions. These observations suggest neutrophil recruitment to the lung occurs before the development of disease lesions and bacterial growth in the absence of CXCR2. Anti-LcrV treated *Cxcr2*$^{-/-}$ mice eventually developed pneumonia, but with a delayed time course compared to untreated WT or mutant mice. Bacterial colonies were visible in areas of lung injury surrounded by inflammatory cells, many of which appeared to be neutrophils judged by morphology and positive staining for Gr-1 (Table 4.1). Together these data suggest that after anti-LcrV treatment, neutrophils are attracted to *Y. pestis* through multiple, perhaps redundant, chemotactic pathways. CXCR2-expressing cells are able to control the infection while signaling through other chemotaxis receptors, perhaps CC or C5a

receptors, may allow recruitment to the infection site, but little to no effector function that could result in bacterial clearance.

4.4.4. Temporary Ablation of Neutrophils Slows Progression of Pneumonic Plague.

Our experiments thus far suggest that CXCR2 signaling provides protective responses but does not abrogate neutrophil migration to the infected sites of the lungs. To address the contribution of CXCR2-independent neutrophil chemotaxis to the lungs, we first tested wild-type mice, and compared antibody immunity after pretreatment with either PBS or anti-Gr-1 (RB6.8C5), an antibody that ablates circulating neutrophils and some monocytes with a half-life of approximately 1.5 days in C3H-HeN mice [49]. RB6.8C5 or PBS was delivered to wild-type C3H mice by intraperitoneal injection of 100 μg on days -1 and +1 relative to intranasal *Y. pestis* challenge, with anti-LcrV administered 60 minutes before infection. All mice treated with anti-LcrV and RB6.8C5 were initially protected, suggesting that neutrophils are not required for early containment of the infection in the presence of protective antibodies. However, bacteria were not eliminated and all of these mice eventually developed weight loss at higher levels than PBS-treated mice. Only 40% of RB6.8C5-treated mice progressed to lethal disease by day 7, while the others resolved the infection (Figure 4.7A-B). These results suggest that early neutrophil ablation decreases immunity to plague, which is in agreement with recently reported observations of RB6.8C5 treatment in a mouse pneumonic plague model [51].

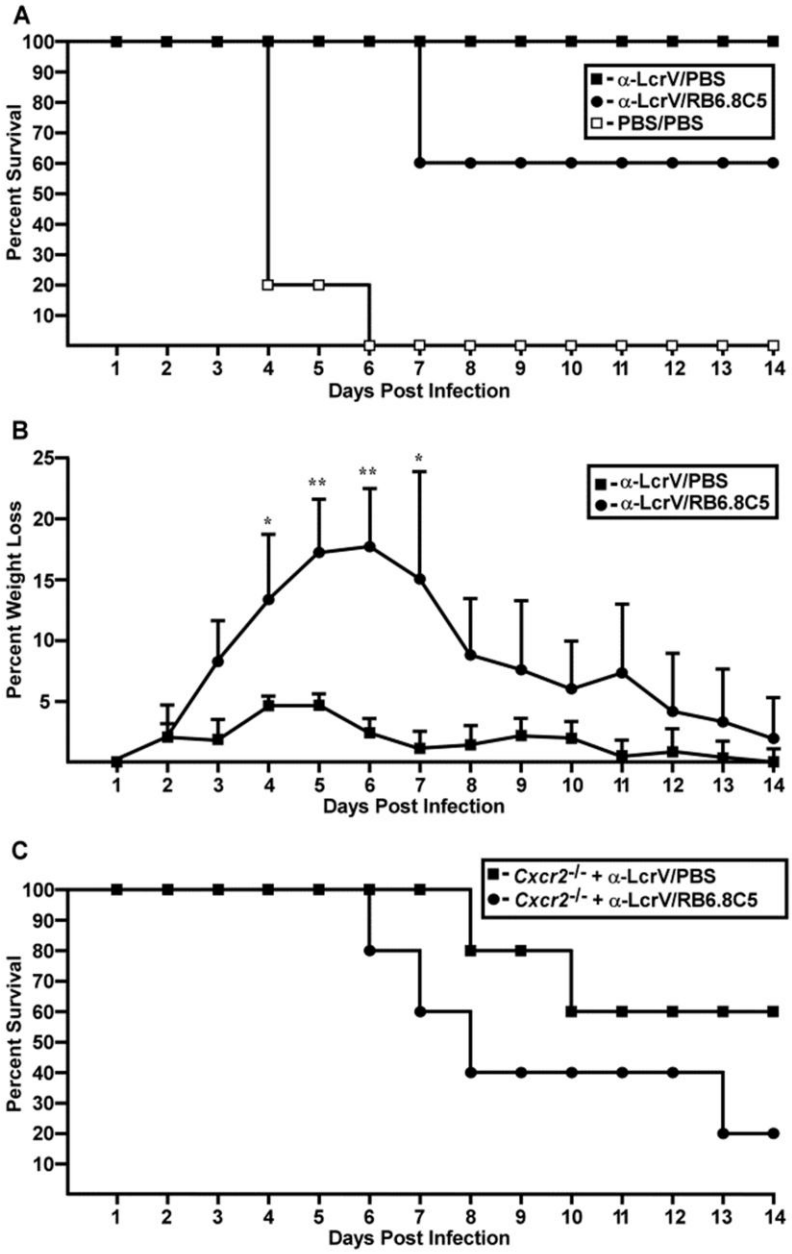

Figure 4.7. Extended time to death but no protection following anti-LcrV treatment and neutrophil ablation in wild-type and *Cxcr2*$^{-/-}$ mice. (A) Wild-type mice (n=5) were given 100 µg anti-Gr-1 monoclonal antibody or PBS on days -1 and +1 post infection and 400 µg anti-LcrV polyclonal antibody or PBS 60 minutes prior to IN infection with 4,000 CFU *Y. pestis* CO92 and survival was monitored over a 14 day period. (B) Percent daily weight loss compared to pre-challenge weight is shown for all surviving mice in each group for the experiment shown in (A). (C) *Cxcr2*$^{-/-}$ mice (n=5) were given 200µg anti-Gr-1 or PBS 60 hpi and 400 µg anti-LcrV 60 minutes prior to IN infection with 4,000 CFU *Y. pestis* CO92 and survival was monitored. **p* <0.05, ***p* <0.005 as determined by Student's *t*-test.

We next treated *Cxcr2*$^{-/-}$ mice with anti-LcrV followed by either PBS or 200 µg RB6.8C5 at 60 hours post-infection, approximately 24-36 hours before acute disease appears in the absence of RB6.8C5 treatment. Both untreated and RB6.8C5-treated *Cxcr2*$^{-/-}$ mice were initially protected from disease similar to treated wild-type mice. On day 5, disease symptoms began in 80% of RB6.8C5 treated animals, and disease progressed to lethality in all of these mice (Figure 4.7C). *Cxcr2*$^{-/-}$ mice treated with anti-LcrV and PBS behaved similarly and 40% developed lethal disease (p >0.05 RB6.8C5 compared to PBS-treated mice). Together, these results are consistent with CXCR2 signaling as the primary mechanism whereby host neutrophils control *Y. pestis* infection but also suggest that initial containment of disease after treatment with protective antibodies is not mediated by Gr-1^{+} cells.

4.4.5 CXCR2 Independent Signaling Clears Mutant Y. pestis.

To address whether *Cxcr2* is a general necessity for host defense against bacterial infections of the lung, we challenged *Cxcr2*$^{-/-}$ mice with a nonpigmented mutant strain of *Y. pestis* CO92 (Δ*pgm*) by intranasal infection. In this model, *Yersinia* colonize the lung and do not cause inflammation or pneumonia, but nevertheless cause septicemic plague and the infection is lethal to mice [33]. Pre-treatment of mice with iron accelerates bacterial access to the blood, resulting in a more uniform and rapid disease. Intranasal challenge of wild-type mice with 1x10^{6} CFU *Y. pestis* CO92Δ*pgm* resulted in approximately 90% lethality within 10 days, consistent with our previous observations [33] (Figure

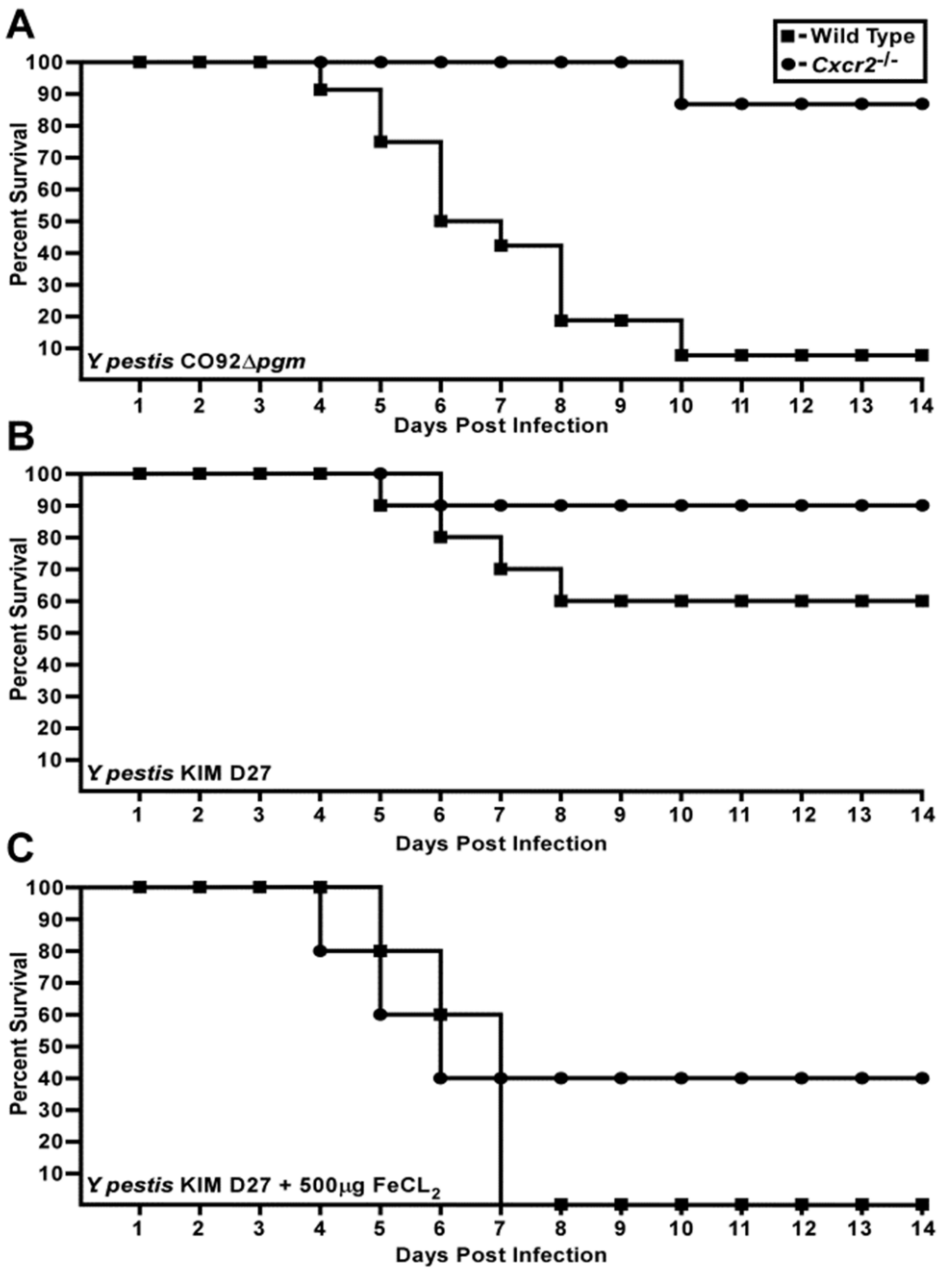

Figure 4.8. CXCR2 increases sensitivity to non-pigmented *Y. pestis* strains. (A) WT (n=12) and *CXCR2*$^{-/-}$ mice (n=7) were challenged by intranasal infection with 1x10^{6} CFU *Y. pestis* CO92Δ*pgm* and survival was monitored over a 14 day period; p <0.005 between wild-type and *CXCR2* mutant mice, evaluated by Mann-Whitney rank sum test. . (B) Wild-type or *CXCR2*$^{-/-}$ mice (n=10) were given PBS prior to intranasal infection with 1x10^{6} CFU *Y. pestis* KIM D27 and survival was monitored for 14 days. (C) 500 μg inorganic iron ($FeCl_2$) in sterile H_2O was injected IP into WT or *CXCR2*$^{-/-}$ mice (n=5) prior to infection with 1x10^{6} CFU *Y. pestis* D27 and survival was monitored over a 14 day period; p >0.05 between wild-type and mutant mice, evaluated by Mann-Whitney rank sum test.

4.8A). Strikingly, *Cxcr2*$^{-/-}$ mice were significantly less susceptible to infection by *Y. pestis* CO92Δ*pgm* and only one of these mice succumbed to infection after 10 days (p <0.005, evaluated by the Mann-Whitney rank sum test). We also tested another nonpigmented strain, KIM D27, which is a laboratory strain first isolated in 1965 from a lineage distinct from CO92, for its ability to cause acute disease in *Cxcr2* mutant mice [42]. In this model, 40% of wild-type C3H-HeN mice succumbed to intranasal challenge with 1x10^6 CFU *Y. pestis* KIM D27 (Figure 4.8B). Treatment with iron before challenge increased overall susceptibility and 100% succumbed to the infection (Figure 4.8C). Both PBS-treated and iron-treated *Cxcr2*$^{-/-}$ mice exhibited similar, if not less, susceptibility to *Y. pestis* KIM D27 in both models, with 10% and 60% lethality, respectively, although these differences may not be significant (Figure 4.8B-C, p >0.05 compared to wild-type with or without iron treatment). Together these results strongly suggest that bacterial virulence factors within the *pgm* locus may prevent neutrophil activation through CXCR2-independent pathways. Furthermore, *Cxcr2*$^{-/-}$ mice are capable of mounting an effective response against a highly similar bacterial infection in the lungs indicating that CXCR2 is not broadly required for host defense against bacterial pathogens in the lungs.

4.5 Discussion

CXCR2 is known to be critical in mediating effective neutrophil responses to invading bacterial and even viral pathogens. In the case of pneumonic plague (an acute disease), CXCR2 activation is unable to keep pace with bacterial

replication and a robust but ineffective inflammatory response occurs that may exacerbate the disease. In this work, we used polyclonal anti-LcrV antibodies, which opsonize the bacteria, as an alternative means to induce multiple pathways of neutrophil recruitment. As with untreated mice, antibody-treated *Cxcr2*$^{-/-}$ mice mounted a neutrophil-mediated inflammatory response. However, this only delayed and did not prevent lethal disease suggesting that while there may be redundancy in neutrophil recruitment, CXCR2 provides unique activation that is necessary for controlling the infection. Because pulmonary infection by the nonpigmented strain could be cleared in the absence of *Cxcr2*, it is likely that bacterial virulence factors within the pigmentation locus contribute to the resistance of *Y. pestis* to neutrophils or other Gr-1^{+} monocytes. Recently, CXCR2-dependent activation of neutrophil extracellular traps (NETs) was shown to be independent of chemotaxis, as small molecule inhibitors of CXCR2 could prevent secretion of NETs without affecting neutrophil recruitment [52]. Thus, it is likely that similar chemotaxis-independent pathways involving CXCR2 may be required for host defense against *Y. pestis*.

Neutralizing antibodies aid in bacterial clearance mechanisms involving neutrophils and other phagocytic cells as well as the complement system. Antibodies that opsonize bacteria promote Fc receptor (FcR) dependent uptake and subsequent secretion of the pro-inflammatory CXC and CC chemokines as well as activation of complement [53]. When activated, FcR signaling results in enhanced killing of the bacterial pathogens which is an important part of

antibody-mediated clearance [54, 55]. In parallel, antibodies also stimulate activation of complement C3a and C5a signaling molecules. Although the classical complement pathway in mice is ineffective against *Y. pestis*, C5a may still be effective in signaling neutrophil recruitment through binding of the C5a receptor (C5aR) which is present on the surface of neutrophils [56, 57]. Moreover, because excess C5a, such as may occur during sepsis, can paralyze neutrophil activation, it is conceivable that the inability of C*xcr2*$^{-/-}$ to clear the infection may be due to this or another aberrant host response that can promote rather than prevent disease [58].

Pneumonic plague in both rodents and humans is not uniform throughout the lungs or between lung lobes, making it difficult to ascertain mechanisms of disease from whole lung cellular samples, or cytokine measurements of bronchoalveolar lavage fluid [25, 27, 31, 59]. Our quantitative assessments of histopathology revealed either more pronounced or more rapid neutrophil recruitment in *Cxcr2* mutants than wild-type mice. Although neutrophils from *Cxcr2* knockout mice cannot respond to MIP-2 or KC they have been shown to exhibit normal migration to C5a and CC chemokines as well as to induce phagocytic processes through FcR [60]. Because *Y. pestis* infection elicits very strong induction of pro-inflammatory cytokines and chemokines, in addition to KC and MIP-2, and opsonizing antibodies are also strong inducers of inflammatory responses, it is likely that neutrophil recruitment in *Cxcr2*$^{-/-}$ mice proceeds by one or more of these alternative, seemingly redundant pathways [15, 26, 31]. In

contrast, defense against other bacterial infections, which elicit a more limited inflammatory response in the host, may rely more heavily on CXCR2 for neutrophil recruitment [9-11]. Thus, although mice require CXCR2 to control *Y. pestis* as with other bacterial pathogens, our results suggest a novel host pathogen interaction that regulates the activity of these phagocytic cells independent of their recruitment.

Anti-LcrV antibody neutralizes the type III secretion system, opsonizes the bacteria for efficient uptake and is effective in promoting protection in the lungs [36, 38-40]. A model for how macrophages and neutrophils might respond to these antibodies is shown in Figure 4.9. In this model, LcrV antibody-opsonized bacteria are likely taken up by the lung or alveolar macrophages or neutrophils via Fc-mediated phagocytosis, and although they may survive inside the phagosome, they may also stimulate production of CC and CXC chemokines for neutrophil recruitment [44, 45, 47]. In parallel, complement recognition of antibody-opsonized bacteria would be expected to activate C5 convertase, resulting in the circulation of C5a and recruitment of neutrophils via the C5a receptor [56]. While each may lead to neutrophil recruitment to infected areas, perhaps only CXCR2 also activates specific effector functions necessary for bacterial killing such as degranulation or extracellular traps (NETs) while other pathways may be disabled by *Yersinia*.

Because *CXCR2*$^{-/-}$ mice treated with anti-LcrV had a significant delay in the development of disease compared to no treatment, it appears that

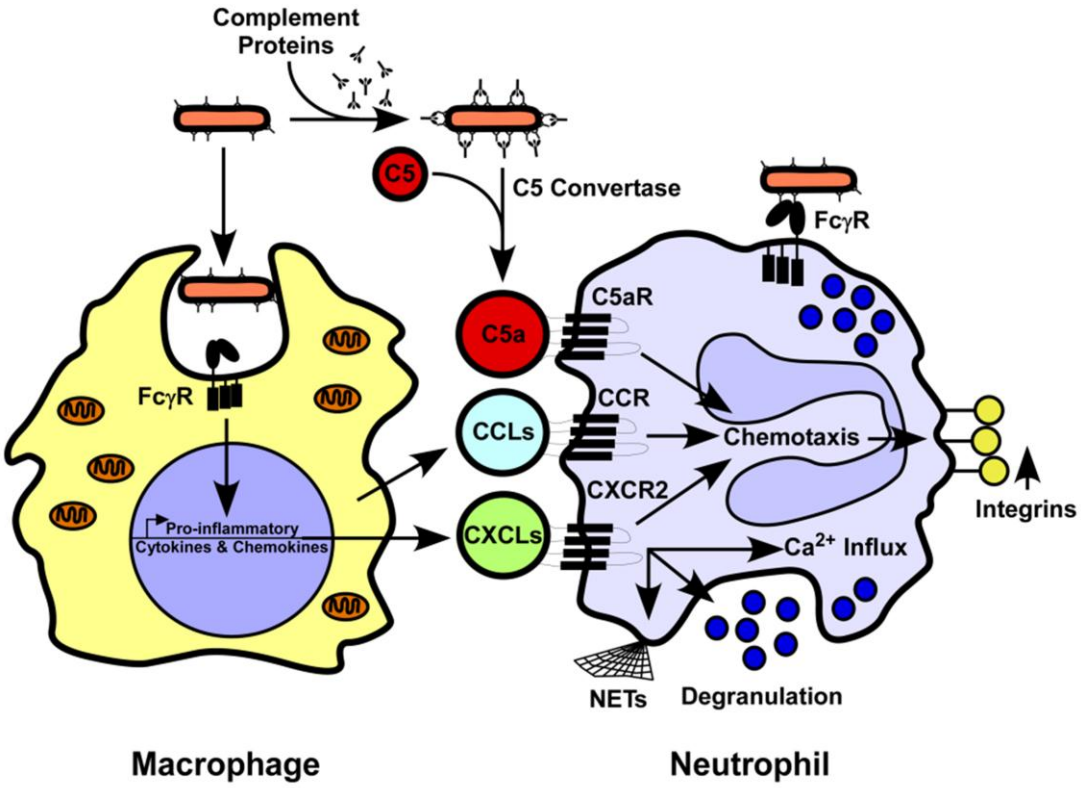

Figure 4.9. Model for the role of CXCR2 in antibody-mediated immunity to pneumonic plague. Antibody-opsonized bacteria are expected to be taken up by macrophages and neutrophils via the FcγR, and although this may not lead to bacterial clearance by either cell type, chemokines may still be secreted. Simultaneously, activation of C5a convertase leads to increased C5a which also acts as a chemoattractant for neutrophils and other cells that express the C5a receptor (C5aR). C5aR and CC receptors would be expected to promote neutrophil chemotaxis but may be prevented from activation because of *Yersinia* virulence factors encoded within the *pgm* locus. In contrast, CXC chemokine signaling may be required to activate effector functions independent of neutrophil chemotaxis such as increased intracellular Ca^{+2}, stimulation of granuole release or secretion of neutrophil extracellular traps (NETs) that promote bacterial clearance and protect the host from disease.

phagocytosis in the lungs without subsequent CXCR2 signaling slows bacterial growth, but does not lead to killing of the engulfed bacterium. Furthermore, because neutrophil ablation resulted in the same phenotype, it is likely that this initial containment is not mediated by neutrophils. *In vitro*, activated macrophages that engulf anti-LcrV treated bacteria are unable to kill them, while deletion of the *pgm* locus renders *Y. pestis* sensitive to activated macrophages

[46, 47]. Our results are consistent with this observation but suggest that bacterial growth may be reduced in this intracellular environment *in vivo*. CXCR2$^{-/-}$ neutrophils also express FcR, thus it may be that this signaling pathway may be targeted by *Yersinia* in both cell types.

Recently, human neutrophils were shown to be able to kill intracellular *Y. pestis in vitro*, but were sensitive to killing by extracellular bacteria expressing a functional type III secretion system [61]. Our model suggests that this activity may be influenced by CXCR2 and that other activation mechanisms may be silenced by virulence factors of the pigmentation locus. Future experiments will aim to distinguish whether Fc, C5a, or CC receptor signaling is silenced by bacterial or host responses and whether human neutrophils respond similarly to antibody opsonized *Y. pestis*.

4.6 Acknowledgements

We are grateful to members of our laboratory for helpful discussions and assistance with the BSL3 experiments and to Dr. Craig Franklin for assistance with statistical analyses. Histology and immunohistochemistry were performed by the Research Animal Diagnostics Laboratory (RADIL; University of Missouri). The *Kc*$^{-/-}$ mice were a kind gift from Dr. Sergio Lira (Mount Sinai School of Medicine).

4.7 Supplementary Data

Table S4.1. Pathology report from formalin fixed lung tissues from *Cxcr2*$^{-/-}$ (C3H-HeN) mice

***Cxcr2*$^{-/-}$ (time point-treatment)**	**Sample ID**	**bacteria**	**alveolar destruction**	**neutrophil infiltration**	**parenchymal congestion**	**pulmonary edema**	**total score**
						ave (SD)[a]	1
Non-infected-1	lobe 1	-	0	1	2	0	3
	lobe 2	-	0	1	1	0	2
	lobe 3	-	0	1	1	0	2
						Total	7
						ave (SD)	2.25 (± 0.50)
Non-infected-2	lobe 1	-	0	1	0	0	1
	lobe 2	-	0	1	2	0	3
	lobe 3	+	3	2	0	2	7
						Total	11
						ave (SD)	3.00 (± 2.83)
Non-infected-3	lobe 1	-	0	0	2	0	2
	lobe 2	-	0	0	2	0	2
	lobe 3	-	0	0	2	0	2
						Total	6
						ave (SD)	1.75 (± 0.50)
Non-infected-4	lobe 1	-	0	1	0	0	1
	lobe 2	-	0	1	0	0	1
	lobe 3	-	0	1	1	0	2
						Total	4
						ave (SD)	1.00 (± 0.82)
60hpi[b]+PBS-1	lobe 1	+	1	3	1	1	6
	lobe 2	-	0	2	0	0	2
	lobe 3	+	3	3	2	0	8
						Total	16
						ave (SD)	4.5 (± 3.00)
60hpi+PBS-2	lobe 1	+	3	2	3	0	8
	lobe 2	+	3	2	3	3	11
	lobe 3	+	3	1	3	1	8
						Total	27
						ave (SD)	7.4 (± 2.61)

60hpi+PBS-3	lobe 1	-	0	2	1	0	3
	lobe 2	+	3	3	3	2	11
	lobe 3	-	0	2	2	0	4
						Total	18
						ave (SD)	6.00 (± 4.36)
60hpi+αLcrV-1	lobe 1	-	0	0	1	0	1
	lobe 2	+	2	1	3	2	8
	lobe 3	+	3	3	3	0	9
						Total	18
						ave	4.75 (± 4.35)
60hpi+αLcrV-2	lobe 1	+	2	2	2	2	8
	lobe 2	-	0	0	0	0	0
	lobe 3	-	0	0	0	0	0
						Total	8
						ave (SD)	2.00 (± 4.00)
60hpi+αLcrV-3	lobe 1	-	0	1	1	0	2
	lobe 2	-	0	1	1	0	2
	lobe 3	-	0	1	2	0	3
						Total	7
						ave (SD)	2.00 (± 0.82)
90hpi+αLcrV-1	lobe 1	+	3	3	3	2	11
	lobe 2	-	0	2	0	0	2
	lobe 3	-	0	2	0	0	2
						Total	15
						ave (SD)	4.25 (± 4.50)
90hpi+αLcrV-2	lobe 1	+	3	3	3	3	12
	lobe 2	+	3	3	3	3	12
	lobe 3	-	0	2	2	0	4
						Total	28
						ave (SD)	7.75 (± 4.92)
90hpi+αLcrV-3	lobe 1	-	0	2	2	0	4
	lobe 2	+	3	3	3	3	12
	lobe 3	-	0	0	0	0	0
						Total	16
						ave (SD)	4.00 (± 5.66)

90hpi+αLcrV -4	lobe 1	-	0	2	0	0	2
	lobe 2	+	3	3	3	3	12
	lobe 3	-	0	2	0	0	2
						Total	16
						ave (SD)	4.50 (± 5.00)

a. SD – Standard Deviation
b. hpi – Hours Post-Infection

Table S4.2. Pathology report from formalin fixed liver and spleen tissues from wild type and *Cxcr2*$^{-/-}$ C3H-HeN mice

Sample ID	liver	spleen
WT-60hpi-PBS-1	vasculitis with thrombosis; multifocal suppurative hepatitis	marked congestion, mod granulopoiesis, normal PALS
WT-60hpi-PBS-2	multifocal necrotizing hepatitis; mod multifocal hematopoiesis	marked congestion, minimal hematopoiesis; depleted PALS
WT-60hpi-PBS-3	no significant changes	minimal congestion, mod hematopoiesis; hyperplastic PALS
WT-60hpi-PBS-4	no significant changes	moderate hematopoiesis; normal PALS
WT-60hpi-αLcrV-1	no significant changes	min congestion; marked granulopoiesis, T-cell zone depletion
WT-60hpi-αLcrV-2	no significant changes	minimal congestion, mod hematopoiesis; hyperplastic PALS
CXCR2-uninfected-1	multifocal hematopoiesis; microgranulomas	min congestion; marked granulopoiesis, T-cell zone depletion
CXCR2-uninfected-2	multifocal hematopoiesis	min congestion; marked granulopoiesis, T-cell zone depletion
CXCR2-uninfected-3	multifocal hematopoiesis	minimal congestion, mod hematopoiesis; hyperplastic PALS
CXCR2-uninfected-4	multifocal hematopoiesis	moderate congestion; mild granulopoiesis; normal PALS
CXCR2-60hpi-PBS-1	mod. hematopoiesis; mild steatosis, focal hepatocellular hyperplasia	hemorrhage; marked granulopoiesis; depleted T cell zone
CXCR2-60hpi-PBS-2	focal hematopoiesis, microgranulomas, mild diffuse steatosis	marked congestion, mod granulopoiesis,
CXCR2-60hpi-PBS-3	mod multifocal hematopoiesis	marked congestion, minimal hematopoiesis; depleted PALS
CXCR2-60hpi-αLcrV-1	mod. hematopoiesis	marked congestion, mod granulopoiesis, normal PALS
CXCR2-60hpi-αLcrV-2	mild diffuse steatosis	marked congestion, mod granulopoiesis, hyperplastic PALS
CXCR2-60hpi-αLcrV-3	multifocal suppurative hepatitis; diffuse steatosis	moderate congestion/hemorrhage; moderate granulopoiesis; depleted T cell zone
CXCR2-90hpi-αLcrV-1	multifocal thrombosis; mod multifocal hematopoiesis	marked congestion/hemorrhage; marked granulopoiesis; normal PALS
CXCR2-90hpi-αLcrV-2	multifocal necrotizing septic hepatitis; mod multifocal hematopoiesis	marked hemorrhage; marked granulopoiesis; depleted PALS; bacterial colonies
CXCR2-90hpi-αLcrV-3	multifocal suppurative hepatitis; mod multifocal hematopoiesis	min congestion; marked granulopoiesis, T-cell zone depletion
CXCR2-90hpi-αLcrV-4	multifocal suppurative hepatitis; occasional steatosis	marked congestion/hemorrhage; marked granulopoiesis; depleted T cell zone

Table S4.3. Pathology report from formalin fixed lung tissues from wild type C3H-HeN mice

Wild type (time point-treatment)	Sample ID	bacteria	alveolar destruction	neutrophil infiltration	parenchymal congestion	pulmonary edema	total score
60hpi+PBS-1	lobe 1	-	0	2	0	0	2
	lobe 2	-	0	2	0	0	2
	lobe 3	-	0	2	0	0	2
						Total	6
						ave (SD)	2
60hpi+PBS-2	lobe 1	-	0	2	0	0	2
	lobe 2	-	0	2	0	0	2
	lobe 3	-	0	2	0	0	2
						Total	6
						ave (SD)	2
60hpi+PBS-3	lobe 1	-	0	0	1	0	1
	lobe 2	-	0	0	0	0	0
	lobe 3	-	0	0	1	0	1
						Total	2
						ave (SD)	0.50 (± 0.06)
60hpi+PBS-4	lobe 1	-	0	0	0	0	0
	lobe 2	-	0	0	0	0	0
	lobe 3	-	0	0	0	0	0
						Total	0
						ave (SD)	0
60hpi+αLcrV-1	lobe 1	-	0	1	1	0	2
	lobe 2	-	0	1	1	0	2
	lobe 3	-	0	1	1	0	2
						Total	6
						ave (SD)	1.75 (± 0.50)
60hpi+αLcrV-2	lobe 1	-	0	0	1	0	1
	lobe 2	-	0	0	1	0	1
	lobe 3	-	0	0	1	0	1
						Total	3
						ave (SD)	1
						ave (SD)	7.4 (± 2.61)

a. SD – Standard Deviation
b. hpi – Hours Post-Infection

4.8 References

1. Hamilton, T., et al., *Chemokine and chemoattractant receptor expression: post-transcriptional regulation.* J Leuk Biol, 2007. **82**: 213-9.

2. Nasser, M., et al., *Differential activation and regulation of CXCR1 and CXCR2 by CXCL8 monomer and dimer.* J Immunol, 2009. **183**: 3425-32.

3. Smith, K. and M. Clatworthy, *FcgRIIB in autoimmunity and infection: evolutionary and therapeutic implications.* Nat Rev Immunol, 2010. **10**: 328-43.

4. Oquendo, P., et al., *The platelet-derived growth factor-inducible KC gene encodes a secretory protein related to platelet alpha-granule proteins.* J Biol Chem, 1989. **264**: 4133-7.

5. Tekamp-Olson, P., et al., *Cloning and characterization of cDNAs for murine macrophage inflammatory protein-2 and its human homologues.* J Exp Med, 1990. **172**: 911-9.

6. Zhang, X., et al., *CXC chemokines, MIP-2 and KC induce P-selectin-dependent neutrophil rolling and extravascular migration in vivo.* Brit J Pharmacol, 2001. **133**: 413-21.

7. Chapman, R., et al., *CXCR2 antagonists for the treatment of pulmonary disease.* Phamacol and Therap, 2009. **121**: 55-68.

8. Mehrad, B., et al., *CXC chemokine receptor-2 ligands are necessary components of neutophil mediated host defense in invasive pulmonary aspergillosis.* J Immunol, 1999. **163**: 6086-94.

9. Moore, T., et al., *Bacterial clearance and survival are dependent on CXC chemokine receptor-2 ligands ina murine model of pulmonary Norcardia asteroides infection.* J Immunol, 2000. **164**: 908-15.

10. Tsai, W., et al., *CXC chemokine receptor CXCR2 is essential for protective innate host response in murine Pseudomonas aeruginosa pneumonia.* Infect Immun, 2000. **68**(7): 4289-96.

11. Tateda, K., et al., *Chemokine-dependent neutrophil recruitment in a murine model of Legionella pneumonia: Potential role of neutrophils as immunoregulatory cells.* Infect Immun, 2001. **69**(4): 2017-24.

12. Hotchkiss, R. and D. Nicholson, *Apoptosis and caspases regulate death and inflammation in sepsis.* Nat Rev Immunol, 2006. **6**: 813-22.

13. Nagarkar, D., et al., *CXCR2 is required for neutrophilic airway inflammation and hyperresponsiveness in a mouse model of human Rhinovirus infection.* J Immunol, 2009. **183**: 6698-707.

14. Spehlmann, M., et al., *CXCR2-dependent mucosal neutrophil influx protects against colitis-associated diarrhea caused by an attaching/effacing lesion-forming bacterial pathogen.* J Immunol, 2009. **183**: 3332-43.

15. Herbold, W., et al., *Importance of CXC chemokine receptor 2 in alveolar neutrophil and exudate macrophage recruitment in response to Pneumococcal lung infection.* Infect Immun, 2010. **78**(6): 2620-30.

16. Jacobs, J., et al., *Deficiency of CXCR2, but not other chemokine receptors, attenuates autoantibody-mediated arthritis in a murine model.* Arthritis & Rheumatism, 2010. **62**(7): 1921-32.

17. Mei, J., et al., *CXCL5 regulates chemokine scavenging and pulmonary host defense to bacterial infection.* Immunity, 2010. **33**(1): 106-17.

18. Seki, M., et al., *Critical role of IL-1 receptor-associated kinase-M in regulating chemokine-dependent deleterious inflammation in murine influenza pneumonia.* J Immunol, 2010. **184**.

19. Ritzman, A.M., et al., *The chemokine receptor CXCR2 ligand KC (CXCL1) mediates neutrophil recruitment and is critical for development of experimental Lyme arthritis and carditis.* Infect Immun, 2010. **78**(11): 4593-600.

20. Vanderbilt, J., et al., *CXC chemokines and their receptors are expressed in Type II cells and upregulated following lung injury.* Am J Respir Cell Mol Biol, 2003. **29**: 661-8.

21. Neff, T., et al., *Relationship of acute lung inflammatory injury to Fas/FasL system.* Am J Path, 2005. **166**(3): 685-94.

22. Schmal, H., et al., *Role for macrophage inflammatory protein-2 in lipopolysaccharide-induced lung injury in rats.* J Immunol, 1996. **156**: 1963-72.

23. Wang, Z., et al., *Alveolar macrophages from septic mice promote polymorphonuclear leukocyte transendothelial migration via an endothelial cell Src Kinase/ NADPH Oxidase pathway.* J Immunol, 2008. **181**: 8735-44.

24. Gordon, J., et al., *The combined CXCR1/CXCR2 antagonist CXCL8(3–74)K11R/G31P blocks neutrophil infiltration, pyrexia, and pulmonary vascular pathology in endotoxemic animals* J Leuko Biol, 2005. **78**: 1265-72.

25. Pollitzer, R., *Plague*. 1954, Geneva, Switzerland: World Health Organization.

26. Lathem, W., et al., *Progression of primary pneumonic plague: A mouse model of infection, pathology, and bacterial transcriptional activity.* Proc Natl Acad Sci, 2005. **102**(49): 17786-91.

27. Anderson, D., et al., *Pneumonic plague pathogenesis and immunity in Brown Norway rats.* Am J Path, 2009. **174**(3): 910-21.

28. Huang, X., M. Nikolich, and L. Lindler, *Current trends in plague research: From genomics to virulence.* Clin Med Res, 2006. **4**(3): 189-99.

29. Montminy, S., et al., *Virulence factors of Yersinia pestis are overcome by a strong lipopolysaccharide response.* Nat Immunol, 2006. **7**(10): 1066-73.

30. Auerbuch, V., D. Golenbock, and R. Isberg, *Innate Immune Recognition of Yersinia pseudotuberculosis Type III Secretion.* PloS Path, 2009. **5**(12): 1000686.

31. Agar, S., et al., *Characterization of a mouse model of plague after aerosolization of Yersinia pestis CO92.* Microbiology, 2008. **154**: 1939-48.

32. Agar, S.L., et al., *Characterization of the rat pneumonic plague model: infection kinetics following aerosolization of Yersinia pestis CO92.* Microbes Infect, 2009. **11**(2): 205-14.

33. Lee-Lewis, H. and D. Anderson, *Absence of inflammation and pneumonia during infection with non-pigmented Yersinia pestis reveals new role for the pgm locus in pathogenesis.* Infect Immun, 2010. **78**(1): 220-30.

34. Skrzypek, E. and S. Straley, *Differential effects of deletions in lcrV on secretion of V antigen, regulation of the low-Ca^{2+} response, and virulence of Yersinia pestis.* J Bacteriol, 1995. **177**(9): 2530-42.

35. Hill, J., et al., *Regions of Yesinia pestis V antigen that contribute to protection against plague identified by passive and active immunization.* Infect Immun, 1997. **65**(11): 4476-82.

36. Weeks, S., et al., *Anti-V antigen antibody protects macrophages from Yersinia pestis-induced cell death and promotes phagocytosis.* Microb Path, 2002. **32**: 227-37.

37. Fetherston, J. and R. Perry, *Yersinia pestis -- etiologic agent of plague.* Clin Microbiol Rev, 1997. **10**(1): 35-66.

38. Cowan, C., et al., *Anti-LcrV antibodies inhibits delivery of Yops by Yersinia pestis KIM5 by directly promoting phagocytosis.* Infect Immun, 2005. **73**(9): 6127-37.

39. Eisele, N. and D. Anderson, *Dual-function antibodies to Yersinia pestis LcrV required for pulmonary clearance of plague.* Clin Vacc Immunol, 2009. **16**(12): 1720-7.

40. Quenee, L., et al., *Amino acid residues 196-225 of LcrV represent a plague protective epitope.* Vaccine, 2010. **28**(7): 1870-6.

41. Burrows, T. and S. Jackson, *The virulence-enhancing effect of iron on nonpigmented mutants of virulent strains of Pasteurella pestis.* Br J Exp Path, 1956. **37**(6): 577-83.

42. Brubaker, R., E. Beesley, and M. Surgalla, *Pasteurella pestis: Role of Pesticin I and iron in experimental plague.* Science, 1965. **149**: 422-4.

43. Fetherston, J., P. Schuetze, and R. Perry, *Loss of the pigmentation phenotype in Yersinia pestis is due to the spontaneous deletion of 102kb of chromosomal DNA which is flanked by a repetitive element.* Mol Microbiol, 1992. **6**(18): 2693-704.

44. Pujol, C. and J. Bliska, *The ability to replicate in macrophages is conserved between Yersinia pestis and Yersinia pseudotuberculosis.* Infect Immun, 2003. **71**(10): 5892-9.

45. Grabenstein, J., et al., *The response regulator PhoP of Yersinia pseudotubeculosis is important for replication in macrophages and for virulence.* Infect Immun, 2004. **72**(9): 4973-84.

46. Pujol, C., et al., *Replication of Yersinia pestis in interferon γ-activated macrophages requires ripA, a gene encoded in the pigmentation locus.* Proc Natl Acad Sci, 2005. **102**(36): 12909-14.

47. Noel, B., et al., *Yersinia pestis can bypass protective antibodies to LcrV and activation with gamma interferon to survive and induce apoptosis in murine macrophages.* Clin Vacc Immunol, 2009. **16**(10): 1457-66.

48. Surgalla, M. and E. Beesley, *Congo red-agar plating medium for detecting pigmentation in Pasteurella pestis.* App Microbiol, 1969. **18**(5): 834-7.

49. Brown, C., V. Blaho, and C. Loiacono, *Treatment of mice with the neutrophil-depleting antibody RB6-8C5 results in early development of experimental lyme arthritis via the recruitment of Gr-1 polymorphonuclear leukocyte-like cells.* Infect Immun, 2004. **72**(9): 4956-65.

50. Stillie, R. and A. Stadnyk, *The functional signficance behind expressing two IL-8 receptor types on PMN.* J Leuko Biol, 2009. **86**(3): 529-43.

51. Laws, T., et al., *Neutrophils are important in early control of lung infection by Yersinia pestis.* Microbes Infect, 2010. **12**(4): 331-5.

52. Marcos, V., et al., *CXCR2 mediates NADPH oxidase-independent neutrophil extracellular trap formation in cystic fibrosis airway inflammation.* Nat Med, 2010. **16**(9): 1018-23.

53. Nimmerjahn, F. and J. Ravetch, *Rcg receptors as regulators of immune responses.* Nat Rev Immunol, 2008. **8**: 34-47.

54. Tian, H., et al., *Efficacy of opsonic and nonopsonic serotype 3 Pneumococcal capsular polysaccharide-specific monoclona antibodies against intranasal challenge with Streptococcus pneumoniae in mice.* Infect Immun, 2009. **77**(4): 1502-13.

55. Gondwe, E., et al., *Importance of antibody and complement for oxidative burst and killing of invasive nontyphoidal Salmonella by blood cells in Africans.* Proc Natl Acad Sci USA, 2010. **107**(7): 3070-5.

56. Guo, R., et al., *Divergent Signaling Pathways in Phagocytic Cells during Sepsis.* J Immunol, 2006. **177**: 1306-13.

57. Kolodziejek, A.M., et al., *Outer membrane protein X (Ail) contributes to Yersinia pestis virulence in pneumonic plague and its activity is dependent on the lipopolysaccharide core length.* Infect Immun, 2010. **78**(12): 5233-43.

58. Riddirisch, D., et al., *Functional roles for C5a receptors in sepsis.* Nat Med, 2008. **14**(5): 551-7.

59. Lien-Teh, W., *A Treatise on Pneumonic Plague*. 1926, Geneva: League of Nations Health Organization.

60. Lee, J., et al., *Chemokine binding and activities mediated by the mouse IL-8 receptor.* J Immunol, 1995. **155**: 2158.

61. Spinner, J.L., J.A. Cundiff, and S.D. Kobayashi, *Yersinia pestis type III secretion system-dependent inhibition of human polymorphonuclear leukocyte function.* Infect Immun, 2008. **76**(8): 3754-60.

CHAPTER 5

SUMMARY AND FUTURE PERSPECTIVES

5.1 Summary

The goal of the projects presented within aimed to better define the requirements, as well as the mechanisms driving antibody-mediated clearance of pneumonic plague. As such, we first sought to better understand the role of opsonophagocytosis in humoral immunity to plague (Chapter 2). In order to accomplish this goal, a library of monoclonal antibodies targeting distinct epitopes of LcrV was used. Antibodies were first measured for the ability to block T3S, a property previously known to be important for antibody-based immunity to disease [1]. By assaying for Caspase-3 activation in macrophages, a hallmark of Yop injection, we found that 2 antibodies, BA5 and AH1, were able to significantly block effector protein injection. In addition, combining BA5 and AH1, or adding an additional non-neutralizing antibody (4G2) further improved the T3S blocking capability of antibodies. Thus, we hypothesized that administration of antibody combinations to mice would improve treatment efficacy after pulmonary infection with a lethal dose of bacteria. Unexpectedly, we found that the only treatment regimen capable of protecting mice from challenge was BA5 when

administered alone, and combinations containing BA5 were less effective due to the diminution of the antibody, and not competition for epitope binding.

Thus, we further hypothesized that BA5 displays unique properties that are required for disease clearance. It has been known that T3S neutralizing polyclonal antibodies allow for the phagocytic uptake of opsonized bacteria by macrophages, but it was unclear if this process is required for protection [1]. We therefore measured the ability of single antibodies, or combinations of antibodies for the capability to opsonize bacteria. Strikingly, we found that only BA5 was able to significantly increase the opsonophagocytosis of *Y. pestis* in comparison to AH1 alone or combinations of antibodies, thus directly correlating antibody-mediated protection from pneumonic disease with the ability of anti-LcrV antibodies to both block T3S and opsonize bacteria.

Despite these observations, subsequent data published by Noel et al. indicated that *Y. pestis* is able to survive inside of macrophages, even if pre-opsonized with anti-LcrV antibodies [2]. As a result, the aim of chapter 3 was to better understand intracellular *Y. pestis*-macrophage interactions in the context of T3S. Here, we infected macrophages with T3SS-proficient bacteria or bacteria defective in T3S (Δ*lcrV*) then added gentamicin to eliminate extracellular bacteria. Using this protocol, we found that *Y. pestis* is capable of killing macrophages from within via T3SS-dependent, as well as T3SS-indepdendent mechanisms, as measured by LDH accumulation in infected cell culture supernatants. Interestingly, T3SS-indepdent cytotoxicity toward macrophages

was not contingent on the *pgm* locus or excessive bacterial replication, prompting us to screen a library of Tn*5* transposon mutants for genetic elements that lead to a loss-of-function phenotype with respect to LDH release during intracellular infection. The results of the screen suggest several possible mechanisms intracellular bacteria may use to elicit cytotoxicity toward macrophages, as well as egress the vacuole and/or the cell. Of these, the most intriguing is via a mechanism relying on the ShlBA hemolysin system, the regulators of virulence YmoA and HmsT, or perhaps protein glycosylation.

Nevertheless, only bacteria capable of T3S accumulated in the supernatant outside of infected macrophages. To better understand this observation, we measured the total amount of LDH release possible within an infected cell culture and found that despite elevated LDH levels during infection, this amount could be more than doubled by lysing the remaining cells. Thus, even within an infected cell culture, viable cells make up a significant percentage of the population. As such, we further hypothesized that in the absence of a functional T3SS, bacteria would therefore be sequestered intracellularly by these viable cells, resulting in the inhibition of bacterial replication. In support of this notion, we found that after infecting macrophages with wild-type and Δ*lcrV* bacteria and pulsing with gentamicin, a larger total number of T3SS^{+} bacteria were present in the infection when both intra- and extracellular organisms were quantified.

These observations suggest a model whereby intracellular *Y. pestis* kills macrophages from within via T3SS-dependent, as well as T3SS-independent mechanisms in order to escape the cell. However, only after the thermal up regulation of T3S during infection are bacteria able to remain extracellular due to the injection of phagocytosis-inhibiting effector proteins into viable cells. Moreover, in the absence of functional T3S, bacteria are sequestered intracellularly, limiting replication and improving disease outcome. In further support of this conclusion, previously published data indicate that bacteria pre-opsonized with anti-LcrV antibodies are not killed, yet remain cytotoxic toward macrophages after phagocytosis [2].

Taken together, these results suggest that although macrophages contribute to the anti-LcrV-mediated protection of plague, their role may be indirect, and that an alternative immune cell type is likely responsible for the direct clearance of opsonized bacteria. As such, the aim of chapter 4 was to identify host-factors necessary for the clearance of pneumonic plague in the presence of dual-function anti-LcrV antibodies. Our laboratory and others have shown that massive neutrophil infiltration correlates with extracellular bacterial replication during fulminant pneumonic plague infection [3-5]. In investigating the role of these cells, work published by Laws et. al. showed that ablation of neutrophils during naïve pneumonic plague infection results in increased bacterial burden in the lung and severity of disease, demonstrating a protective role for neutrophils during infection [6]. In addition, analysis of the cytokine and

chemokine profile of lung homogenates taken during late stages of infection indicates that many pro-inflammatory chemokines specifically thought to recruit neutrophils to sites of infection are highly up regulated [5]. Thus, we postulated that recruitment of neutrophils to sites of infection may play an important role in the antibody-mediated protection from disease.

Of the chemokines produced during pneumonic plague infection, the CXC chemokine KC is highly up regulated. To this end, we tested whether C3H-HeN mice deficient in KC production (*Kc*$^{-/-}$) were able to clear pneumonic plague after administration of a normally protective dose of anti-LcrV antibodies. We found that although a modest loss of protection was observed in *Kc*$^{-/-}$ mice, KC was largely dispensable for antibody-mediated protection. Moreover, examining lung tissues taken from mice during infection indicated that neutrophils are still recruited to the lung in the absence of KC, suggesting that additional factors, perhaps additional CXC chemokines, could compensate for the loss of KC. Thus, we hypothesized that mice lacking the major receptor for CXC chemokines, CXC Receptor-2 (CXCR2), would display further susceptibility toward lung infection.

Accordingly, we infected anti-LcrV treated *Cxcr2*$^{-/-}$ mice intranasally with a lethal dose of *Y. pestis* and measured susceptibility to disease. Although anti-LcrV treated mice were initially protected compared to sham treated mice, as measured by prolonged survival, decreased bacterial titers in the lung, and less severe histopathology, animals eventually succumbed to pneumonic disease.

Strikingly, neutrophil recruitment was not eliminated in the absence of CXCR2 signaling, indicating the presence of CXCR2-independent pathways of neutrophil recruitment to the sites of *Y. pestis* infection in the lung. To investigate the role of CXCR2-independent neutrophil recruitment, we ablated neutrophils in anti-LcrV treated mice and measured survival after intranasal infection. Although we saw a modest increase in survival in mice that still contained CXCR2-independent neutrophils, the overall survival of both treatment groups was longer than that of PBS-treated mice alone (compare figures 4.2 and 4.7). Taken together, these data suggest that early antibody-mediated protection from pneumonic plague does not rely on neutrophils, yet only in the presence of neutrophils and CXCR2 chemokine signaling are mice able to eliminate bacteria and fully clear disease.

Cumulatively, the data presented in chapters 2-4 support the following mechanism of humoral immunity against pneumonic plague (Figure 5.1). In the presence of protective, dual-function anti-LcrV antibodies, bacteria are simultaneously neutralized in T3S activity and opsonized for directed phagocytic uptake by alveolar macrophages, or perhaps inflammatory monocytes. Nevertheless, bacteria persist inside of macrophages and eventually escape through inducing cell death independent of T3S. Since the T3SS maintains bacteria in the extracellular milieu, it is likely that in the presence of anti-LcrV antibodies bacteria remain opsonized and are re-phagocytosed by viable cells, paralleling results obtained for strains lacking LcrV. This results in a cycle that

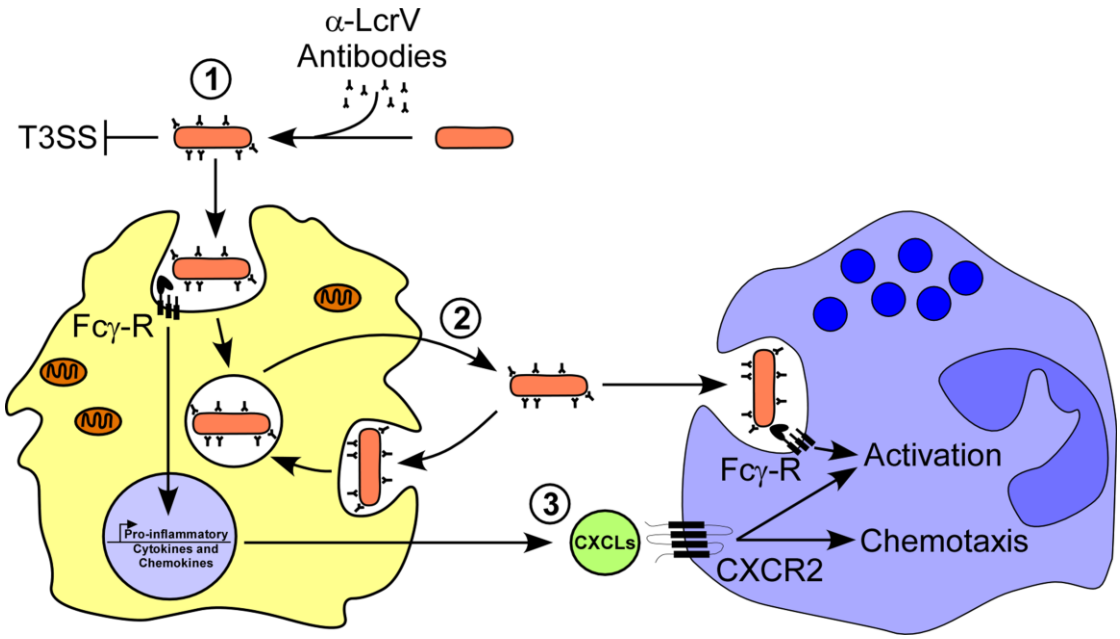

Figure 5.1: Model for the antibody-mediated clearance of pneumonic plague. 1) Dual-function anti-LcrV antibodies both block T3S and opsonize bacteria for phagocytic uptake by macrophages. 2) Intracellular bacteria are then able to kill the macrophage and escape the cell, but are subsequently re-phagocytosed by viable cells, leading to a cycle that limits bacterial replication. 3) Upon Fcγ-R interactions with the macrophage, CXC chemokines are produced that result in the recruitment and activation of neutrophils, which ultimately kill opsonized bacteria and clear the infection.

leads to intracellular sequestration of bacteria, ultimately limiting the number of extracellular organisms. In order to fully clear infection, alveolar macrophages, or possibly other lung cells (such as type II pneumocytes or bronchial epithelial cells), detect and respond to the presence of bacteria and initiate a program of inflammation, leading to the production of proinflammatory cytokines and chemokines. Given the opsonized state of the bacterium, this may also occur through interactions with Fcγ-Receptors expressed on the surface of macrophages, further stimulating proinflammatory gene expression. Upon production of chemokines, yet in a manner that is at least partially independent of CXC chemokine signaling, neutrophils begin to accumulate at the sites of

infection. However, only in the presence of CXC signaling are infiltrating neutrophils activated and able to directly eliminate bacteria.

5.2 Future Directions

Although the data directly support many aspects of this model, several assumptions were made that will need to be examined further. Upon antibody-mediated immune complex formation and opsonophagocytosis of *Y. pestis* by macrophages, we propose that interactions with Fcγ-Receptors may stimulate proinflammatory gene expression that results in the recruitment and activation of neutrophils. Although IgG-mediated immune complex formation with *Y. pestis* likely elicits an inflammatory response from macrophages or other cells along the airway epithelium, it is unclear how robust this response is [7]. Thus we aim to determine the repertoire and concentration of chemokines and cytokines elicited by opsonized *Y. pestis* in the lung to identify factors that could be leading to neutrophil infiltration and contributing to protective responses.

Although we assign this role to a putative cell type(s) in the lung, immune complex-mediated recruitment of neutrophils could also be independent of innate immune cells altogether. While *Y. pestis* is resistant to complement-mediated lysis, it is likely that complement protein C1q binds to antigen-antibody complexes on the surface of opsonized bacteria [8]. This would lead to the initiation of the classical pathway and the subsequent activation of C5 convertase and production of the potent neutrophil chemokine C5a. To test this, we are currently investigating the role of C5a Receptor (C5aR) during pneumonic plague

infection. Preliminary data suggest that antibody neutralization of C5aR results in an increased susceptibility toward disease in wild-type mice, as measured by increased bacterial titers and decreased survival compared to untreated mice (Andrew Kocsis, personal communication). Future experiments aim to determine the role of C5aR in the antibody-mediated clearance of disease, as well as CXCR2-independent neutrophil recruitment in response to *Y. pestis* lung colonization.

It has previously been shown that human neutrophils kill *Y. pestis* after phagocytic uptake [9]. Thus, taken in consideration with our data, we propose that neutrophil bactericidal activity toward opsonized *Y. pestis* relies on CXCR2-dependent signaling. To test this hypothesis, we are currently performing *in vitro* infection studies to identify specific effector functions (such as Ca^{2+} influx, ROS production, NETs, and degranulation) that may be regulated by CXCR2, as well as their role in controlling *Y. pestis* infection. Furthermore, although histopathology indicates that neutrophils accumulate at sites of *Y. pestis* lung colonization independent of CXCR2 signaling, we did not determine if small differences in total neutrophil numbers between wild-type and *Cxcr2*$^{-/-}$ mice may be contributing to disease clearance. To this end, we also plan to measure the total number of neutrophils in the lungs of infected wild-type and *Cxcr2*$^{-/-}$ mice using flow cytometry to determine if mice require CXCR2 signaling to maximally recruit the necessary number of protective neutrophils to sites of infection.

Finally, our model predicts that macrophages indirectly contribute to protection from pneumonic plague by sequestering bacteria intracellularly while contributing to the production of proinflammatory cytokines and chemokines, including protective CXC chemokines. In support of this notion, Das et al. have shown that intracellular *Y. pestis* induces the up regulation of MIP1-α, MIP1-β, MIP2-α, IL-1β, IL-6 and TNF-α in human monocytes [10]. However, although *in vitro* data support this model, additional experimentation will be needed in order to further validate this claim and determine the biological relevance of these observations. To this end, we have been investigating the role of Monocyte Chemotactic Protein-1 (MCP-1) which has been previously shown in to elicit monocyte recruitment to sites of bacterial infection in the lung in murine models of *Burkholderia mallei* and *E. coli* models of infection. Interestingly, Balamayooran et. al. showed that during *E. coli* infection, MCP-1 signaling also leads to the recruitment of neutrophils through stimulating the production of the CXC chemokines KC and MIP-2, further supporting an indirect role for macrophages during infection.

After intranasal instillation of *Y. pestis* in wild-type C3H-HeN and *Mcp1*$^{-/-}$ mice, significantly higher titers of bacteria are present in the lung tissues of mice defective for MCP-1 signaling 48 hours after infection (Figure 5.2A). However, by 72 hours post-infection, titers in wild-type mice reach that of *Mcp1*$^{-/-}$ mice. In addition, *Mcp1*$^{-/-}$ mice are largely protected from pneumonic plague when given a protective dose of anti-LcrV antibodies (Figure 5.2B), supporting the hypothesis

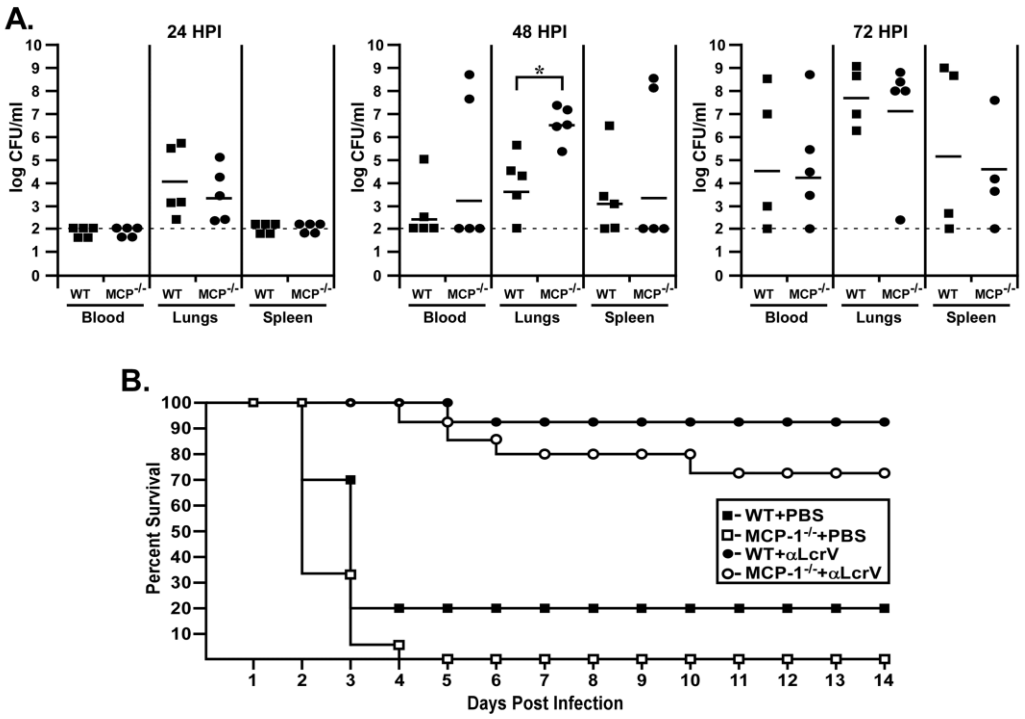

Figure 5.2. MCP-1 contributes to protection from pneumonic plague. Wild-type or *Mcp1*$^{-/-}$ C3H-HeN mice were infected with 6000 CFU *Y. pestis* CO92 intranasally. A) Mice were euthanized at 24, 48, and 72 hours post-infection and bacterial titers were measured in the indicated organs. Each data point indicates and individual mouse, *p<0.05 by students t-test. B) 60 minutes prior to infection, mice were given 400 µg polyclonal anti-LcrV antibodies or PBS. Survival was then measured over a 14 day period.

that although macrophages limit bacterial replication, additional factors are required to fully clear *Y. pestis* lung infection. Nevertheless, these data do not address the role of resident alveolar macrophages, or directly demonstrate that inflammatory monocytes are taking up and sequestering bacteria intracellularly. Thus, we are currently investigating whether anti-LcrV opsonized bacteria are limited in their replication in a similar manner to Δ*lcrV* strains in cell lines more relevant for lung infection, such as mouse MH-S alveolar macrophages and THP-1 human monocytes. Perfroming these important experiments will not only allow us to better understand the role of macrophages in the immune clearance of

pneunonic plague, but also shed light on the role of intracellular infection for *Y. pestis* pathogenesis in the lung.

5.3 Contributions to the Field

Along with laying the groundwork for the experiments proposed above, the research presented within makes several significant contributions to the fields of microbial pathogenesis and vaccine/therapeutics development. Previously, it was unclear if T3S blocking anti-LcrV antibodies merely neutralize bacteria and allow for phagocytic uptake, or if antibodies opsonize bacteria for directed uptake. Our data show for the first time that protective antibodies require both neutralizing and opsonophagocytic properties to elicit protection in a mouse model of pneumonic plague (Chapter 2). This information is absolutely essential for the development of passive antibody therapies that could be used to treat plague in affected individuals. Moreover, it broadens our knowledge of the correlates of immunity needed for the development of plague vaccines that rely on anti-LcrV antibodies.

In addition, we propose a mechanism of macrophage-based protection during pneumonic plague (Chapter 3). Until these experiments were performed, the role of monocytes and macrophages during infection was unknown. We show here for the first time that macrophages are likely playing an ancillary role in the innate and immune clearance of *Y. pestis* from the lung. Although future studies are needed to better define the precise mechanisms used by these cells to contribute to protection from disease, the collective data clearly demonstrate

that cell types other than macrophages are needed to fully clear *Y. pestis* from the lung. Nevertheless, the activity of macrophages appears to limit bacterial replication and improve disease outcome.

Although previous data suggested that neutrophils serve to limit bacterial replication at early time points during infection, their role in immune clearance was unknown [6]. To this end, we show here unequivocally that neutrophils are required for both innate protection and humoral immunity against pneumonic plague (Chapter 4). Moreover, we also demonstrate for the first time that CXC chemokine signaling is required for this activity and that neutrophils defective in CXCR2 signaling remain capable of mobilizing to sites of infection. This was an unexpected observation as CXC signaling had been previously shown to be essential for neutrophil chemotaxis toward sites of bacterial and fungal infection in the lung, suggesting unique mechanisms of neutrophil recruitment during pneumonic plague [11-14]. Together, these data bring attention to novel pathways of immunity elicited by neutrophils that can be exploited for therapeutic development.

In conclusion, the research presented within this dissertation makes significant contributions toward our understanding of *Y. pestis* pathogenesis and the immune clearance of pneumonic plague. However, the most important contribution of this work is the discovery of essential pathways and factors that can be exploited for development of novel therapeutics. For instance, designing a combinatorial therapy that utilizes humanized dual-function anti-LcrV antibodies

with compounds that stimulate CXCR2-dependent neutrophil activities may improve disease clearance. Translational projects of this nature are absolutely essential as protective anti-LcrV antibodies must currently be delivered within an extremely short period of time after infection (24-48 hours). Extending this window of time must remain a priority for researchers, policy makers, and grant funding agencies as effective and fast acting therapeutics must be available in the event of an outbreak, albeit natural or malicious.

5.4 References

1. Weeks, S., et al., *Anti-V antigen antibody protects macrophages from Yersinia pestis -induced cell death and promotes phagocytosis.* Microb Pathog, 2002. **32**(5): 227-37.

2. Noel, B.L., et al., *Yersinia pestis can bypass protective antibodies to LcrV and activation with gamma interferon to survive and induce apoptosis in murine macrophages.* Clin Vaccine Immunol, 2009. **16**(10): 1457-66.

3. Lathem, W.W., et al., *Progression of primary pneumonic plague: a mouse model of infection, pathology, and bacterial transcriptional activity.* Proc Natl Acad Sci U S A, 2005. **102**(49): 17786-91.

4. Lee-Lewis, H. and D.M. Anderson, *Absence of inflammation and pneumonia during infection with nonpigmented Yersinia pestis reveals a new role for the pgm locus in pathogenesis.* Infect Immun, 2010. **78**(1): 220-30.

5. Agar, S.L., et al., *Characterization of a mouse model of plague after aerosolization of Yersinia pestis CO92.* Microbiology, 2008. **154**(Pt 7): 1939-48.

6. Laws, T.R., et al., *Neutrophils are important in early control of lung infection by Yersinia pestis.* Microbes and Infection, 2010. **12**(4): 331-5.

7. Nimmerjahn, F. and J.V. Ravetch, *Fcgamma receptors as regulators of immune responses.* Nat Rev Immunol, 2008. **8**(1): 34-47.

8. Bartra, S.S., et al., *Resistance of Yersinia pestis to complement-dependent killing is mediated by the Ail outer membrane protein.* Infect Immun, 2008. **76**(2): 612-22.

9. Spinner, J.L., J.A. Cundiff, and S.D. Kobayashi, *Yersinia pestis type III secretion system-dependent inhibition of human polymorphonuclear leukocyte function.* Infect Immun, 2008. **76**(8): 3754-60.

10. Das, R., et al., *Study of proinflammatory responses induced by Yersinia pestis in human monocytes using cDNA arrays.* Genes Immun, 2007. **8**(4): 308-19.

11. Greenberger, M.J., et al., *Neutralization of macrophage inflammatory protein-2 attenuates neutrophil recruitment and bacterial clearance in murine Klebsiella pneumonia.* J Infect Dis, 1996. **173**(1): 159-65.

12. Mehrad, B., et al., *CXC chemokine receptor-2 ligands are necessary components of neutrophil-mediated host defense in invasive pulmonary aspergillosis.* J Immunol, 1999. **163**(11): 6086-94.

13. Tateda, K., et al., *Chemokine-dependent neutrophil recruitment in a murine model of Legionella pneumonia: potential role of neutrophils as immunoregulatory cells.* Infect Immun, 2001. **69**(4): 2017-24.

14. Tsai, W.C., et al., *CXC chemokine receptor CXCR2 is essential for protective innate host response in murine Pseudomonas aeruginosa pneumonia.* Infect Immun, 2000. **68**(7): 4289-96.

VITA

Nicholas A. Eisele was born in Etobicoke, Ontario Canada in 1985 and is son to Karen and Rod Eisele, brother to Kirstin Bradshaw, brother-in-law to Lawrence Bradshaw, and uncle to Luke Bradshaw. He and his family emigrated to the United States in 1987 where he grew up in Corpus Christi, Texas and graduated from Gregory-Portland High School in 2003. He is proud to have naturalized as a citizen of the United States of America in 2012. He enjoys outdoor activities such as hiking, camping, and marksmanship, is an avid music enthusiast, and enjoys watching Texas Longhorn football.

Nicholas began college at the University of Texas at San Antonio, and then transferred to the University of Texas at Austin. While in school, Nicholas worked in the laboratory of Shelley Payne and played bass for the band *Copper Child*. After graduating with Bachelor of Science degree in Microbiology in 2007, he moved to Columbia, Missouri to begin graduate school in the laboratory of Deborah Anderson at the University of Missouri. After completion of his graduate work, Nicholas will begin a post-doctoral fellowship at Stanford University in the laboratory of Denise Monack.